2020

Divergence in Neuronal Calcium Dysregulation in Brain Aging and Animal Models of AD

Adam Ghoweri

University of Kentucky, aogh222@uky.edu

Author ORCID Identifier:

https://orcid.org/0000-0003-4750-5519

Digital Object Identifier: https://doi.org/10.13023/etd.2020.521

Right click to open a feedback form in a new tab to let us know how this document benefits you.

DIVERGENCE IN NEURONAL CALCIUM DYSREGULATION IN BRAIN AGING
AND ANIMAL MODELS OF AD

_____

DISSERTATION

_____

A dissertation submitted in partial fulfillment of the
requirements for the degree of Doctor of Philosophy in the
College of Medicine
at the University of Kentucky

By
Adam Omar Ghoweri
Lexington, Kentucky
Director: Dr. Olivier Thibault, Professor of Pharmacology and Nutritional Sciences
Lexington, Kentucky
2020

ABSTRACT OF DISSERTATION

DIVERGENCE IN NEURONAL CALCIUM DYSREGULATION IN BRAIN AGING AND ANIMAL MODELS OF AD

Neuronal calcium dysregulation first garnered attention during the mid-1980's as a key factor in brain aging, which led to the formulation of the Ca^{2+} hypothesis of brain aging and dementia. Indeed, many Ca^{2+}-dependent cellular processes that change with age, including an increase in the afterhyperpolarization, a decrease in long-term potentiation, an increased susceptibility to long-term depression, and a reduction in short-term synaptic plasticity, have been identified. It was later determined that increased intracellular Ca^{2+} with age was due to increased Ca^{2+} channel density, elevated release from intracellular Ca^{2+} stores, and decreased Ca^{2+} buffering or clearance. Further, changes in intra- and intercellular Ca^{2+}-dependent processes can lead to poor learning and spatial mapping in aged animals. As these are clear deficits in hippocampal function, many early studies assumed Ca^{2+} dysregulation phenotypes in animal models of aging were similar to the dysregulated cellular mechanisms seen in Alzheimer's disease (AD) and other types of dementia. However, with the development of transgenic models to recapitulate hallmark AD phenotypes over the past 20 years, it has become apparent that the mishandling of Ca^{2+} is notably different across models.

Importantly, many of these results were obtained while measuring Ca^{2+} indirectly and at limited ages. Thus, the once generalizable phenotypes associated with Ca^{2+} dysregulation, including increased intracellular Ca^{2+} and reduced synaptic communication, appear to diverge in normal brain aging and AD. The following dissertation investigates direct and indirect Ca^{2+} measures across the widely used 5xFAD familial AD mouse, as well as the less common $Aldh2^{-/-}$ sporadic AD mouse model. Based on previous evidence, it was hypothesized that a decrease in intracellular Ca^{2+} and associated processes would manifest in both models across age. Key results showed a reduction in resting Ca^{2+} in the 5xFAD mice, while in the $Aldh2^{-/-}$ model only minor Ca^{2+}-dependent processes showed a genotype effect. These results highlight the non-generalizable nature of the Ca^{2+} hypothesis of brain aging to AD phenotypes and emphasize the importance of genetic background characterization, as well as underscore the complexity of cellular alterations in the divergence of aging and neurodegeneration.

Adam Omar Ghoweri

(Name of Student)

11/17/2020

Date

DIVERGENCE IN NEURONAL CALCIUM DYSREGULATION IN BRAIN AGING
AND ANIMAL MODELS OF AD

By
Adam Omar Ghoweri

Dr. Olivier Thibault
Director of Dissertation

Dr. Rolf Craven
Director of Graduate Studies

11/17/2020
Date

DEDICATION

To my wonderful friends, family, and mentors: Life is a journey with no instruction manual. You must follow the guidance of those who you trust and, importantly, the gravity of intuition. Every day is a new adventure to be had and story to be told. You inspire me to pursue new endeavors with the knowledge that purpose is married to human spirit. Selflessness cultivates happiness.

ACKNOWLEDGMENTS

The following dissertation is the product of years of training under the mentorship of Dr. Olivier Thibault. Olivier, you have my sincerest gratitude and respect for the time that you have invested in me. Not only do I feel like a better scientist, but I feel like an overall better person. Wherever I may end up in life, I hope to carry the same fervor for learning and excitement to share knowledge as you do. During my time in the lab, you challenged me to better myself through writing, engagement with others, and critical interpretation of data and literature, thus developing my perception of what it means to do "good science." I recognize now that I will never truly know *everything*, but that is the excitement of being a life-learner. As long as I have the passion to continue to learn, grace to accept and improve my shortcomings, and wisdom of open-mindedness, I know I will be wealthy in life experience.

I would be remiss if I did not extend my gratitude to my lab mates: Hilaree, Ruei-Lung, and Katie, as well as current/former members of the department: Chris Gant, Ellie, Lucy, Courtney, Kendra, Ms. Kelley, Véronique, and Lawrence. I am a firm believer that people thrive when they are immersed in an environment conducive to growth. We are far more than just a department; we are a strong collaborative community. Fostering friendships to lean on in addition to discussing science with sharp minds has truly been an unexpected blessing during these past few years. Thank you for lending me your support, wisdom, insight, and expertise. The cadence of your friendship has become an extension of who I am and I intend to impart such values in my future relationships.

Lastly, I must express appreciation for the guidance provided to me by my graduate committee consisting of Drs. Olivier Thibault, Donna Wilcock, Nada Porter, Chris Norris,

TABLE OF CONTENTS

LIST OF TABLES

LIST OF FIGURES

CHAPTER 1. NEURONAL CALCIUM HANDLING IN AGING AND AD

1.1   The Calcium Hypothesis of Brain Aging and Dementia

In the mid-1980's, a novel proposal revolutionized modern Alzheimer's disease (AD) research. This was the recognition of Ca^{2+} dysregulation as a variable involved in brain aging and dementia which was subsequently coined the "Calcium Hypothesis of Brain Aging and Dementia" [1-6]. In the initial proposal it was postulated that increased neuronal intracellular Ca^{2+}, with age, warrants excitotoxicity and subsequent cell death. Since this early hypothesis, it has been shown that rather than an excitotoxicity phenotype, neuronal hyperexcitability due to sustained intracellular Ca^{2+} levels and reduced clearance are more accurate biomarkers of Ca^{2+} dysregulation. Some of this early work in rat and rabbit animal models of brain aging showed aged neurons exhibiting enhanced influx of Ca^{2+} through voltage-gated channels which led to both a larger Ca^{2+}-dependent afterhyperpolarization (AHP) and reduced short-term synaptic plasticity [2, 7-11]. Further, alterations to mitochondrial and endoplasmic reticulum (ER) cytosolic Ca^{2+} buffering [12-16], decreased release from intracellular stores [17], and reduced cytosolic clearance [18-21] are recognized as important hallmarks of perturbed Ca^{2+} homeostasis in neurons.

Detection of these markers of dysregulated Ca^{2+} have led to advances in understanding the complex regulatory mechanisms involved in neuronal network communication, memory encoding, and cognition. Despite these encouraging insights, there have been therapeutic limitations and misalignments of outcome measures between normal brain aging and AD. **Chapter 1** of this dissertation aims to address the current status of Ca^{2+} homeostasis literature in normal brain aging and how it diverges during AD progression. **Chapters 2** and **4** are studies that measured Ca^{2+} in two different mouse

models of amyloidogenesis across age, while **Chapter 3** highlights the differences between the animals and the utility of using various models. **Chapter 5** will conclude the dissertation by summarizing and discussing results, addressing limitations of the studies, and suggesting future directions.

1.2 Ca^{2+} Handling in Neuronal Physiology

Ca^{2+} is a versatile second-messenger signaling ion that has a fundamental role in many cellular processes such as apoptosis, neurotransmitter release, mitochondrial bioenergetics and free radical species formation, gene regulation, cell proliferation and growth, membrane excitability, synaptic transmission, and plasticity [22-24]. Its functional role in a neuron is carefully regulated, so much so that the concentration of intracellular Ca^{2+} (50-200 nM) is 10,000 times less than in the extracellular space (1-2 mM) [25-28]. To maintain this sheer difference in concentration gradient, many protein complexes are involved at the plasma membrane, cytosol, mitochondria, and ER [29].

At the plasma membrane, voltage-gated Ca^{2+} channels (VGCCs), ligand-gated Ca^{2+} channels (LGCCs) such as N-methyl-D-asparate (NMDA) and α-amino-3-hydroxy-5-methylisoxazole-4- propionate (AMPA) receptors, and store-operated Ca^{2+} entry (SOCE) channels regulate Ca^{2+} influx, while plasma membrane Ca^{2+} ATPase (PMCA) and Na^+/ Ca^{2+} exchangers (NCX) are prominent regulators of Ca^{2+} efflux [24, 30-34]. NCX flux Ca^{2+} into the extracellular space with low affinity, but high capacity during the recovery phase of an action potential (AP) firing [35], while the PMCA has high affinity for Ca^{2+}, yet slow transportation in the extracellular matrix, positioning the PMCA channels to be better equipped for maintaining resting state levels of Ca^{2+} [36, 37]. Within the intracellular

space, the ER's ryanodine (RyR) and inositol (1, 4, 5)-trisphosphate (IP$_3$) receptors and the mitochondrial transport system play a critical role in maintaining intracellular Ca^{2+} store homeostasis through release and clearance mechanisms [38-44]. It is through calcium-induced calcium release (CICR) and RyR/IP$_3$R activation that cytosolic Ca^{2+} levels can rise to 1-5 μM and trigger Ca^{2+}-dependent signaling pathways. Intracellular Ca^{2+} stores in the ER are then replenished via Ca^{2+} uptake through the sarco-endoplasmic reticulum Ca^{2+}-ATPase (SERCA) pumps. Further, through a mechanism called capacitive Ca^{2+} entry (CCE) or store operated Ca^{2+} entry (SOCE), crosstalk between ORAI subunits at the plasma membrane and STIM proteins at the ER aid in the regulation of ER Ca^{2+} levels [45-47]. The following sections will describe in greater detail the cellular physiology of Ca^{2+} handling, alterations during aging, and changes to these processes in AD.

1.3   Membrane-bound Ca^{2+} Channels

1.3.1   NMDA Receptors

At the post-synapse are the hetero-tetrameric protein complex NMDA receptors. A type of ligand-gated Ca^{2+} channel (LGCC), NMDARs are ionotropic glutamate receptors that regulate the passing of Na$^+$, K$^+$, and Ca^{2+} ions into the intracellular space. Because neurons have a negative resting membrane potential and the reversal potential of NMDARs is ~0 mV, receptor activation is always an excitatory response. These excitatory responses (*i.e.* excitatory postsynaptic potentials or EPSPs) grow in amplitude as the receptor is activated, which influxes extracellular Ca^{2+} into the post-synaptic neuron. Importantly, the inclusion of Ca^{2+} influx into the cytosolic space activates a signaling cascade of CICR. Additionally, through nonspecific activation involving glutamate and glycine co-agonist

binding, as well as the depolarization of the plasma membrane to remove a Mg^{2+} that occludes the NMDA channel, NMDARs facilitate long-term potentiation (LTP) and long-term depression (LTD) processes [48, 49]. It is through repetitive, synchronous stimulation of the pre- and post-synapse at high and low frequencies that LTP and LTD are elicited, respectively. These synaptic plasticity processes are believed to be largely associated with memory encoding and erasure [50-54]. Moreover, Ca^{2+} influx via NMDA receptors at the postsynaptic dendritic spines is necessary for LTP to be induced [55]. Conversely, when NMDA receptors are either inhibited or quantitatively in deficit, depression of the synapse may ensue [56]. With ties to memory and attention, it has been of interest to investigate NMDA receptors and their function in brain aging research.

In aging, it has been shown that NMDA proteins and function are altered; however, this has been relatively region specific, as such changes were noted in the hippocampus, but not in cortical tissue. More specifically, reduced expression of NMDA protein localized to region Cornu Ammonis-1 (CA1) has been observed in aged mice, rats, and rhesus monkeys [57-67]. This observation is coupled with decreased NMDAR-mediated synaptic response in aging, as electrophysiological studies have shown reduced EPSP amplitude by 50% [68, 69]. Various theories have been postulated to explain the overall reduction in NMDAR density, such as decreased subunit expression, altered posttranslational modification via kinase/phosphatase activity states, and decreases in local supporting cells that are the source of essential amino acids [64, 67, 69-83]. However, due to inconsistencies and contrasting outcomes in age-related loss of NMDARs, an explanation has remained elusive. With the crucial role NMDARs have in synaptic communication, reductions in

NMDA proteins and function are expected in memory impairment and cognitive decline. Thus, NMDA alterations are a robust marker of neuronal aging and deficits.

1.3.2 Voltage-gated Ca^{2+} Channels

Another source of neuronal Ca^{2+} influx from the extracellular space is through the voltage-gated Ca^{2+} channels (VGCCs). These hetero-multimer protein channels are embedded within the plasma membrane and are activated upon depolarization of the membrane. Two classes of VGCCs have been identified: high-voltage-gated and low-voltage-gated. As their names imply, high-voltage is dependent on a strong membrane depolarization while low-voltage relies on a weak depolarization. High-voltage VGCCs have been further classified as the L (Ca_v 1.1-3), P/Q (Ca_v 2.1), and N (Ca_v 2.2) type channels, while low-voltage VGCCs are classified as either T (Ca_v 3.1) or R (Ca_v 2.3) type based on their respective biophysical and pharmacological properties [84-94]. There has been a wealth of evidence suggesting VGCCs are affected during brain aging as well. In CA1 hippocampal neurons of aged rats, increased L-type voltage-gated calcium channel (L-VGCC) density, Ca^{2+} currents, mRNA protein expression levels, and post-translational phosphorylation state have been well characterized [80, 95-102]. That being said, the application of Ca^{2+} channel blockers to reverse the effect of aging on L-VGCCs has generated a lot of research interest.

Many previous studies have applied L-VGCC blockers such as nifedipine and nimodipine to hippocampal slices to investigate Ca^{2+}-mediated processes like the AHP and long and short-term plasticity. Importantly, by inhibiting L-VGCC activity with blockers, age-related deficits to synaptic strength and behavioral learning have been rescued [80, 103, 104]. Further, it has been observed that through blocking L-VGCCs, the amplitude of

the age-enhanced AHP is reduced and, notably, LTP induction is facilitated at lower frequency stimulation while LTD induction is inhibited in aged animals [80, 105]. The translatability of these findings is apparent too, as a multitude of studies have shown robust improvements in hippocampal learning and memory through the blockade of L-VGCCs in *both* aged animals and humans [8, 100, 106-119]. Surprisingly, L-VGCC alterations seem to only be related to hippocampal-dependent memory, as expression patterns and function of L-VGCCs in cortical neurons are not altered with age [120, 121]. Of interest, there is also crosstalk between estrogen and L-VGCC expression, as they are negatively correlated; L-VGCC density increases with age as estrogen decreases, perhaps underscoring a sex difference that may be present in memory decline [122]. Thus, it comes with little surprise that the use of L-VGCC blockers in studies of aging and cognitive impairment has been widely explored. The clinical application of L-VGCCs is discussed in greater detail in **Chapter 1.8**.

1.4   Intracellular Calcium Stores (ICS)

1.4.1   Endoplasmic Reticulum

CICR is a physiologic phenomenon to amplify the release of Ca^{2+} at the ER. Through Ca^{2+} influx at the plasma membrane and activation of IP$_3$Rs at the ER, Ca^{2+} is released into the cytosol and further activates RyRs at the ER for even greater Ca^{2+} release. Age-related decreases in IP$_3$ receptor density have been reported in cerebellum and cortex. Interestingly, however, these reductions do not seem to correlate with reduced IP$_3$-induced Ca^{2+} release [123-127]. Similarly, it should be noted that increased RyR responsiveness to CICR has been observed in the presence of age-mediated increases in oxidative stress,

which incidentally has been suggested to increase IP_3 receptor function, perhaps highlighting the complexity of compensatory effects, especially when IP_3 receptor function is modified [128-132]. Further, in aged F344 rats, it has been shown that inhibiting the age-dependent enhancement of CICR in hippocampal neurons reduces the AHP amplitude, enhances LTP, inhibits LTD, and promotes NMDAR-mediated synaptic plasticity, underscoring the widespread physiologic implications that dysregulated Ca^{2+} handling can have on synaptic communication [133, 134]. Moreover, direct Ca^{2+} measures show increased somatic Ca^{2+} and slow release (decreased rise time) from intracellular stores in aged F344 rats [135]. These age-related differences are attenuated when the CICR antagonist ryanodine is administered, further emphasizing the global effect that dysregulated Ca^{2+} homeostasis has on a neuron.

1.4.2 Mitochondrial Ca^{2+} Handling

Mitochondria have a prominent role in maintenance of bioenergetics necessary for cell survival and programmed death through the production of adenosine triphosphate (ATP) and caspase activators/proteins needed for apoptosis [136, 137]. Of interest, mitochondria also function as regulators of intracellular Ca^{2+} transients through uptake via the mitochondrial Ca^{2+} uniporter (MCU), which in turn regulates mitochondrial metabolism [38, 138-140]. Ca^{2+} is also transported back to the cytosol via the mitochondrial NCX (mNCX) [141]. In aged cortical tissue of F344 rats, reduced mitochondrial uptake of Ca^{2+} has been observed in comparison to younger aged animals [142]. However, when elevated levels of Ca^{2+} enter the mitochondria, reactive oxygen species (ROS) production increases, ATP synthesis is inhibited, and apoptosis is initiated, highlighting a delicate threshold of mitochondrial Ca^{2+} regulation [143, 144]. In addition

to decreased Ca^{2+} uptake in aging, mitochondrial regulation of free oxygen radicals has been observed to decline with age [145]; thus, it is perhaps unsurprising that the relationship between Ca^{2+} dysregulation and ROS has garnered attention in brain aging and dementia literature. Both Ca^{2+} dysregulation and ROS have been implicated in the genesis of amyloid beta plaques and all three are believed promote one another. **Chapter 1.10** goes into greater detail on these phenotypes.

1.4.3   Cytosolic Ca^{2+} Transportation

To regulate the dynamic increases in cytosolic Ca^{2+} during depolarization and keep intracellular concentrations of the cation low during resting state, neurons have robust Ca^{2+} signaling mechanisms to clear excess Ca^{2+} ions from the cytosolic space [146]. Ca^{2+} transport is achieved through the signaling of over 200 Ca^{2+} binding proteins (CBPs) that are key modulators of Ca^{2+} signaling pathways [147]. CBPs can be subdivided into Ca^{2+} buffers (*e.g.* calbindin, parvalbumin, and calretinin) and Ca^{2+} sensors (*e.g.* calmodulin and protein kinase C) [147, 148]. The CBPs help facilitate the flux of Ca^{2+} back into the ER and mitochondria (sequestration), as well as the exchange of Ca^{2+} back into the extracellular milieu (extrusion). The involvement of CBPs in aging has been unique to CBP-type, as well as to tissue region specificity.

Many studies have examined different types of CBPs across age, yet findings have been notably widespread. For example, decreased levels of CBPs such as calbindin and calretinin have been observed in the hippocampus of aged rats [149, 150], while their levels remained unchanged in the cerebellum [149]. Similarly, when calbindin immunoreactivity was measured across age in rats and rabbits, significant decreases were detected in *both* the dentate gyrus and subregion CA1 of the hippocampus in aged rats, but *only* in the dentate

8

gyrus of aged rabbits [151]. In contrast to calbindin, interneurons containing parvalbumin in the hippocampus had no changes in aged rats [150], but reduced levels of parvalbumin in the medial septum-diagonal band that leads to the hippocampus have been noted [152]. Others have also suggested that a reduction in CBPs during aging may lead to decreased function of the embedded proteins involved in sequestration and extrusion transport systems, hence heightened intracellular Ca^{2+} levels [153-158]. Reductions of CBPs during aging is not generalizable though, as the Ca^{2+} and Ca^{2+}/calmodulin binding protein phosphatase, calcineurin, has been demonstrated to play a direct role in increasing L-VGCC function in aging [101, 159]. Further, it is important to note that *decreased* Ca^{2+} binding may be region or cell specific, as *increased* Ca^{2+} binding has been identified in basal forebrain neurons during aging, perhaps suggesting the presence of an underlying compensatory mechanism to regulate Ca^{2+} ion concentrations [16, 160, 161]. Irrespective of irregular CBP results, there is clearly an important role that CBPs have in neuronal Ca^{2+} regulation that should continue to be explored.

1.5   Synaptic Plasticity

As highlighted in previous sections, age-dependent NMDAR loss and L-VGCC functional increases (coupled with alterations to ICS signaling) impact both the excitability and overall neural activity of hippocampal neurons. A classic measure of the association between synaptic plasticity and memory is sustained synaptic strength using LTP outcome measures [162]. A well-characterized phenotype of synaptic plasticity in aging is the elevated activation threshold for LTP induction and reduced LTP duration [51, 52, 163], perhaps meaning greater difficulty to encode memories. It is curious, however, that the

larger AHP and enhanced Ca^{2+} levels during stimulation that are observed in aging do not contribute to a *lower* activation threshold in LTP. Importantly though, the AHP is a *post-synaptic* potential, which likely explains the lack of effect it may impose on the *synaptic* LTP activation threshold. Reduced LTD threshold, increased susceptibility to activating LTD, and depotentiation (reduction in synaptic strength after it was initially potentiated) have been illustrated as markers of poor synaptic plasticity in aging as well [18, 52, 164, 165]. Moreover, aging phenotypes of synaptic strength have not been exclusive to long-term synaptic plasticity. Another phenotype of impaired synaptic plasticity in aging has been observed during repetitive synaptic stimulation (frequency facilitation), a form of short-term synaptic plasticity, where failure to elicit growth of EPSPs is seen in aged F344 rats [10]. This finding has been coupled with the elevation of both postsynaptic intracellular Ca^{2+} as well as L-VGCC activity in aged CA1 pyramidal neurons, a testament to the global impact of dysregulated Ca^{2+} on network communication [11].

1.6   Afterhyperpolarization (AHP)

The communication between neurons is profoundly unique, incredibly complex, and, importantly, well-regulated. In a sense, an AP can be thought of as the language used to facilitate communication between neurons. Through repeated firing of APs, neurons release neurotransmitters at their synapses to communicate with one another. It is through specific patterns and frequencies that memories are encoded or forgotten. As a regulator of repetitive AP firing, the post-burst afterhyperpolarization (AHP) is a neuronal mechanism that prevents overexcitation [166] and its amplitude is dependent on the number and frequency of APs during stimulation [167, 168]. In addition to the number and frequency

10

of APs affecting AHP amplitude, the AHP of hippocampal pyramidal neurons has two sub-components, medium and slow afterhyperpolarizations, that are Ca^{2+}-dependent [169, 170]. The amplitude and duration of the AHP correlates with intracellular Ca^{2+} concentrations. Moreover, the AHP has been shown to be directly associated with learning, as reductions in its amplitude have been previously described in rat and rabbit models undergoing hippocampal-dependent tasks such as eyeblink conditioning [171-173], context-fear conditioning [174], olfactory-discrimination [175, 176], and the Morris water maze [177].

Conversely, when learning is impaired in aged animals, the post-burst AHP amplitude is enhanced [171]. Though learning tasks ameliorate the amplitude of the Ca^{2+}-sensitive AHP, pharmacological treatments are effective in truncating the AHP magnitude too. L-VGCC blockers nifedipine and nimodipine have been historically used to reduce Ca^{2+} influx and decrease the AHP [80, 103, 104, 178-180], while 1,25VitD treatment on cultured neurons has been proven effective as well [181]. Importantly, it has been widely demonstrated that CA1 pyramidal neurons of aged animals have AHPs of significantly greater amplitude compared to young counterparts [2, 9, 182]. This increase in AHP amplitude of aged animals is due in part to higher concentrations of intracellular Ca^{2+} and reflects perturbed Ca^{2+} regulatory mechanisms such as channel density at the plasma membrane and clearance, buffering, and extrusion processes [133, 135, 165, 170, 183, 184]. Because the AHP relies so heavily on other Ca^{2+} regulating biophysical mechanisms, it is considered a reliable indirect measure of neuronal Ca^{2+} handling.

1.7   Sex Differences in Ca^{2+} and Ca^{2+}-dependent Processes of Aged Neurons

Notably, sex hormones have been described to impact Ca^{2+} homeostasis as well, and this is of considerable interest in aging research, as sex is considered a predisposing feature of AD development [185]. For example, treatment with estrogen has been shown to increase NMDA receptor density in aged animals [186], as well as elevate dendritic spines of CA1 neurons in young rats [187], but alterations were only present in those specific age groups. However, estrogen treatments in ovariectomized primates elicit greater hippocampal spines and performance of hippocampus-dependent cognitive tasks in *both* young and aged animals, highlighting a clear role estrogen plays in learning and memory [188, 189]. Why there is a disconnect between estrogen effects across species remains to be determined. As estrogen has demonstrated an effect on learning and memory, its use in synaptic plasticity is of interest as well.

Through whole cell electrophysiological recordings, application of 17beta-estradiol (a potent estrogen) to medial vestibular nucleus neurons of rat brainstem slices induces synaptic LTP and inhibits LTD induction, while dihydrotestosterone induces synaptic LTD, which was corroborated by an abundance of estrogen and androgen receptors in MVN neurons [190]. Further, high doses of 17beta-estradiol have been shown to inhibit intracellular Ca^{2+} release in gerbil CA1 pyramidal neurons [191]. This work has been corroborated through the identification of an enhanced AHP in aged ovariectomized F344 rats and the reduction in amplitude upon direct application of 17beta-estradiol benzoate to hippocampal slices [102], as well as an estradiol-mediated increase in the slow afterdepolarization amplitude of mice [192]. Interestingly, 17beta-estradiol benzoate bath occludes the attenuation of the AHP with the L-channel blocker nifedipine, suggesting

estrogen derivatives modulate the AHP through a different mechanism other than L-VGCC blockade. Through and through, it is evident that the crosstalk between estrogen and Ca^{2+} is essential to neuronal homeostasis and supports the importance of including sex difference investigation in studies of aging.

1.8 Ca^{2+} and Cognition

Arguably the most forthright phenotype of brain aging, cognitive decline has been long thought to be the result of neuronal loss with age in contemporary culture. However, many studies have illustrated a non-significant reduction in neurons across human, monkey, and rodent models, questioning the validity of this theory [193-198]. Rather, decline in cognition has been suggested to depend on synaptic alterations and neurotransmission limitations [199]. These changes with age, however, are more-subtle than reductions in synaptic density and have been mostly absent in hippocampal tissue during aging [199, 200]. Instead, alterations in synaptic communication during aging have manifested in Ca^{2+}-dependent processes like a reduced excitatory postsynaptic potential [10, 18, 201] and an increased AHP current (reduces neuronal excitability), as previously noted in **Chapters 1.1** and **1.3.1** [165, 202]. Thus, it has been of interest in clinical trials to test the effect of Ca^{2+} blockers on cognitive deficits in aging human populations, especially AD.

As the purpose of basic research is the hopeful translatability for clinical use in humans, the identification of perturbed neuronal Ca^{2+} handling in AD led to the exploration of Ca^{2+} channel blockers as a form of treatment. Nimodipine has been a commonly used drug in clinical trials due to its ability to readily traverse the blood-brain barrier, yet these

results have been controversial. Indeed, improved memory and attention from nimodipine treatment was observed in patients of age-related dementia in early trials [117, 203, 204]. However, because nimodipine is an antihypertensive drug used in the prevention of subarachnoid hemorrhaging as a vasodilator, it has been speculated that its effectiveness in AD pertains specifically to treating vascular-related symptoms of vascular dementia [205, 206]. Moreover, meta-analyses suggest VGCCs have a limited role in vascular dementia progression [205]. Nevertheless, the use of other Ca^{2+} channel blockers in the treatment of dementia prevention have also been tested, but yielded similarly inconsistent results. Antihypertensive Ca^{2+} channel blockers like nitrendipine and nilvadipine have been shown to temporarily reduce mild cognitive impairment progression, while nifedipine, diltiazem, verapamil, and amlodipine were found to be ineffective [207-209]. Thus, while Ca^{2+} channel blockers may play a potential role in treating AD, they clearly are not enough to effectively address the multi-faceted cellular alterations that drive disease progression.

1.9   Alzheimer's Disease

AD is a devastating neurodegenerative disease state first described by Alois Alzheimer in 1906, that is characterized by beta amyloid (Aβ) deposits, hyperphosphorylated tau protein tangles, dysregulated Ca^{2+} homeostasis, elevated oxidative stress, and altered neuroinflammatory markers. The global impact of each of these hallmarks can promote impaired cognitive function, memory deficits, and behavioral problems, leading to reduced quality of living and need for assisted care. To elucidate the underlying mechanisms that drive AD progression, multiple hypotheses have been proposed to pinpoint an initiating marker that propagates other pervasive cellular

alterations and, ultimately, poor cognition and behavior. However, though there is substantial evidence suggesting that amyloid, tau, dysregulated Ca^{2+}, inflammation, oxidative stress, and even metal ion dysregulation each participate in the pathogenesis of AD, no singular biomarker accounts for the extensive cascade of detrimental cellular events that promote AD [210, 211].

Despite the lack of a single AD hypothesis to explain phenotype progression, this should not detract from the importance of the data that has been collected within each respective hypothesis' field of research. The paucity of identifying an AD treatment that addresses each hallmark speaks to the complexity of the disease and likely suggests *multiple* initiating events are intertwined and occur much earlier than the manifestation of amyloid and tau, synaptic loss, and cognitive decline. Thus, the interplay of early AD phenotypes such as Ca^{2+} dysregulation and oxidative stress may be important to further investigate. Because normal brain aging is devoid of amyloid plaque deposits and phosphorylated tau and there is a prevalence of altered Ca^{2+} handling in both aging proper and AD, an assumption that AD may be an advanced form of aging has been suggested. However, a growing body of evidence detailing a misalignment of outcome measures between aging and AD suggests a potential divergence at the neuronal level. Further, these misaligned phenotypes may even suggest that the Calcium Hypothesis of Brain Aging and Dementia is not as generalizable as previously thought. The following sections highlight deviations in Ca^{2+}-dependent processes in AD models of aging and segue into two studies that investigate Ca^{2+} outcome measures across age in mouse models of AD.

1.10 Aβ and Ca^{2+} in Culture and Animal Models of AD

The amyloid precursor protein (APP) is a type I membrane protein that is proteolytically processed to generate toxic Aβ species in AD [212]. Though APP is expressed in many tissue types, its expression and improper splicing in AD gives rise to insoluble extracellular Aβ monomers and oligomers in the brain. It is through the processing via β and γ secretases and aggregation of insoluble Aβ peptides that amyloid deposits accumulate in the AD brain, which led to the synthesis of the amyloid hypothesis [213-217]. Early evidence has suggested Aβ as an influencing factor in dysregulated Ca^{2+} homeostasis in AD, such that Aβ oligomers may create Ca^{2+}-permeable channels in the cell membrane [218, 219]. In initial cell culture studies, the addition of Aβ to cultured neurons was shown to elevate intracellular Ca^{2+} concentrations [220, 221]. Further, Aβ has also been shown to elicit ROS production and subsequent membrane lipid peroxidation, leading to impairments of Ca^{2+} transporters at the plasma membrane and elevating intracellular Ca^{2+} concentrations [222, 223]. With clear detrimental impact to neuronal health, studies have also measured the influence Aβ has on cell-to-cell neuronal communication such as synaptic plasticity.

Reduced synaptic strength and synaptic loss are key markers of AD progression. As such, studies have investigated the impact of Aβ oligomers on synaptic plasticity. Not only have decreased surface NMDA receptors in APP mutated transgenic models [224] been identified, but an inhibition of LTP induction in both *in vivo* and *in vitro* models has been observed as well, although this was not present with LTD [225-228]. The latter result is especially surprising, considering both mechanisms are widely thought to be involved in memory encoding and erasure. Interestingly, Aβ oligomers have also been shown to induce

the production of ROS through NMDAR-dependent activation in hippocampal cultures [229]. In pyramidal neurons of Sprague-Dawley rats, Aβ reduces dendritic spine density, impairs electrophysiologically active synapses [230], and facilitates NMDA-mediated excitotoxicity [229, 231], which may underscore why such pronounced synaptic deficits are present in AD. It is important to note, however, that while Aβ increases intracellular Ca^{2+}, elevated intracellular Ca^{2+} can also promote Aβ production, which suggests a cyclic relationship between the two events and further complicates detection of the initiating factor(s) that begin the AD cascade [232-235].

1.11 Plasma Membrane Ca^{2+} Handling in AD Models

1.11.1 Ca^{2+} Influx Via VGCCs at the Plasma Membrane in AD Models

In an attempt to gain a greater understanding of Aβ's effect on Ca^{2+}-mediated processes at the plasma membrane such as Ca^{2+} influx via VGCCs, studies have looked at VGCC density and function in culture and animal models of amyloidogenesis. Growing evidence has shown Aβ impacts neuronal health through increased L-type VGCC influx of current, increased intracellular Ca^{2+}, and impaired synaptic plasticity [236]. In studies of cultured rat neurons, Aβ treatment increases free radical production and subsequently elevates Ca^{2+} influx through L- and N-VGCCs [237], while also elevating N- and P-type VGCC current amplitude [238]. Similarly, L-type $Ca_v1.2$ and 1.3 subunit surface proteins and channel activity have been observed to increase in the presence of acute Aβ oligomer exposure in culture [239, 240], although chronic exposure evoked decreased L-type $Ca_v1.2$ surface proteins [239]. Though many cell culture studies have provided evidence of a

negative impact of Aβ on VGCCs, it has been of interest to investigate VGCCs in AD animal models to uncover physiologic alterations in the progression of AD.

A limited number of studies have investigated L-VGCCs in models of AD with the inclusion of aging. Of these, an age-dependent increase in L-VGCC density specific to CA1 neurons of 3xTg mice has been observed, but not in neurons of subfield CA3 or the dentate gyrus [241]. Strangely, in a similar study conducted by our group using a double knock-in mouse model and the same patch-clamp electrophysiological technique, *reductions* in L-VGCC channel activity was observed in mice of the same age (12-14 mo.) [242]. Further, a reduction in $Ca_v1.2$ protein expression has been seen in 2xTg mice of 9 months compared to WT littermates using a similar biochemical approach [243]. Perhaps such drastic differences in phenotypes between the similar mouse models can be attributed to the inclusion of the *MAPT* (tau) gene mutation in the 3xTg design, although many other factors may be influencing the generation of the phenotype as well. Nevertheless, these deviations from the early findings of increased L-VGCC density and activity in aged F344 rats by Thibault and Landfield highlight a clear misalignment between normal brain aging and brain aging in AD [97]. Considering the growing body of literature linking L-VGCC alterations to cognitive and spatial memory deficits [244, 245] and the controversial evidence of L-VGCC blocker effectiveness in clinical trials [246-250], it is of interest to continue efforts to elucidate the role of these channels in AD progression.

1.11.2 Synaptic Dysfunction and Tau in AD Models

Studies exposing NMDAR to concentrations of Aβ *in vitro*, *ex vivo*, and *in vivo* have illustrated a direct negative impact on synaptic connectivity. Some of the markers of synaptic dysfunction include the reduction of activity to the NMDA subunit GluN2A and

downregulation of synaptic proteins PSD-95 and synaptophysin [251], subunit GluN2B-mediated LTP impairment [252], and even rescuing learning and memory through the enhancement of GluN2B NMDAR surface trafficking [253]. There have also been studies linking synaptic dysfunction in AD to the hyperphosphorylation of tau, which adds to the complexity of cellular changes as they transpire. As tau protein is normally localized to neuronal axons, it is indeed problematic that in the AD brain, tau is aberrantly translocated to the somatodendritic region of cells [254, 255]. Of particular interest, recent evidence has suggested that this mislocalization of tau protein and subsequent hyperphosphorylation may be due, in part, to overexcitation of NMDA and AMPA receptors resulting from excess glutamate stimulation [256], which aligns with epilepsy phenotypes that have been observed in AD [257-260]. However, as tau mislocalization to dendritic spines has been implicated in the degeneration of synaptic activity [261], it is clear that a better establishment of a time orientation between the manifestation of synaptic dysfunction and somatodendritic tau accumulation is necessary to more carefully link the coupled phenotypes [262].

1.11.3 Ca^{2+} Efflux at the Plasma Membrane in AD Models

Given the direct impact that Aβ has on NMDA receptors [224], it is unsurprising that Aβ oligomers impact NCX and PMCA as well. Existing as three different isoforms with varying tissue-specific expression patterns [263], increased NCX activity has been observed in post-mortem cerebral brain tissue of AD patients [264]. This very well may be a compensatory mechanism to reduce increased levels of cytosolic Ca^{2+} caused by Aβ load. When co-localized with Aβ, NCX isoforms are increased in synaptosomes [265], and overproduction of Aβ promotes calpain-mediated cleavage of isoform NCX3, a regulator

19

protein of Ca^{2+} current during synaptic activation [266, 267]. Despite this, contradictory findings have revealed a downregulation of protein and mRNA levels of NCX2 and NCX3 isoforms in hippocampal CA1 neurons of APP transgenic mice [268]. It is unclear whether there is a brain region-specific difference in NCX expression or if Aβ oligomers affect this Ca^{2+} transporter differently across human and rodent tissue preparations. Treatment with Aβ oligomers, tau, and H_2O_2 have been shown to inhibit the functional activity of PMCAs as well [269, 270].

1.12 ICS in AD Models

1.12.1 Endoplasmic Reticulum and Presenilin Mutations

In addition to the substrate APP, ER presenilin (PS) mutations are commonly incorporated into the genetic makeup of mouse models of familial AD [271]. The inclusion of the PS mutation in these models has been crucial to the progression of Ca^{2+} dyshomeostasis research in AD since a link between PS and Ca^{2+} was first identified in fibroblasts of patients with familial AD (fAD) [272, 273]. This discovery launched many subsequent studies showing PS mutations are linked to increased Ca^{2+} release through 'leaky channels' of the ER in human fibroblast samples, cell culture, and animal models [127, 272, 274-281]. Resting cytosolic Ca^{2+} is elevated in the 3xTg and APP(SWE) transgenic models compared to WT controls; however, this difference is partially attenuated with the application of either an IP_3R blocker or VGCC blocker, but not with a RyR antagonist [282]. One hypothesis to explain increased ER Ca^{2+} release has been that ER Ca^{2+} stores are simply overloaded, hence greater expulsion [277, 283, 284].

Despite findings showing enhanced ER Ca^{2+} stores, many studies have also observed either no changes or even *reductions* in ER Ca^{2+} [285-288]. Nevertheless, previous studies investigating neuronal Ca^{2+} either directly or indirectly in transgenic AD models have often reported increased resting or stimulated cytosolic Ca^{2+} levels compared to WT littermates [281, 289-300]. This, perhaps, implicates PS mutations as participating in perturbed cytosolic Ca^{2+} levels. However, with so many inconsistent outcome measures and the lack of PS mutations in the more common form of AD, sporadic AD (sAD), PS-dependent Ca^{2+} measures cannot be generalized to all AD models. Further, it is important to note that most direct measures of Ca^{2+} in these models were acquired at single time-points, which precludes observing associations between Ca^{2+} and aging. Thus, there is a complication as to whether increased intracellular Ca^{2+} is merely the product of failed ER Ca^{2+} channels, aging, or both.

1.12.2 Endoplasmic Reticulum and IP$_3$R

In an attempt to better understand ER Ca^{2+} release in models of AD, it has been of interest to look at IP$_3$R changes as well. Compared to reductions of IP$_3$R primarily observed in cerebellar and cortical rodent samples, it has been shown that in autopsied human AD patients, IP$_3$R density is significantly reduced in both hippocampus and parietal lobe tissue, while no significant decreases are present in the frontal, occipital, or temporal lobes [301]. Interestingly, in a transgenic model that overexpresses the IP$_3$ receptor regulatory protein IP$_3$K-A three-fold in excitatory hippocampal neurons, presynaptic release probability of evoked responses and miniature excitatory postsynaptic current amplitudes were increased and LTD was inhibited, while novel object recognition and radial arm maze tasks were partially impaired, indicating overcorrections are not always beneficial [302]. This is

surprising, considering previous evidence has indicated IP$_3$K-A is highly involved in synaptic plasticity, as it accumulates in dendritic spines and has critical dual roles in developing and mature synapses [127, 303]. That being said, an increase in resting Ca^{2+} of pyramidal cortical neuron spines and dendrites has been reported in AD transgenic animals [282, 304], suggesting deficits in IP$_3$R may be contributing to synaptic impairments in AD. More evidence is needed to better define the relationship between IP$_3$R and synaptic loss in AD.

1.12.3 CBPs in AD Models

Similar to what has been observed in aging, decreases in calbindin gene expression have been seen in both hippocampus and nucleus basalis of AD human brain samples, suggesting a failed Ca^{2+} buffering mechanism may contribute to dysregulated Ca^{2+} levels as well [305]. Conversely, when either calbindin or calsenilin CBPs are overexpressed in culture, Aβ-induced intracellular Ca^{2+} level elevations are significantly reduced [306-308]. Perhaps reminiscent of early CBP studies, calbindin and parvalbumin proteins in the hippocampus of young (3 mo.) knock-in APPswe/PS1dE9 mice have increased immunoreactivity compared to WT counterparts, suggesting an underlying mechanism to regulate Ca^{2+} and synaptic plasticity in early disease-state [309]. Comparatively, by 12 months of age, calbindin immunoreactivity is significantly reduced, illustrating a threshold for compensation being met and failing, which could contribute to the increased resting Ca^{2+} phenotype commonly observed in APP/PS1 transgenic models. Importantly, in a novel study comparing the classic 5xFAD AD mouse model to a calbindin KO 5xFAD crossbreed (CBKO.5XFAD), the calbindin KO model has significantly greater neuronal loss, reduced NMDA receptor density, and decreased synaptophysin in the subiculum,

further highlighting the need for a robust Ca^{2+} buffering system in maintenance of synaptic strength [310]. Failure of neuronal Ca^{2+} buffering in AD likely enhances widespread impact to overall cell health and network communication.

1.12.4 Mitochondrial Changes in AD

Considering the dire nature of regulated mitochondrial function in providing optimal bioenergetics for cell health, it comes with little surprise that impaired mitochondrial function in AD results in a cascade of cellular deficiencies and even cell death. With mitochondrial impairment during the progression of AD, the generation of ROS becomes less regulated, and damage to lipid membranes of both internal organelles and the plasma membrane ensues [311]. In fact, in a delicate study examining APP transgenic mice gene profiles before, during, and after the development of amyloid plaque deposits, a compensatory upregulation of mitochondria-specific genes was detected as amyloid plaque deposits progressed [312]. Surely, this can be interpreted as an internal defense mechanism in order to preserve mitochondrial integrity. However, in a disease state like AD, the magnitude of Aβ and tau-induced cellular impairments is likely too great for compensatory mechanisms to override in an attempt to maintain cell integrity.

In models of overexpressed tau protein, decreases in mitochondrial complex I (the largest and most complex enzyme of the electron transport chain), ATP, morphology, fusion/fission proteins, and oxidative stress protection have been noted [313, 314], while increases in free oxygen radicals, synaptic deficits, and cognitive decline are propagated [314, 315]. In fact, point-mutations to induce phosphorylation on various sites of tau has been shown to be impactful to the gravity of mitochondrial damage, further highlighting the extent of biological variability in animal models that genetic mutations influence [315].

23

Additionally, because AD is a complicated disease saturated with etiologies of both Aβ *and* tau tangles, in a study looking at AD-related protein mutations in aged 3xTg transgenic mice, 24 APP and tau-dependent mutations were detected and 1/3 were linked to dysregulated complexes of the oxidative phosphorylation system, synthesis of ATP, and regulation of ROS [316]. Thus, changes in mitochondrial Ca^{2+}, though seemingly minor, can have a devastating impact on many downstream signaling pathways.

1.13 Synaptic Plasticity and Oxidative Stress in Models of AD

As neuronal connectivity and synaptic plasticity impairments are closely linked to cognitive decline, modeling physiologic changes of synaptic deficits in the context of AD pathologies demonstrates the fragility of regulatory cellular mechanisms. Many studies have demonstrated a profound correlation between elevated Aβ and memory impairment [317-320]. However, while decline in synaptic connectivity, rather than neuronal loss, has been suggested to more closely bode cognitive reduction in AD [321], it is interesting to note that in several AD models with overexpressed APP, impaired LTP precedes synaptic loss and neuronal death [322-324]. Moreover, in triple transgenic mice with both tau and amyloid mutations, drastic synaptic deficits (including reduced LTP) have been observed in an age-dependent manner prior to tau and amyloid manifestation [325]. Of interest, while similar results are observed in a double transgenic model of APP and PS1 overexpression, short-term memory is impaired first, followed by long-term months later as amyloid burden worsened [326]. However, in a unique model of only tauopathy (devoid of amyloid or APP mutations), severe impairment in LTP maintenance are observed with aging, which

underscores how tau-like pathologies alone are enough to drastically inhibit synaptic plasticity in AD [327].

While the impact of amyloid and tau on synaptic plasticity is certainly a relevant association to be studied in AD, the link between mitochondrial damage/oxidative stress and synaptic loss is of importance too, as increased ROS is a common hallmark of the AD brain. Strangely, the results of observing the relationship between oxidative stress and synaptic plasticity have been unexpected. Studies have shown that in young transgenic mice with overexpressed intracellular and extracellular superoxide dismutase 1 (SOD-1), an enzyme that reduces oxidative stress, an LTP impairment and memory deficit is observed [328-330]. However, in older mice these phenotypic impairments were not only rescued, but actually improved compared to older WT counterparts and young transgenic mice [331, 332]. Similarly, in a transgenic model of Aβ-induced LTP impairment, both the overexpression of mitochondrial SOD-2 and administration of antioxidant ROS scavenger MitoQ are able to rescue synaptic deficits [319, 333]. Together, this evidence supports previous work suggesting physiologic concentrations of ROS are necessary in synaptic events (such as LTP induction) in both adolescence and aging [334]. It has become a paradox, however, as aging studies have found hydrogen peroxide inhibits LTP in both young and aged animals [331].

Given the growing body of evidence that Aβ proximity to neurons increases neuronal hyperexcitability [335-340] and impairs glutamatergic neurotransmission [341-343], perhaps increased resting Ca^{2+} in AD is to be expected. It is important to note that in addition to studies illustrating an increase in neuronal hyperexcitability when in close proximity to Aβ plaques, others have also shown that soluble Aβ will not only reduce

glutamate reuptake, but promote LTD [344]. Reduction of glutamate reuptake and excess

glutamate remaining in the synaptic cleft, aligns well with the promotion of

hyperexcitability. Bezprozvanny and colleagues have even posited changes in ER Ca^{2+}

stores and handling may be a compensatory mechanism to counterbalance increased

neuronal hyperexcitability and impaired neuronal network activity previously observed in

AD mouse models [257, 304, 335, 345-347]. Given synaptic impairment and loss are so

devastating to functional cognition, maintaining neuronal health integrity during

deleterious conditions caused by Aβ is likely a high priority of many organelles.

1.14 Afterhyperpolarization in AD

As the post-synaptic AHP has historically been shown to be enhanced with aging,

it has been of interest to measure this Ca^{2+}-dependent phenotype in the context of AD as

well, especially considering the observation of elevated Ca^{2+} in response to Aβ load. The

evidence implicating an enhanced AHP alongside increased cytosolic Ca^{2+} in models of

AD have been inconsistent, however, as measuring patch clamp recordings of Wistar rat

cortical tissue sections exposed to low and high concentrations of Aβ has provided

counterintuitive results [347]. Low concentrations of Aβ elevates the amplitude of the AHP

as well as expectedly reduces neuronal excitability. Surprisingly, however, the

administration of high Aβ concentration reduced the AHP amplitude of these neurons and

increased their excitability. Importantly, as the authors speculate, Aβ could be acting on

ion channels in both a time- and concentration-dependent manner, such that internalization

or expression patterns of channels on the plasma membrane are affected. Given AD is a

disease of progressive worsening phenotypes, the inclusion of aging in a physiologic system may offer a broader scope of characterizing the AHP in AD.

Indeed, measures of the AHP over a time course in animal models of AD offers a physiologically relevant modality that single-timepoint studies lack. Similarly, an elevated AHP and reduced neuronal excitability have been characterized in the 5xFAD mouse by 8 months of age compared to WT littermates using the whole-cell patch clamp technique [294]. However, measuring the AHP in non-Tg, PS1KI, 3xTg, and APPSweTauP301L models at 1.5, 6, and 18 months using the same approach has shown an increased AHP by 18 months and only within each respective model, not across genotype [127]. Interestingly, in a recent study by our group looking at the AHP in young (2 mo.) genetically modified 5xFAD mice with slower-developing phenotypes and using the sharp electrode technique, a *reduction* in the AHP amplitude was observed in comparison to WT littermates [348]. Unfortunately, due to a limited number of studies measuring the AHP across aging in models of amyloidogenesis, variance in the genetic makeup, and use of different electrophysiological techniques, more data is needed to sufficiently address the lack of consistencies in prior work.

1.15 Estrogen and Ca^{2+} in AD

Women are more than 1.5-3 times as likely as men to develop Alzheimer's disease [185]. This could be due to the large shift in endogenous hormones that women experience during post-menopause, which downregulates the neuroprotective effect of sex steroids in the brain and their involvement in Aβ accumulation [349-352]. Of interest, estrogen replacement therapy has been shown not only to reduce the incidence of AD in post-

menopausal women [96, 353-357], but also improve cognition in women AD patients as well [358-361]. Thus, the inclusion of sex and estrogen therapies in neuronal Ca^{2+} research is an important consideration that should not be overlooked.

As estrogen therapies have been long thought to possess neuroprotective properties, the accumulating evidence of their effect on Ca^{2+} therapies comes with little surprise. A recent study examined the magnitude of injury that cultured PC12 cells exposed to Aβ endure when treated with the genistein, a phytoestrogen compound. Down-regulation of CaM-CaMKIV signaling pathway protein expression is observed in the genistein treated cells, as well as improved cell rate survival and decreased cell damage [362]. Similarly, genistein has also been shown to prevent Aβ-mediated reductions in Ca^{2+}-dependent protein complexes like PKC pathway activity for neuronal plasticity, generation of ROS, synaptic markers synaptophysin and PSD-95, and NMDAR subunits NR1 and NR2B [363-365]. These findings are not exclusive to one estrogen derivative, however, as the use alpha-ZAL phytoestrogen not only ameliorates Aβ-induced apoptosis, but also prevents the increase of calpain2, a marker indicative of intracellular Ca^{2+} overload [366]. Additionally, the estrogen receptor agonist hesperetin protects against hydrogen peroxide induced oxidative stress and the subsequent rise in cytosolic Ca^{2+} and caspase-3 activity [367]. Beta-estradiol can also mitigate C31-, an APP derivative, mediated increases in VGCC current activity as well [368]. Though the clear link between estrogen and Ca^{2+} processes is robust, the inclusion of an aging component in rodent models would bolster the understanding of their relationship in the progression of AD.

1.16 Divergence between Normal Aging and AD

Undoubtedly, the last 40 years of investigating the role of Ca^{2+} in AD research has been invaluable to understanding the underlying mechanisms of the disease state. As Ca^{2+} is an essential secondary messenger in neuronal function, it comes without surprise that an innumerable amount of evidence has illustrated a role of Ca^{2+} in both normal brain aging and in the pathogenic AD brain. Indeed, altered Ca^{2+} signaling and levels are present in both states. However, a misalignment of outcome measures, as well as inconsistent findings, warrant the question of whether Ca^{2+} dysregulation is the byproduct of aging or a precipitating factor that promotes AD progression.

As aging is the top risk factor for AD development [369-375], perhaps the misalignment of Ca^{2+} dysregulation phenotypes in normal brain aging and AD suggest perturbed Ca^{2+} homeostasis results from a common mechanism that, when altered, diverges normal brain aging and AD. The presence of intra- and extracellular alterations like hyperphosphorylated tau and $A\beta$ in AD may exacerbate Ca^{2+}-dependent alterations through bi-directional interplay, hence the capacity of phenotypes such as $A\beta$ and Ca^{2+} dysregulation to cyclically promote one another. Without the presence of $A\beta$ deposits ubiquitously targeting Ca^{2+} channels, signaling elements, and synaptic plasticity proteins in the normal aged brain, it could be that Ca^{2+} dysregulation is a more linear process that aligns better with aging. However, because AD phenotypes are obviously not present in normal brain aging, it is challenging to accurately characterize the presence and relationship of Ca^{2+} dysregulation in aging proper and AD.

Unfortunately, there have been a limited number of studies that have carefully measured neuronal Ca^{2+} handling progression in alignment with aging. Many of the early

studies investigating the relationship between Ca^{2+} and $A\beta$ were conducted in culture, which may have hindered the consideration of aging on physiological variables. In *in vivo* work (where in-tact physiologic connections are considered), these animal models often have aggressive phenotypes at young ages and subtle underlying phenotypes like neuronal Ca^{2+} handling are veiled by more severe cellular alterations. Clearly there is a relationship between the regulation of Ca^{2+} and $A\beta$, yet culture preparations do not reflect the impact of synaptic deficits on cognitive impairment that is demonstrated in *in vivo* models of aging. Considering synaptic loss and reductions in LTP have been observed prior to $A\beta$ and tau burden, along with the essential role Ca^{2+} plays in synaptic plasticity, it appears that initial and progressive neuronal Ca^{2+} changes require greater attention.

With respect to a paucity of studies exploring neuronal Ca^{2+} handling *ex vivo* across age, the following two studies aimed to accomplish 1) measuring direct and indirect Ca^{2+} before, during, and after amyloidogenesis timepoints, 2) comparing these outcome measures between models of fAD and sAD, and 3) aligning these results with previous evidence of Ca^{2+} dysregulation in normal brain aging and transgenic AD animal models. Because fAD only represents a fraction of total AD cases, the first study looked at Ca^{2+} and Ca^{2+}-dependent processes in an alternative sporadic model of AD that generates unregulated quantities of lipid peroxidation byproduct HNE at a young age to elicit AD-like phenotypes. The second study focused on acquiring the same direct and indirect measures of Ca^{2+} in a genetically altered 5xFAD mouse model that generates AD phenotypes more slowly to better align with aging. Additionally, sex differences were assessed in the latter study. With the inclusion of distinct age time-points in the acquisition of electrophysiological and direct Ca^{2+} imaging measures, a linear relationship between

Ca^{2+} dysregulation, oxidative stress, Aβ, and cognitive impairment could be derived. It was hypothesized that Ca^{2+} dysregulation would be present in each model before the development of Aβ deposit or oxidative stress phenotypes, and progressively worsen with age as Aβ load and ROS increased.

Aldh2$^{-/-}$ mouse colonies were maintained at Queen's University via the lab of B.M. Bennett and shipped to the University of Kentucky in several cohorts. All electrophysiological recordings and Ca^{2+} imaging experiments were performed by A.O. Ghoweri through the guidance of O. Thibault and J.C. Gant. LTP electrophysiological recordings and analyses were conducted by P. Gagolewicz under the guidance of R.D. Andrew and B.M. Bennett. Manuscript writing and editing was established by A.O. Ghoweri, O. Thibault, H.N. Frazier, and B.M. Bennett. The purpose of the following study was to identify a relationship between Ca^{2+} dysregulation and oxidative stress in a mouse model of increased free oxygen radical burden through the knock down of the *ALDH2* gene. In this model of sporadic Alzheimer's disease, early-life elevated levels of oxidative stress lead to severe synaptic deficits, the presence of amyloid deposits, and cognitive decline in a progressive age-dependent manner [376-378]. Oxidative stress is a neuronal marker with the capacity to elicit Ca^{2+} dysregulation, and vice versa, however, while both are present in AD, their relationship during the initiating stage of disease development is poorly understood. As homeostatic Ca^{2+} is necessary for important neuronal processes like action potential signaling and synaptic plasticity, it was of interest to measure Ca^{2+} handling across age in the context of heightened oxidative stress via *ALDH2* knockout. We hope that the novelty of this sporadic AD mouse model helps to broaden the understanding of disease progression beyond the scope of *APP* and *PSEN1* gene mutations that are commonly featured in familial AD models.

CHAPTER 2. NEURONAL CALCIUM IMAGING, EXCITABILITY, AND PLASTICITY CHANGES IN THE ALDH2$^{-/-}$ MOUSE MODEL OF SPORADIC ALZHEIMER'S DISEASE

Adam O. Ghoweri [a], Peter Gagolewicz [b], Hilaree N. Frazier [a], John C. Gant [a], R. David

Andrew [b],

Brian M. Bennett [b], and Olivier Thibault [a]

Pharmacology and Nutritional Sciences University of Kentucky [a]

University of Kentucky Medical Center, UKMC, MS-231; 800 Rose Street, Lexington,

KY 40536

Biomedical and Molecular Sciences and Centre for Neuroscience Studies [b]

Faculty of Health Sciences, Queen's University; Kingston, ON, Canada K7L 3N6

2.1 Abstract

Dysregulated signaling in neurons and astrocytes participates in pathophysiological alterations seen in the Alzheimer's disease brain, including increases in amyloid-β, hyperphosphorylated tau, inflammation, Ca^{2+} dysregulation, and oxidative stress. These are often noted prior to the development of behavioral, cognitive, and non-cognitive deficits. However, the extent to which these pathological changes function together or independently is unclear. Little is known about the temporal relationship between Ca^{2+} dysregulation and oxidative stress, as some reports suggest that dysregulated Ca^{2+} promotes increased formation of ROS, while others support the opposite. Prior work has quantified several key outcome measures associated with oxidative stress in aldehyde dehydrogenase 2 knockout ($Aldh2^{-/-}$) mice, a non-transgenic model of sporadic Alzheimer's disease. Here, we tested the hypothesis that early oxidative stress can promote Ca^{2+} dysregulation across aging by measuring Ca^{2+}-dependent processes using electrophysiological and imaging methods and focusing on the afterhyperpolarization (AHP), synaptic activation, somatic Ca^{2+}, and long-term potentiation in the $Aldh2^{-/-}$ mouse. Our results show a significant age-related decrease in the AHP along with an increase in the slow AHP amplitude in $Aldh2^{-/-}$ animals. Measures of synaptic excitability were unaltered, although significant reductions in long-term potentiation maintenance were noted in the $Aldh2^{-/-}$ animals compared to wild-type. With so few changes in Ca^{2+} and Ca^{2+}-dependent processes in an animal model that shows significant increases in HNE adducts, Aβ, p-tau, and activated caspases across age, the current findings do not support a direct link between neuronal Ca^{2+} dysregulation and uncontrolled oxidative stress.

2.2   Introduction

Alzheimer's disease (AD) is a devastating condition underscored by progressive memory loss and profound reductions in quality of life. Currently, there are no effective disease-modifying pharmaceutical interventions, and those that are available provide only symptomatic relief. It is estimated that 5.4 million Americans currently suffer from AD and this number is projected to grow to 13.8 million individuals by the year 2050 [185]. Moreover, the cost of patient care is cumbersome to society, healthcare providers, and, importantly, the families involved. Although much progress has been made in identifying underlying causes and mechanisms, a treatment for AD, much less a cure, remains elusive.

Several dysregulated intracellular signaling pathways that participate in the development of cognitive, as well as non-cognitive, declines have been described for dementias, including frontotemporal, vascular cognitive impairment, and AD [379-382]. AD has been characterized by several pathological markers including amyloid-β (Aβ) plaque deposition, neurofibrillary tangles, impaired glutamatergic and cholinergic neurotransmission, increased production of inflammatory cytokines and oxidative stress, as well as neuronal Ca^{2+} dysregulation. A number of transgenic animal models have been developed in an attempt to recapitulate these pathological events, with the goal of identifying how they manifest and promote disease progression [383-389]. Perhaps not surprisingly given the complexity and etiology of the disease, few studies have provided clarity regarding the onset of changes and the temporal associations between these pathological events. For example, while there is strong evidence that neuronal Ca^{2+} dysregulation can drive oxidative stress, there is also ample evidence to support the contrary; that is, that oxidative stress can dysregulate Ca^{2+} homeostasis [23, 348, 390-395].

To address this, it is advantageous to determine the exact temporal associations between these markers in an attempt to highlight their role in disease progression [396-400].

Oxidative stress-induced damage is critical in the pathogenesis of AD [401-403]. While this damage also occurs as part of normal aging, it appears significantly increased in the brains of AD patients compared to age-matched elderly controls, suggesting the involvement of additional oxidative factors in AD [404-407]. Oxidative damage can be mediated through lipid peroxidation (LPx), protein and DNA oxidation, decreases in mitochondrial metabolism, and increases in advanced glycation end products [408]. For example, 4-hydroxynonenal (HNE) is a reactive aldehydic byproduct of oxidative stress-induced LPx, and increases in free HNE and HNE protein adducts have been observed in both the brain and cerebral spinal fluid of AD patients [406, 407, 409-412]. Studies have shown that overproduction of HNE can inhibit dephosphorylation of tau, target key mitochondrial enzymes, alter Aβ peptide deposition, mediate cell death, reduce synaptic processes/communication, and impair cognition [376, 413-416]. These findings squarely position HNE as a mediator of cellular damage in oxidative stress, and perhaps also as an initiating factor in AD pathogenesis. Early and widespread manifestation of oxidative stress byproducts in AD patients and in AD animal models precede the development of Aβ plaques, NFTs, and cognitive decline [417-423]. These temporal associations lead to the formulation of the oxidative stress hypothesis of AD [401-403]. While electrophysiological and synaptic structure/function relationships linked to oxidative stress can impact cellular communication and throughput [333, 424-426], the onset of these changes with respect to the manifestation of the phenotype has not been carefully characterized.

While some studies have investigated the association between Ca^{2+} dysregulation and oxidative stress, few labs have directly measured neuronal Ca^{2+} in the presence of rising oxidative stress loads with aging. In the current study, we used an oxidative stress-induced model of age-related cognitive impairment with a gene deletion of ALDH2, an enzyme important for the detoxification of endogenous aldehydes arising from LPx [376-378]. This model presents with marked increases in LPx byproducts (*i.e.* HNE protein adducts) from as early as 3 months of age, followed by age-related increases in Aβ, phosphorylated tau protein (p-tau), and activated caspases, as well as by decreases in synaptic proteins [376]. Moreover, deficits in hippocampus-dependent working and spatial memory tasks, together with reductions in dorsal CA1 dendritic arborization and spine density, are also present in this animal model [376, 377]. The slow, age-driven progression of LPx byproduct accumulation highlights the model's utility and uniqueness in recapitulating AD phenotypes in the context of aging, and therefore represents a valuable model of sporadic AD. Here, we sought to characterize the relationship between neuronal Ca^{2+} dysregulation and oxidative stress in an animal model that overproduces HNE adducts at an early age. We chose specific ages to frame the onset of the histopathology in the model before (1.5 months), soon-after (4 months), and well-after (10 months) AD pathology manifestation. Oregon Green Bapta-1 (OGB-1)-based neuronal Ca^{2+} fluorescence, synaptic and post-synaptic excitability, and long-term potentiation (LTP) changes were characterized to test the hypothesis that early oxidative stress drives Ca^{2+} dysregulation. Only mild alterations in physiological parameters were seen. This result, combined with small changes in Ca^{2+}-dependent processes and LTP, do not support the

proposal that oxidative stress in this model leads to Ca^{2+} dysregulation within CA1 neurons undergoing AD-like dysfunction.

2.3 Methods

2.3.1 Animals

Aldehyde dehydrogenase 2 knockout (*Aldh2*^{-/-}) mice, derived from a C57BL/6J background and generated by a gene-targeting knockout (KO) as previously described [427], were kindly provided by Dr. T. Kawamoto (University of Occupational and Environmental Health, Kitakyushu, Japan). The wild-type (WT) and *Aldh2*^{-/-} cohorts used in the current study were generated by the mating of heterozygotes (obtained by backcrossing *Aldh2*^{-/-} mice with WT C57BL/6J mice for more than 10 generations) and genotyping of the progeny using PCR analysis of genomic DNA (extracted from ear punches) utilizing primers previously reported [428]. This process allowed the generation of age- and gender-matched WT and *Aldh2*^{-/-} littermates. Experimenters were blinded to the genotype of the animals during all data acquisition and throughout analyses.

LTP experiments were conducted on 8-month old animals derived and maintained at Queen's University (Kingston, Ontario, Canada). Young-adult (1.5 months), adult (4 months), and mid-age (10 months) mice were shipped to the University of Kentucky in several cohorts. Each cohort represented animals (male and female *Aldh2*^{-/-} mice and their WT littermates) at a particular age (e.g. 4.5 weeks, 3.5 months, and 9.5 months). As only one animal could be recorded per day, recording for each cohort was staggered across 3-5 weeks. The average age of each cohort was 1.5, 4, and 10 months. Male mice were housed individually while females were paired together. All animals were maintained on a 12 h

on/12 h off light cycle and were fed Teklad Global 18% protein rodent diet *ad libitum*. Routine assessment of animal health was performed by a veterinarian and animals exhibiting signs of morbidity were excluded from the study. Treatment and handling of all animals was in accordance with both university's Institutional Animal Care and Use Committee guidelines.

2.3.2 Intracellular Recordings and Ca^{2+} Imaging

2.3.2.1 Slice Preparation

Mice were anesthetized using inhalable isoflurane (5%) followed by decapitation. Brains were quickly removed and incubated in ice-cold low Ca^{2+}, high magnesium artificial cerebral spinal fluid (ACSF): (in mM) 114 NaCl, 3 KCl, 10 glucose, 1.25 KH_2PO_4, 26 $NaHCO_3$, 0.096 $CaCl_2$ anhydrous, and 7.98 $MgCl_2$ anhydrous. Slices (350 µm thick) from the dorsal hippocampus were sectioned using a Vibratome® 3000 (TPI; St. Louis, MO) and incubated for at least 2 hours at 32°C in a humidified (95% O_2 – 5% CO_2) interface-type chamber in normal Ca^{2+} ACSF: (in mM) 114 NaCl, 3 KCl, 10 glucose, 1.25 KH_2PO_4, 26 $NaHCO_3$, 2 $CaCl_2$ anhydrous, and 2 $MgCl_2$ anhydrous. Slices were then placed on a net in a heated recording chamber (RC-22C; Warner Instruments, Co., Hamden, CT) at 32°C with a $TC^2Bip/HPRE2$ in-line heating system (Cell Micro Controls; Norfolk, VA) and perfused (above and below the slice) with a continuous flow of oxygenated normal Ca^{2+} ACSF at the rate of 1.5 mL/min. Slices were visualized under a Nikon Eclipse E600FN microscope.

2.3.2.2 Current Clamp Electrophysiology

Sharp electrodes (~80 – 120 MΩ) were pulled from 1.0 mm diameter borosilicate glass capillaries (World Precision Instruments, Inc.; Sarasota, FL) on a Sutter Instruments P80 pipette puller (Novato, CA). Tips were initially backfilled with a bolus of 1.25 mM OGB-1, pH 7.4 (ThermoFisher Scientific, Catalog number: O6806; Waltham, MA). The rest of the electrode was filled with 1 M potassium methyl sulfate ($KMeSO_4$) in 10 mM HEPES. A bipolar stimulating electrode was placed on the Schaffer collaterals (SC) for stimulation (0.1 ms duration) and the sharp electrode was slowly advanced through *stratum pyramidale* of field CA1 to record primary neurons. A stimulator (SD9K, Astro Med Inc., Grass Instruments; Warwick, RI) was used for synaptic activation. Responses were recorded through an AxoClamp-2B amplifier (Molecular Devices LLC.; San Jose, CA) and digitized at ~ 5-10 KHz with a Digidata® 1550B (Molecular Devices LLC.). Data were processed through pClamp (v10.7, Molecular Devices LLC.). While other cell types, including interneurons and astrocytes, are present in field CA1, compactness of the pyramidal layer, morphology of the cell imaged, and spiking properties of the cell were used to limit our recordings to only primary pyramidal neurons.

2.3.2.3 Afterhyperpolarization (AHP)

For measures of post-synaptic excitability, cells were held at -65 mV and action potential (AP) threshold was set to -55 mV. Four AP bursts were evoked (depolarizing 150 ms current injection) to generate the Ca^{2+}-dependent AHP every 30 s for 5 min. Three measures of the AHP were quantified: the medium AHP (mAHP), the slow AHP (sAHP), and the AHP duration. The mAHP was defined as the peak hyperpolarization observed immediately after the end of current injection. The sAHP was measured as the change in

amplitude at 800 ms post-current injection compared to baseline. Quantification of the AHP duration was defined as the time between peak amplitude of the AHP and the return to baseline. We report data on 12 neurons/8 mice (1.5 months), 11 neurons/8 mice (4 months), and 11 neurons/7 mice (10 months) in the WT dataset, and on 17 neurons/15 mice (1.5 months), 9 neurons/7 mice (4 months), and 13 neurons/6 mice (10 months) in the *Aldh2*$^{-/-}$ dataset.

2.3.2.4 *Input/Output* (*I/O*) Curves

For measures of synaptic excitability, cells were held at -70 mV and stimulated every 10 s. Excitatory post-synaptic potential (EPSP) amplitudes were measured from an increasing series of activation voltages. Amplitudes were used to determine the threshold for an AP and then plotted to generate *I/O* curves and their slopes. We report on data from 10 neurons/7 mice (1.5 months), 10 neurons/8 mice (4 months), and 11 neurons/7 mice (10 months) in the WT dataset, and 16 neurons/15 mice (1.5 months), 8 neurons/6 mice (4 months), and 11 neurons/6 mice (10 months) in the *Aldh2*$^{-/-}$ dataset.

2.3.2.5 Repeated Synaptic Stimulation

Synaptic stimulation intensity during repeated synaptic stimulation (RSS; 10 s, 7 Hz) was set at the threshold for an AP. Outcome measures included synaptic hyperpolarization and EPSP facilitation in relation to the first EPSP (baseline) in the train. Synaptic hyperpolarization was measured as the mean peak hyperpolarization amplitudes following the 6th through 9th EPSPs. The growth of the EPSP during the train was measured early (EPSPs 6 through 9) and late (last four EPSPs) during RSS. We report on data from 10 neurons/7 mice (1.5 months), 10 neurons/8 mice (4 months), and 11 neurons/7 mice (10

months) in the WT dataset, and 15 neurons/14 mice (1.5 months), 8 neurons/6 mice (4 months), and 11 neurons/6 mice (10 months) in the $Aldh2^{-/-}$ dataset.

2.3.2.6 Ca^{2+} Imaging

Cells were visualized under a 40x objective using a filter cube (Ex: 470/40 nm; Em: 525/50; Dichroic 495 nm; Chroma Technology Corp.; Bellows Falls, VT). Imaging Workbench (INDEC BioSystems; Los Altos, CA) was used to quantify signals. A Lambda DG-4 (Sutter Instruments; Novato, CA) was used as a source to activate the fluorophore with exposures in the range of 250-800 ms, depending on the depth of the cell imaged. OGB-1 dye was allowed to diffuse from the tip of the recording electrode for 10-15 min prior to initiation of Ca^{2+} imaging experiments. A photometrics camera (Teledyne Photometrics; Tucson, AZ) was used to image Ca^{2+} fluorescence and kinetics. Two regions of interest (ROI) were created: one around the cell body and another of similar size in tissue adjacent to the imaged cell. Background subtraction and normalization to baseline ($\Delta F/F\%$) were used during analysis of OGB-1 signal. For quantification of resting fluorescence, values were averaged before RSS and normalized to the depth of the recorded cell. Outcome measures included rise time, peak amplitude, decay time, and area-under-the-curve (AUC) ($\Delta F/F \%*s$) during RSS and were derived using ClampFit (Molecular Devices LLC.; San Jose, CA) and SigmaPlot (Systat Software, Inc.; San Jose, CA). Data reported here were taken from 8 neurons/7 mice (1.5 months), 7 neurons/5 mice (4 months), and 9 neurons/6 mice (10 months) for the WT dataset, and 8 neurons/8 mice (1.5 months), 6 neurons/5 mice (4 months), and 11 neurons/6 mice (10 months) for the $Aldh2^{-/-}$ dataset.

2.3.2.7 Cell Health and Exclusion Criteria

Only neurons that fit the following criteria were included in this study: input resistance $\geq$ 30 MΩ, holding current $\leq$ than -350 pA, and AP peak $\geq$ 0 mV. If the number of APs during RSS was greater than two standard deviations (SD) from the mean, the cell was deemed an outlier and removed from the analysis. A summary of these values is reported in Table 1.

2.3.3 LTP Induction and Measures

2.3.3.1 Slice Preparation

Hemi-brain slices from the dorsal hippocampus were obtained from male KO and WT mice at 8 months of age. Animals were sacrificed by decapitation, and the brain was rapidly extracted and transferred into a slicing chamber containing ice-cold ACSF ([in mM] 124 NaCl, 26.2 NaHCO$_3$, 4.4 KCl, 1.3 MgSO$_4$, 1 NaH$_2$PO$_4$, 2.5 CaCl$_2$, 10 glucose, and 19.7 mannitol; pH 7.3-7.4) saturated with carbogen (95% O$_2$/ 5% CO$_2$). The brain was split into two hemispheres using a scalpel and sectioned into 400 μm transverse slices using a vibratome (Leica VT1200s; Leica Microsystems, Concord, ON). Slices were then transferred into a submerged incubation chamber filled with ACSF, continuously bubbled with carbogen, maintained at 33.5°C, and allowed to recover for 2 hours prior to recording.

2.3.3.2 Extracellular Recordings

Following incubation, each slice was transferred into a submersion-type recording chamber maintained at 32°C and continuously perfused with carbogen-saturated ACSF at a rate of 2-3 mL/min. A concentric bipolar stimulating electrode (Rhodes Medical instruments, Catalog Number SNE-100X; Tujunga, CA) was placed in the SC fibers, while a glass recording electrode (tip resistance 1-2 MΩ) containing ACSF was placed within the

stratum radiatum of area CA1 of the dorsal hippocampus. Stimulation (0.1 ms duration) was delivered by an electrode connected to a stimulus isolation unit (FE180 Stimulus Isolator; AD Instruments, Colorado Springs, CO, USA) providing a constant current output. The field postsynaptic potentials (fPSPs) in CA1 were recorded with glass electrodes referenced against an Ag/AgCl pellet in the recording chamber bath. The recording electrode was connected to an Axopatch-200A amplifier (Molecular Devices LLC.) and A/D converter (PowerLab 4/35 running v8 LabChart; AD Instruments), allowing the signal to be filtered (low pass at 1 kHZ), digitized (10 kHz), and stored for offline analysis. The signal was additionally conditioned online using the Hum Bug (Quest Scientific, Vancouver, BC).

2.3.3.3 *I/O* Curves

I/O curves were established by stimulating the SC at increasing intensities (0.5-2.0mA in 0.1mA increments). Data reported here were taken from 15 WT and 10 *Aldh2*$^{-/-}$ mice (an error was made saving the data resulting in the loss of one observation point). Based on these curves, a stimulation intensity yielding ~50-60% of the maximal fPSP amplitude was used for baseline and LTP induction recording.

2.3.3.4 LTP Induction

Data reported here were taken from 15 WT and 11 *Aldh2*$^{-/-}$ mice. Hippocampal fPSPs (every 30 s) were recorded until 30 min of stable baseline was achieved ($\leq$ 10% difference between successive data points for fPSPs, averaged over 5 min epochs). Subsequently, high frequency stimulation (HFS) consisting of 100 single pulses (0.1 ms at 100 Hz) per burst (pulse intensity as determined above) was delivered to the SC fibers.

Two trains of HFS were delivered in total, with 30 s between trains. Hippocampal fPSPs were recorded for 60 min following the second HFS episode.

2.3.3.5 Statistical Analyses

Electrophysiological and imaging data were tested for significance on main effects of age and genotype using two-way ANOVAs (SigmaPlot; Systat Software, Inc.; San Jose, CA). Sex differences using three-way ANOVAs (SigmaPlot; Systat Software, Inc.; San Jose, CA) were also investigated, but are not reported here (see results). Two-way repeated measures mixed ANOVAs (GraphPad Prism 8) were used to determine differences in the extent of LTP in WT and *Aldh2*$^{-/-}$ mice. Greenhouse-Geisser corrections were applied where appropriate. Student's *t*-tests (unpaired) were used to investigate LTP maintenance 40-60 min after induction. For all LTP experiments, only one recording was obtained per animal. A p value of < 0.05 was considered to be significant for all measures. All data are reported as means ± standard error of the mean (SEM).

2.4   Results

Previous work using *Aldh2*$^{-/-}$ mice has shown little evidence of sex differences in this KO model [376, 429]. Because statistical significance was quantitatively consistent across the variables measured irrespective of the inclusion of sex, and because of the low number of recorded/imaged cells in some groups, sexes were combined for measures of Ca^{2+} and both pre- and post-synaptic excitability (Figures 2.1-4). Nevertheless, we present ANOVA results on key outcome measures either with sex combined or separated by sex. LTP measures were only conducted in male WT and KO mice (Figure 2.5).

2.4.1 Neuronal Health Measures

Table 2.1 shows outcome measures describing neuronal health during electrophysiological recordings and Ca^{2+} imaging experiments. Resting fluorescence normalized to cell depth showed no differences across age or genotype ($p > 0.05$). Input resistance and AP amplitude were unaltered across aging and genotype ($p > 0.05$). A significant main effect of aging was observed on holding current measures ($F_{(2,74)} = 5.288$, $p < 0.01$; two-way ANOVA), however, post hoc analysis revealed this was only present in the WT group (WT $p = 0.025$, *Aldh2*$^{-/-}$ $p > 0.05$). Additionally, a significant main effect of aging was present in the number of APs elicited during imaging across both genotypes ($F_{(2,48)} = 17.756$, $p < 0.001$; two-way ANOVA). While the number of APs at 4 months was significantly higher (stimulation setting error), this had no noticeable impact on Ca^{2+} levels (Figures 4E and 4F). In fact, normalization of AUC data to the number of action potentials triggered during activation did not alter outcomes (*i.e.* no significant change in Ca^{2+} with age or genotype; *data not shown*).

Table 2.1. Measures of Neuronal Health and Resting Fluorescence.

Genotype	Age (months)	Holding Current (pA)	Input Resistance (MΩ)	Action Potential Amplitude (mV)	# of Action Potentials	Resting Fluorescence (ΔF/F)
WT	1.5	-83.3 ± 25.4	67.0 ± 5.4	12.8 ± 1.7	69.9 ± 0.1	68.6 ± 20.2
	4	-182.5 ± 21.3	63.0 ± 3.3	7.3 ± 1.6	75.6 ± 0.4	51.0 ± 17.5
	10	-152.7 ± 36.2	55.8 ± 4.7	11.4 ± 1.6	70.2 ± 1.3	79.2 ± 19.7
$Aldh2^{-/-}$	1.5	-105.6 ± 21.2	65.3 ± 4.6	11.3 ± 1.4	70.0 ± 0	73.3 ± 27.9
	4	-167.8 ± 29.6	55.2 ± 4.4	9.9 ± 1.5	76.0 ± 0	63.9 ± 23.6
	10	-143.8 ± 20.1	68.1 ± 4.3	7.5 ± 1.1	70.5 ± 1.5	105.8 ± 24.0
Significance	-	*$p < 0.01$	n.s.	n.s.	*$p < 0.001$	n.s.

Table 2.1. Measures of Neuronal Health and Resting Fluorescence. Properties of neuronal health were compared across age and genotype. Holding current and input resistance measures reflect plasma membrane integrity and "leakiness." Additionally, action potential amplitude during AHP data acquisition and the number of action potentials during Ca^{2+} imaging are reported. Resting fluorescence was normalized to the depth of each cell imaged. While a significant aging effect on holding current was seen from 1.5 to 4 months ($p < 0.01$), this was only present within the WT group. A main effect of age on the number of action potentials triggered during imaging was seen ($p < 0.001$), however this did not have an impact on Ca^{2+} (see results). Asterisks (*) represent significant main effect of age. Numbers represent means ± SEM and "n.s." indicates non-significance.

2.4.2 Post-Synaptic Excitability Changes (AHP)

We characterized the Ca^{2+}-dependent AHP in WT and *Aldh2*$^{-/-}$ animals across age (Figure 2.1A) and identified a significant age-dependent reduction in the amplitude of both the mAHP (Figure 2.1B; $F_{(2,74)} = 4.391$, $p < 0.02$; two-way ANOVA) and sAHP (Figure 2.1C; $F_{(2,74)} = 5.050$, $p < 0.01$; two-way ANOVA). A slightly larger sAHP was also present in the *Aldh2*$^{-/-}$ group, highlighted by a main genotype effect ($F_{(2,74)} = 4.765$, $p < 0.04$; two-way ANOVA). Despite these observations, the AHP duration remained unaltered (Figure 2.1D; $p > 0.05$). Of interest, a main effect of sex was also observed in the mAHP ($F_{(2,74)} = 4.141$, $p < 0.05$; three-way ANOVA) in which female mice displayed an overall reduction in AHP amplitude irrespective of genotype (*data not shown*). No significant sex differences were present in the sAHP or AHP duration ($p > 0.05$). These findings suggest that a reduction in the AHP seems to develop with age in this animal model irrespective of genotype. Interestingly, our lab has previously shown that in 14 month old APP/PS1 mice, a reduction in L-VGCC density is seen in CA1 neurons when compared to WT [242]. These results differ from those seen in aging rats and rabbits where significant *increases* in Ca^{2+}-mediated processes (including the AHP) are typically observed [2, 8, 9]. Perhaps this divergence is reflective of the particular genetic background in the *Aldh2*$^{-/-}$ model, and highlights the nongeneralizable nature of the Ca^{2+} hypothesis of brain aging and dementia.
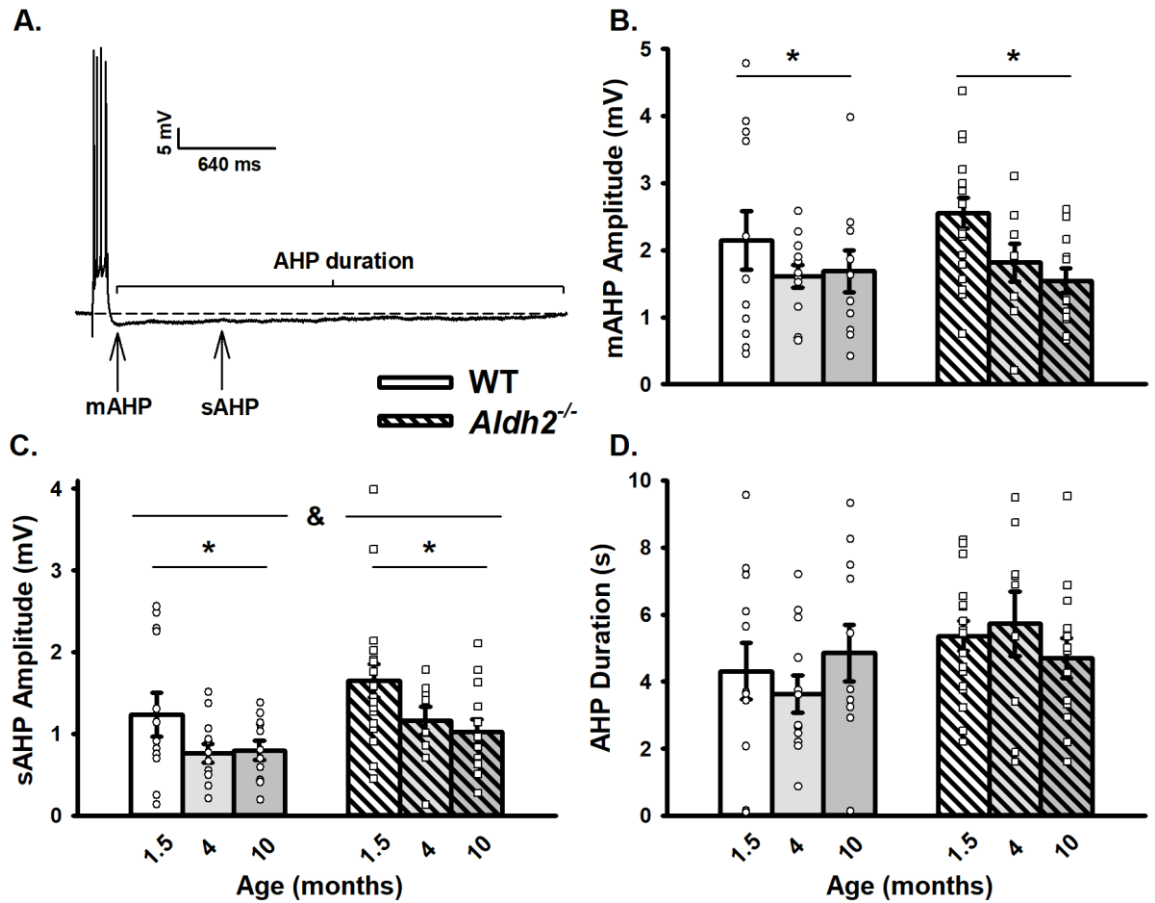
Figure 2.1. AHP in WT and Aldh2-/- Mice Across Age.

A. Representative AHP following post-synaptic depolarization with 4 action potentials. **B.- C.** A main effect of aging ($p < 0.02$) on the mAHP and sAHP was observed within each genotype. A main effect of genotype was also present on the sAHP ($p < 0.04$). **D.** Measures of the AHP duration were unaltered across aging or genotypes. We report data on 12 neurons (1.5 months), 11 neurons (4 months), and 11 neurons (10 months) in the WT dataset, and on 17 neurons (1.5 months), 9 neurons (4 months), and 13 neurons (10 months) in the *Aldh2^-/-* dataset. Asterisks (*) represent significance across aging (above left and right bars) and genotype (top horizontal bar separated by an ampersand) at $p < 0.05$.

2.4.3 Synaptic Excitability

Neuronal synaptic excitability was derived from measures of *I/O* curves (Figure 2.2), as well as from EPSP amplitudes during RSS (Figure 2.3). Given prior work showing significant decreases in synaptophysin (an integral membrane protein of synaptic terminals [376]), and reports of altered dendritic morphology in the *Aldh2$^{-/-}$* mouse, including reduced dendritic length and spine density [377], it is surprising that measures of neuronal excitability (Figure 2.2B) and short-term potentiation (Figures 2.3C-E) were not significantly different across age or genotype ($p > 0.05$). This could reflect the resilience of this mouse model to significant alterations in dendritic morphology, highlight the presence of a successful compensatory mechanism, or provide evidence that physiological activation under relatively low frequencies is spared. Sex differences were also investigated, but no significant differences were detected on either *I/O* or RSS measures ($p > 0.05$; *data not shown*).

2.4.4 Ca^{2+} Imaging

Somatic Ca^{2+} kinetics before, during, and after RSS were compared across genotype and age (Figures 2.4A and 2.4B). No significant alterations in Ca^{2+} handling were seen (Figures 2.4C-F; $p > 0.05$). Given that minor, if any, changes in the AHP were present, these results are perhaps not surprising. Indeed, larger AHPs are often associated with increases in direct/indirect Ca^{2+} measures [11, 97, 106]. Sex differences were not seen on any of the Ca^{2+} measures quantified ($p > 0.05$; *data not shown*).
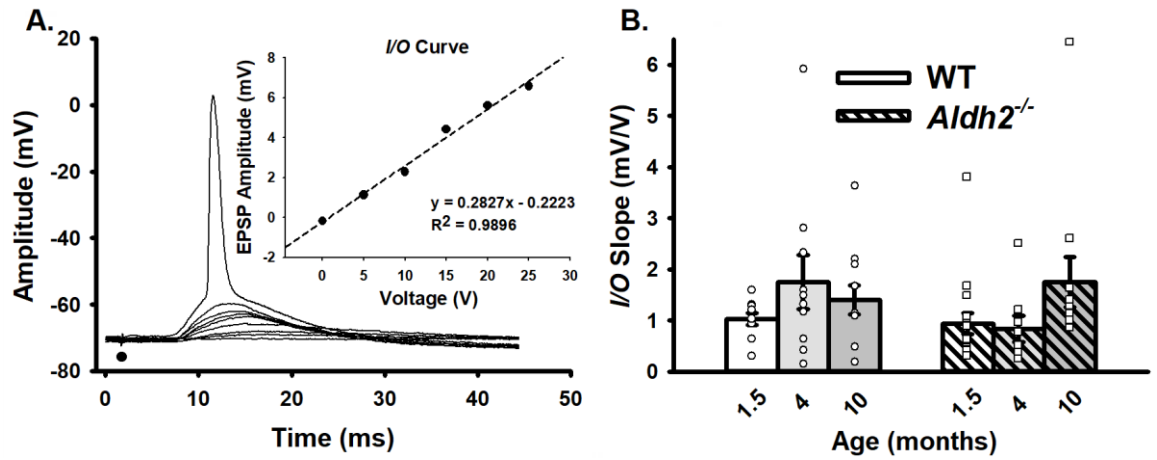
Figure 2.2. Extracellular Synaptic Activation.

A. Example of EPSPs recorded below and at threshold of an action potential. Inset shows *I/O* plot fit from EPSP amplitudes with increasing stimulation intensity. **B.** Synaptic excitability derived from *I/O* measures (slopes). Black dot represents the time at which synaptic stimulation was initiated. We report on data from 10 neurons (1.5 months), 10 neurons (4 months), and 11 neurons (10 months) in the WT dataset, and 16 neurons (1.5 months), 8 neurons (4 months), and 11 neurons (10 months) in the *Aldh2*$^{-/-}$ dataset. Results showed no differences across genotype or age ($p > 0.05$).
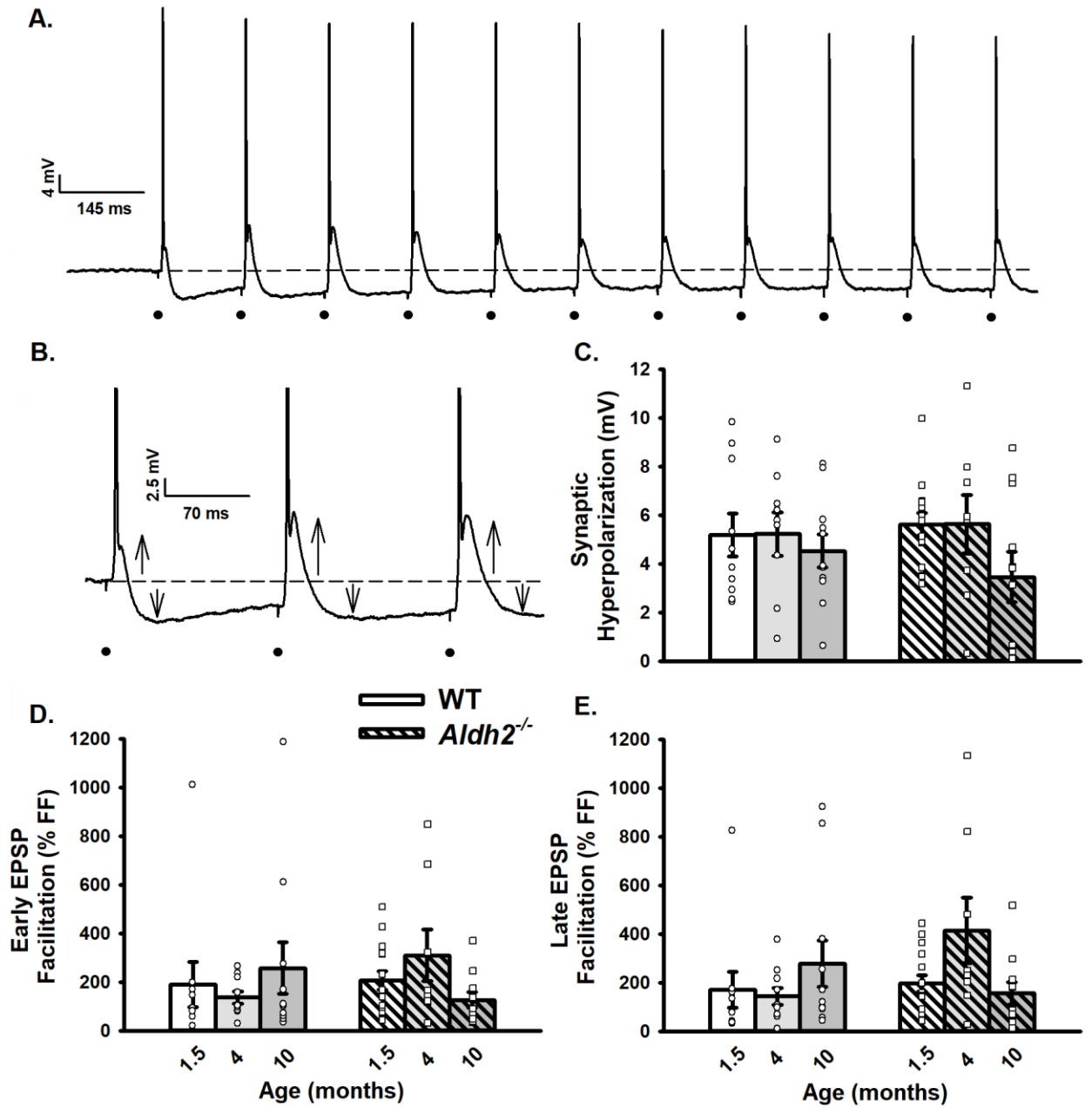
Figure 2.3. Repeated Synaptic Stimulation (RSS).

A. Example of RSS showing EPSP potentiation and synaptic hyperpolarization. **B.** Upward arrows illustrate growth in EPSP amplitude during repeated activation (7 Hz for 10 s), while downward arrows show increased amplitude in the synaptic hyperpolarization. Action potentials were truncated for illustration. **C.-E.** Synaptic hyperpolarization measured during RSS and EPSP facilitation taken during the first (early) and last (late) periods of RSS. Black dots represent the time at which synaptic stimulation was initiated. We report on data from 10 neurons (1.5 months), 10 neurons (4 months), and 11 neurons (10 months) in the WT dataset, and 15 neurons (1.5 months), 8 neurons (4 months), and 11 neurons (10 months) in the *Aldh2$^{-/-}$* dataset. No differences in synaptic hyperpolarization, early EPSP facilitation, or late EPSP facilitation were detected across age or genotype ($p > 0.05$).

A.

B.

Peak Amplitude

Rise Time

Decay Time

Area-Under-the-Curve

ΔF/F (%)

Time (s)

C.

WT

Aldh2$^{-/-}$

Rise Time (s)

D.

Decay Time (s)

E.

Peak Amplitude ΔF/F (%)

Age (months)

F.

AUC ΔF/F (%)*s

Age (months)
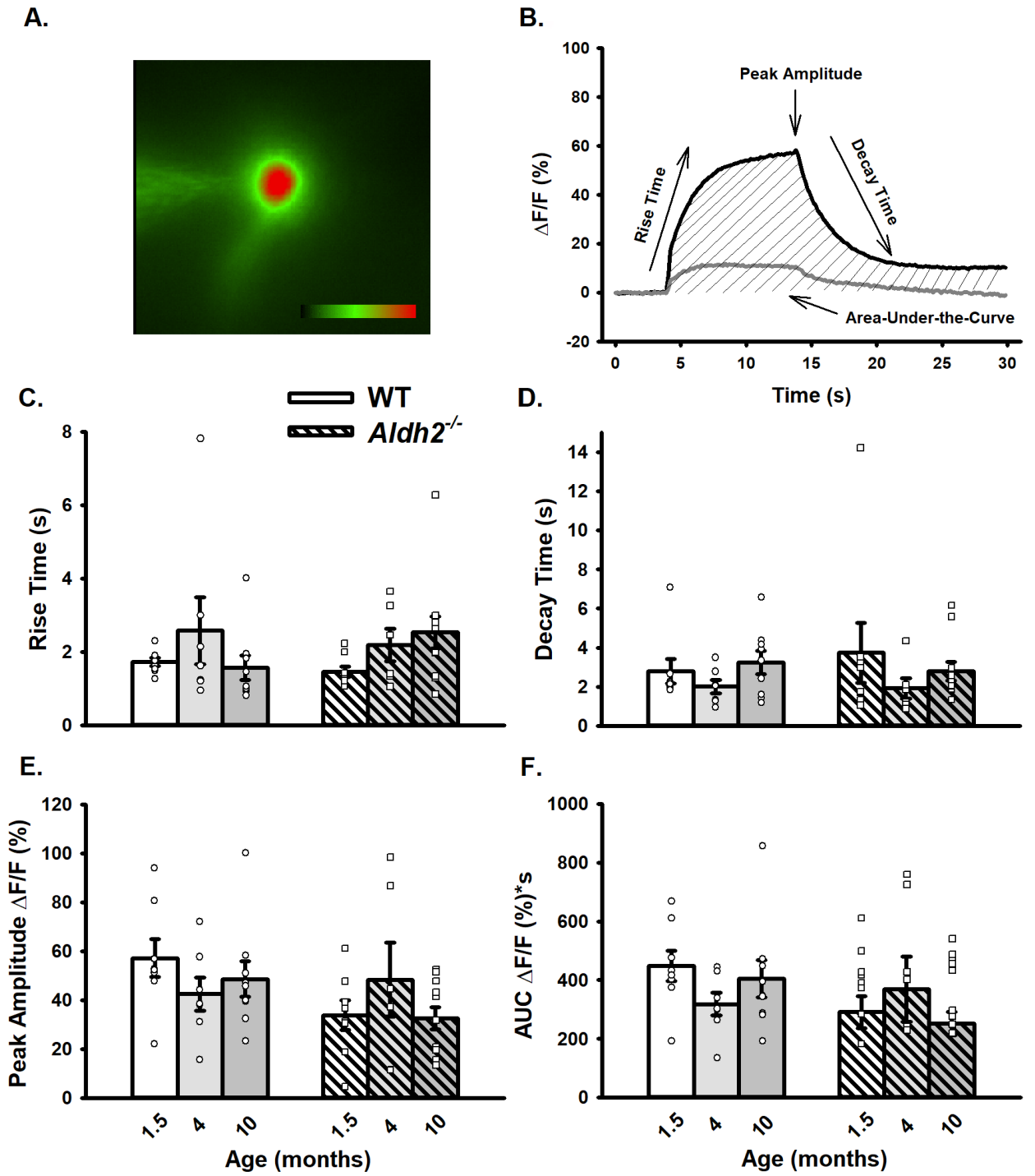
Figure 2.4. Changes in OGB-1 Fluorescence During 10 s RSS.

A. Example of an imaged neuron loaded with OGB-1. **B.** Normalized fluorescence change across time (% ΔF/F) before, during, and after synaptic stimulation in the cellular compartment (dark line) and in the extracellular space adjacent to the cell (gray line). **C.-F.** Measures of Ca^{2+} kinetics (rise and decay time) and somatic Ca^{2+} levels (peak amplitude and AUC). Data reported here were taken from 8 neurons (1.5 months), 7 neurons (4 months), and 9 neurons (10 months) for the WT dataset, and 8 neurons (1.5 months), 6 neurons (4 months), and 11 neurons (10 months) for the *Aldh2$^{-/-}$* dataset. No significant differences across age or genotype were detected (p > 0.05).

2.4.5 Long-term Synaptic Plasticity Changes

The slope of fPSPs recorded in dorsal CA1 of WT and *Aldh2*$^{-/-}$ mice increased with higher stimulation intensities ($F_{(1.827, 42.02)}$ = 166.2, p < 0.0001; two-way repeated measures mixed ANOVA); however, no significant effects were noted (Figure 2.5A; p > 0.05), highlighting a lack of difference in excitability between the two groups. LTP changes were measured following a robust LTP induction protocol in a subset of mid-age (8 months) male mice. While no main effect of genotype was detected on measures of fPSP slopes across the multiple phases of LTP induction and maintenance (Figure 2.5B; p > 0.05), analysis of the data during the maintenance phase of LTP (the last 20 min) revealed a significant genotype effect with greater fPSP slopes in WT (201 ± 5%) compared to *Aldh2*$^{-/-}$ mice (180 ± 5%; t = 16.84, p < 0.0001; unpaired *t*-test). Perhaps the use of a strong protocol for LTP induction (2X 100 Hz) masked differences in the initial phases of the potentiation.
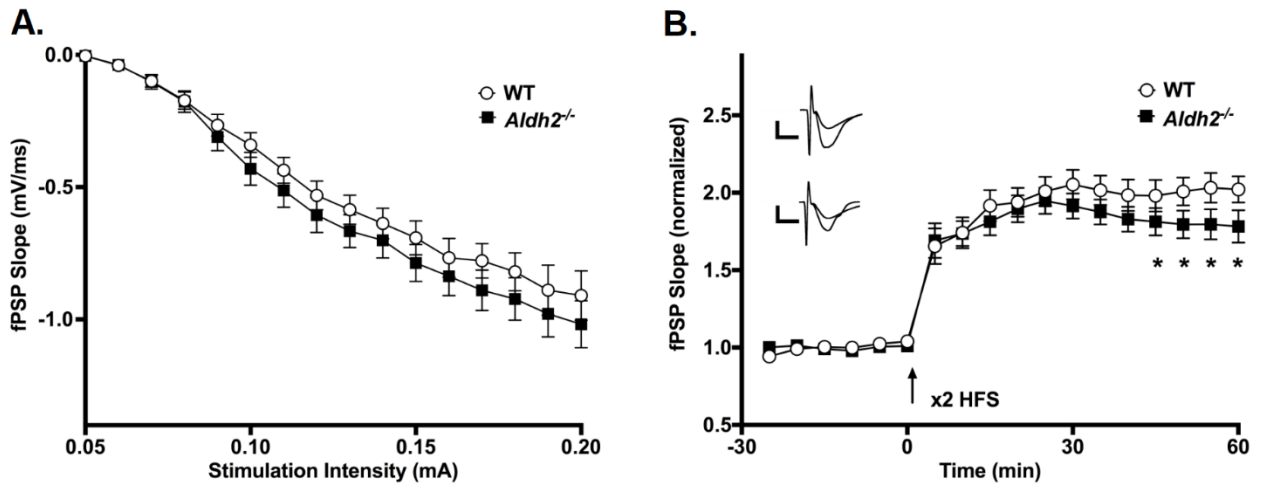
Figure 2.5. LTP Outcomes.

A. *I/O* curves for fPSP slopes (mV/ms; mean ± SEM) elicited in CA1 by single pulse stimulation of the SC in WT and *Aldh2*^{-/-} mice. The fPSP slope increased with higher stimulation intensities, but no statistical differences between the two groups were detected ($p > 0.05$). **B.** fPSP slope (mV/ms; mean ± SEM; normalized to baseline) before and after HFS (arrow) in WT and *Aldh2*^{-/-} mice. Delivery of HFS reliably increased the fPSP slope, however no main effect of genotype was detected ($p > 0.05$). Data reported here were taken from 15 WT and 11 *Aldh2*^{-/-} mice for LTP induction and 15 WT and 10 *Aldh2*^{-/-} mice for *I/O* curves. Analysis of the maintenance phase of LTP (the last 20 min) revealed a significant genotype effect with somewhat reduced potentiation in the *Aldh2*^{-/-} animals ($t = 16.84$, $p < 0.0001$; unpaired *t*-test). Asterisks (*) represent significant group fPSP slope differences at specific time points (*t*-test) at $p < 0.05$. Insets depict typical fPSP before (smaller downward deflection) and after (larger downward deflection) HFS in WT (top) and *Aldh2*^{-/-} mice (bottom; calibration is 0.5 mV and 5 ms).

58

2.5   Discussion

Measures of Ca^{2+}-dependent potentials in single neurons are a historically-reliable method of indirectly detecting alterations to Ca^{2+} homeostasis. Indeed, changes in the AHP with aging reflect Ca^{2+} channel density and function, as well as Ca^{2+} buffering and signaling [80, 97, 103, 161, 430]. In this study, we measured Ca^{2+}-related processes in *Aldh2*^{-/-} and WT mice at different ages in order to draw temporal associations between dysregulated Ca^{2+} and age-mediated increases in oxidative stress byproducts. Based on previous literature thoroughly characterizing the onset of both behavioral and cellular biomarkers, we hypothesized that in this sporadic model of AD with uncontrolled oxidative stress, early oxidative stress could promote Ca^{2+} dysregulation. To our surprise, however, Ca^{2+}-dependent processes were largely unaltered. Further, while age-dependent reductions in the mAHP and sAHP were present, alterations in synaptic processes (both short-term and long-term), as well as Ca^{2+} kinetics, remained relatively unchanged. However, we did note the presence of a small, albeit significant, reduction in LTP maintenance in the *Aldh2*^{-/-} animals compared to WT.

In this animal model, behavioral deficits are present as early as 3.5 (novel object recognition and Y-maze) or 6 months of age (Morris water maze) [376]. Aβ and p-tau accumulation is significant by 6 months, while HNE adducts and several caspases are clearly elevated by 3 months when compared to controls. Our analysis of Ca^{2+}-dependent processes at early time-points (1.5-4 months) does demonstrate a significant reduction in the mAHP and sAHP. However, given that the mAHP and sAHP were reduced in both the WT *and* the *Aldh2*^{-/-} groups with age, we cannot dissociate the effect of aging from that of the genetic manipulation. While there has been some evidence of genotype-mediated

reductions in Ca^{2+} processes in animal models of AD [242, 348], it is surprising that a significant age-dependent *reduction* in the AHP was present here. Given the importance of the genetic backgrounds in animal models and their impact on physiological processes [431-435], it is likely that this particular mouse model, irrespective of the ALDH2 manipulation, presents with a reduction in the AHP across age, thus reflecting on the non-generalizable nature of neuronal Ca^{2+} dysregulation with age across AD models. Previous work from different labs has reported no loss of hippocampal neurons as well as similar levels of synaptic proteins in behaviorally-impaired aged animals compared to young counterparts [432, 433, 436]. Perhaps the mechanism underlying the age-dependent reduction in the AHP presented here in both the WT and *Aldh2$^{-/-}$* groups is dependent on the genetic background of the animals, and may highlight an increase in the resilience of the animal to the impact of elevated HNE adducts. Overall, however, it does not appear that the presence of a greater LPx burden specifically *induces* Ca^{2+} dysregulation. While the electrophysiological phenotype and outcome measures were only minimally affected, several potential mechanisms are discussed.

Firstly, in the current study, animals may not have been exposed to sufficient cumulative oxidative stress to alter neurophysiological properties. No electrophysiological studies investigating the *Aldh2$^{-/-}$* mouse at more mature ages (*i.e.,* 18 months) have been published. Nevertheless, evidence from other models of AD does suggest a worsening of the phenotype with age. Indeed, while there is a paucity of aging studies characterizing Ca^{2+}-mediated AD phenotypes at much later ages, a significant age-dependent increase in hippocampal L-VGCC density and AHP amplitude has been reported in transgenic AD mouse models at 12-18 months of age [127, 241]. Given that our work specifically

addresses alterations in Ca^{2+} homeostasis in a sporadic model of AD, it is not clear how these changes align with prior literature that has commonly used transgenic models of familial AD. Thus, it is possible that the *Aldh2$^{-/-}$* mouse presents with mild electrophysiological alterations during early to mid-life that worsen with more advanced age. Alternatively, the use of a '2-hit' model could unmask more robust changes at a younger age in this particular model, as previous evidence has demonstrated the effectiveness of using a secondary insult in models of traumatic brain injury (TBI), Parkinson's disease, and even schizophrenia to detect complex or less-sensitive processes [437-440]. In fact, a previous study using this animal model in combination with mild (TBI) recently reported significant increases in inflammatory cytokines, as well as sustained cognitive deficits, when compared to sham controls [441]. In this work, administration of anti-inflammatory agents post-TBI ameliorated both inflammatory and cognitive impairments of the *Aldh2$^{-/-}$* mice.

Moreover, reports conducted in the dorsal hippocampus of *Aldh2$^{-/-}$* mice have highlighted morphological changes in this area only, with no alterations detected in the ventral hippocampus or primary sensory cortex [377], suggesting that the impact of oxidative stress may be region-selective. In this animal model, the dissociation between the poor behavioral phenotype and the paucity of Ca^{2+}-mediated electrophysiological changes in the hippocampus support the notion that brain regions other than the hippocampus can also participate in the encoding, storing, and recalling of memory processes [442-446]. Further, the location of the K_{Ca} AHP channels is important to consider. K_{Ca} channels, which are critical to neuronal repolarization and the AHP, have been mostly identified in the somatodendritic region of pyramidal neurons [447-451].

Thus, it is possible that recordings of mostly somatic potentials using the sharp electrode technique did not permit identification of synaptic changes in dendritic spines or finer processes negatively impacted in the *Aldh2$^{-/-}$* model [377]. Finally, the possibility that the genetic manipulation may have induced a series of compensatory cellular events including increases in Ca^{2+} buffering, mitochondrial metabolism, or changes in the location and density of Ca^{2+} or K^+ channels, should be considered. Future studies investigating these potential mechanisms are clearly needed.

With respect to the small, albeit significant, reduction in LTP in the *Aldh2$^{-/-}$* mouse, it is possible that the robust induction protocol used here may have thwarted more subtle differences in synaptic plasticity. Previous evidence has shown that age-related deficits in LTP induction were only seen when less robust (perithreshold) stimulation protocols were used [51, 452-455]. Future studies investigating Ca^{2+} dysregulation across different cell types and brain regions at more advanced ages in this animal model should be initiated to better characterize the potential impact of oxidative stress on behavioral outcomes. In summary, with so few changes in Ca^{2+} and Ca^{2+}-dependent processes detected in an animal model with significant increases in HNE adducts, Aβ, p-tau, and activated caspases across age, the current findings do not support a direct link between neuronal Ca^{2+} dysregulation and uncontrolled oxidative stress.

2.6 Acknowledgments

2.7 Conflict of Interest/Disclosure Statement

The authors have no conflict of interest to report.

CHAPTER 3. THE SPORADIC AND FAMILIAL AD MOUSE MODELS

3.1   Aldh2$^{-/-}$ Study Results

The work in **Chapter 2** explored the utility of a nontraditional model of sporadic AD (sAD), the *Aldh2$^{-/-}$* mouse, as a way of further characterizing the relationship between oxidative stress and Ca^{2+} dysregulation with aging. Previous evidence has shown that in the *Aldh2$^{-/-}$* mouse model, knockdown of the *ALDH2* gene elicits a significant accumulation of lipid peroxidation byproduct 4-hydroxynonenal (HNE) by 3 months of age and remains elevated throughout life [376]. This early elevation of HNE warrants a progressive increase in phosphorylated tau, Aβ, and caspases 3 and 6, while concurrently reducing synaptic strength markers synaptophysin, total CREB, and PSD-95. Additionally, considering the wealth of literature supporting the proposal that HNE has a role as an initiating factor in AD pathogenesis [406, 407, 410, 411, 456-459], as well as the observation of an impaired performance in learning and memory tasks by 6 months of age [376], the *Aldh2$^{-/-}$* mouse is positioned as a unique model for studying AD-like pathology without the genetic manipulation of *APP* or *PSEN* genes. Despite a wide range of phenotypes characterized in the *Aldh2$^{-/-}$* mouse model, a lack of reporting on direct and indirect neuronal Ca^{2+} markers was apparent. Thus, in collaboration with Queen's University, we sought to characterize measures of neuronal Ca^{2+} handling in alignment with similar ages previously studied.

The relationship between Ca^{2+} dysregulation and oxidative stress in aging and AD is complicated, as each have been proposed as initiating elements in AD pathogenesis while also having been shown to promote one another when one is increased [460-466]. Indeed, if oxidative stress propagates the dysregulation of Ca^{2+} then the knockdown of the

regulatory *ALDH2* gene from birth would ideally result in changes pertaining to Ca^{2+} and Ca^{2+}-mediated processes. However, much to our surprise, few changes in Ca^{2+} handling were detected as the animals aged. Given both Aβ and phosphorylated tau are present in *Aldh2^{-/-}* mice [376] and that a recent morphometric characterization of this model has shown deleterious alterations to the dendritic morphology of dorsal and ventral CA1 pyramidal neurons [376, 377], it is difficult to address the lack of Ca^{2+} changes here. Even if this was evidence to disprove a relationship between oxidative stress and Ca^{2+} dysregulation, surely the well-documented ties between Ca^{2+} and Aβ [218, 220, 221], Ca^{2+} and phosphorylated tau [467-469], and Ca^{2+} and synaptic dysfunction [55, 56, 165] would have manifested into a Ca^{2+}-related alteration of some capacity. Perhaps a compensatory alteration of Ca^{2+} binding proteins or plasma membrane/ER Ca^{2+} channel density or function could explain the lack of Ca^{2+} changes, but only additional experimentation can truly address this. Additional insights regarding the lack of Ca^{2+} alterations are discussed in **Chapter 2.5**. Nevertheless, these findings underscore a lack of consistency in aging and AD models' phenotypic expression as mentioned in **Chapter 1**, highlight the complexity of AD progression, and emphasize the necessity of using a wide range of models to elucidate underlying mechanisms of AD development and pathogenesis.

3.2   Mouse Models of AD

3.2.1 The Utility of Mouse Models

Since the synthesis of the first transgenic mouse model by virologist Rudolph Jaenisch in 1974 [470], the use of genetically modified animals in basic research has

radically changed how scientists study disease states. Transgenic mouse models are typically developed through the introduction of complementary DNA with a transgene to the pronucleus of a zygote and then subsequently implanted into a pseudopregnant dam for gestation [471, 472]. Animal research models provide investigators with high throughput information on physiologic measures in controlled environments. Such data is invaluable to identifying biological nuances at molecular, cellular, histological, and behavioral levels. Further, as these are living organisms, intrinsic biological variables such as aging, sex, and circadian rhythm can be measured and accounted for when genetically modifying mice. Homologous genes between rodents and humans can lead to translatability of data that bolster advancements in novel therapeutics. It has been through the utilization of genetically modified mice of AD that researchers have learned more about the precipitation of AD hallmarks during aging and in alignment with physiology. Moreover, the identification of the *APP* and *PSEN* genes and their involvement in AD progression has been instrumental to developing better models that adequately recapitulate AD-like pathology [473-477].

3.2.2 AD-like Pathology in Mouse Models

With over 100 models of AD-like pathology available for commercial use [478], the decision of selecting the right one for experiments can be challenging. Adding to this cumbersome endeavor is the lack of a perfect AD surrogate amongst many established models (*i.e.* it is incredibly difficult and complex to produce rodent offspring with desired genetic modifications that mimic all AD neuropathology) [471, 478]. Thus, generally a mouse model will not exhibit all of the classic hallmarks of AD pathogenesis (Aβ, tau, neurodegeneration such as atrophy and neuronal loss, etc.). Since the development of the

first successful mouse of amyloidogenesis [479], dozens of subsequent models have been designed to mutate the *APP* gene at various sites that recapitulate APP processing through the β- and γ-secretase pathway in a time- and concentration-dependent manner that mimics human AD. Despite this, while low concentrations of hyperphosphorylated tau have been detected in some of these models, characteristic neurofibrillary tangles of human AD are seldom present, if at all [480]. The same can be said for many other models exhibiting tauopathies or neurodegeneration, but other hallmarks like Aβ amyloidosis or neuronal loss may not be present [478]. This has led researchers to investigate alternative methods to recapitulate AD pathology such as viral vector transgenesis through lentivirus and adeno-associated virus techniques [471, 478, 481-483].

3.2.3 Viral Gene Delivery for Modelling AD

Viral gene delivery or transgenesis is an effective tool for eliciting region-specific long-term transgene expression. In AD, amyloid and tau pathologies have been recapitulated in both rat and mouse models using these techniques, although APP mutations have yielded considerably less success in amyloidogenesis [478]. The use of viral transgenesis can be advantageous as it is cheaper than germline modifications, allows for neuronal projection analysis of specific brain regions, and can be used in young or aged animals. However, like using genetic modification, virus gene therapy has drawbacks that limit its application. Limitations such as brain injury from stereotaxic injection, the finite packaging size of a viral vector, and occasional difficulty with genomic integration require important consideration when planning experiments [471, 478]. Nevertheless, the growing optimization of these techniques will surely cultivate novel and safer application methods that promote AD-like pathological progression in animal models in future studies.

3.2.4 Sporadic and Familial AD Mouse Models

As previously mentioned in **Chapter 3.2.2**, the development of many AD mouse models stems from the identification of the *APP* and *PSEN* genes, and the ability to promote amyloidogenesis in a mouse [479]. Importantly, *APP* and *PSEN* are two genes known to promote familial AD (fAD), which represents only 5% of total AD cases, while the remaining 95% are sporadic cases [185]. However, despite this disproportion within total cases, sAD mouse models are less frequently used in research. As environmental, lifestyle, and genetic modifying factors are key components that define sAD, it is important that these aspects are included into a sAD model design. Naturally, these are difficult to recapitulate into a model using a reproducible design that also elicits AD pathology. Though the *Aldh2$^{-/-}$* model in **Chapter 2** may not rely on environmental or lifestyle alterations to warrant AD development and progression, the early generation of lipid peroxidation byproduct HNE and subsequent AD hallmarks without influencing the *APP* or *PSEN* genes positioned the model as being amenable to study.

Despite selecting the *Aldh2$^{-/-}$* mouse for experimentation, it is important to once again note that the perfect AD surrogate has yet to be identified. While a great host of information can be acquired by studying AD through the lens of the *Aldh2$^{-/-}$* model, it too has limitations. For example, like many models, the *Aldh2$^{-/-}$* mouse does not form neurofibrillary tangles, but only concentrations of phosphorylated tau [376]. Considering the well-established evidence that increased neurofibrillary tangle density correlates with reduced cognition in human AD [484-489], a model devoid of true neurofibrillary tangles could be perceived as a shortcoming. Further, Aβ peptides both monomerize and oligomerize in *Aldh2$^{-/-}$* mice, but do not form amyloid deposits [376]. With consideration

of the immense amount of literature highlighted in **Chapter 1** showing Ca^{2+} changes with aging and AD, and the few Ca^{2+} changes observed here, this may be a limitation as well. Nevertheless, alongside increases in HNE, Aβ, and p-tau, the presence of irregularities in synaptic proteins and cognitive impairment support use of this model to study sAD. Irrespective of the *Aldh2*$^{-/-}$ mouse's utility to study sAD, we decided it was of interest to make a direct comparison of our findings to a model of fAD. As many fAD models possess pathological features that are useful markers for studying age-dependent changes in both neuronal and behavioral aspects, we decided to look at similar outcome measures of Ca^{2+} dysregulation in the 5xFAD mouse.

3.3   The 5xFAD Familial Model of AD

The decision to use the 5xFAD mouse in our second study was due to the model's reliable manifestation of many AD-like pathologies in an age-dependent manner. Through genetic manipulation of 3 *APP* and 2 *PSEN1* mutations, 5xFAD mice on a C57BL6 genetic background exhibit extracellular amyloid deposits by 2 months [490], synaptic deficits at 2-3 months [491], and spatial working memory impairment between 3 and 6 months of age [492]. Like many other transgenic fAD models, 5xFAD mice do not develop any neurofibrillary tau tangles during aging. Importantly, only a few studies have reported indirect Ca^{2+}-related changes in the 5xFAD mouse [294, 348, 493, 494]. An increased afterhyperpolarization was noted in 8-month old 5xFAD mice compared to WT using the whole-cell patch clamp technique and a strong (25 action potentials) post-burst stimulation protocol [294]. However, a reduction in the AHP and L-VGCC function has also been observed in 2-month old 5xFAD mice compared to WT littermates [348]. Additionally, a

reduction in calretinin and parvalbumin-positive interneurons has been noted in the hippocampi of 12-month old 5xFAD mice [493], while 8-month old 5xFAD mice had elevated expression of calcineurin-dependent transcription factor nuclear factor of activated T cells 4 compared to WT [494]. Despite these inconsistent observations, no direct measures of neuronal Ca^{2+} have been measured in the 5xFAD model. In collaboration with the University of Michigan, we sought to characterize Ca^{2+} and Ca^{2+}-mediated processes during aging in a re-established design of the 5xFAD mouse model using sharp electrode electrophysiological and Ca^{2+} imaging techniques.

The following manuscript was accepted for publication at the Journal of Alzheimer's Disease. 5xFAD mouse colonies were maintained at the University of Michigan via the lab of G.G. Murphy and managed by R. Parent. Mice were shipped to the University of Kentucky in several cohorts. All electrophysiological recordings and Ca^{2+} imaging experiments were performed by A.O. Ghoweri through the guidance of O. Thibault and J.C. Gant. Morris water maze behavior experiments were done by L. Ouillette under the guidance of G.G. Murphy. Amyloid plaque staining and quantification was performed by S. Moore. Manuscript writing and editing was established by A.O. Ghoweri, O. Thibault, H.N. Frazier, S. Moore, and G.G. Murphy. The purpose of the following study was to characterize neuronal Ca^{2+} dysregulation before, during, and after the generation of amyloid plaques in a re-established design of the 5xFAD mouse. The classic 5xFAD mouse model of familial AD was first derived by Oakley and colleagues in 2006 to recapitulate Alzheimer's disease-like phenotypes through 5 genetic mutations of the *APP*, *PS1*, and *PS2* genes [495]. Though this model has provided valuable insights to the understanding of intracellular mechanisms involved with Aβ plaque generation, the fast-paced nature of amyloidogenesis by 2 months of age in the original 5xFAD design may have masked the characterization of important phenotypes preceding plaque development. Thus, our collaborators at the University of Michigan crossed hemizygous 5xFAD mice with WT C57BL/6Tac mice to generate 5xFAD mice that exhibit AD-related pathology and cognitive deficits 2-4 months later than the original design. We hoped that by measuring neuronal Ca^{2+} handling across age, sex, and genotype in this new 5xFAD design with slower amyloidogenesis, we could potentially elucidate subtle Ca^{2+}-mediated markers that participate in AD pathology progression.

CHAPTER 4. ELECTROPHYSIOLOGICAL AND IMAGING CALCIUM BIOMARKERS OF AGING IN MALE AND FEMALE 5XFAD MICE

Adam O Ghoweri [a], Lara Ouillette [b], Hilaree N Frazier [a], Katie L Anderson [a], Ruei-Lung Lin [a], John C Gant [a], Rachel Parent [b], Shannon Moore [b], Geoffrey G Murphy [b], Olivier Thibault [a]

UKMC MS313, Pharmacology and Nutritional Sciences, University of Kentucky, 800 Rose St., Lexington, KY 40536 [a]

5037 BSRB, Molecular and Integrative Physiology, University of Michigan, 109 Zina Pitcher Place, Ann Arbor, MI 48109 [b]

4.1 Abstract

In animal models and tissue preparations, Ca^{2+} dyshomeostasis is a biomarker of aging and Alzheimer's disease that is associated with synaptic dysfunction, neuritic pruning, and dysregulated cellular processes. It is unclear, however, whether the onset of Ca^{2+} dysregulation precedes, is concurrent with, or is the product of pathological cellular events (*e.g.* oxidation, amyloid-β production, and neuroinflammation). Further, neuronal Ca^{2+} dysregulation is not always present in animal models of amyloidogenesis, questioning its reliability as a disease biomarker. Here, we directly tested for the presence of Ca^{2+} dysregulation in dorsal hippocampal neurons in male and female 5xFAD mice on a C57BL/6 genetic background using sharp electrodes coupled with Oregon-green Bapta-1 imaging. We focused on 3 ages that coincide with the course of amyloid deposition: 1.5, 4, and 10 months old. Outcome variables included measures of the afterhyperpolarization, short-term synaptic plasticity, and Ca^{2+} kinetics during synaptic activation. Quantitative analyses of spatial learning and memory were also conducted using the Morris water maze. Main effects of sex, age, and genotype were identified on measures of electrophysiology and Ca^{2+} imaging. Additionally, measures of resting Oregon-green Bapta-1 fluorescence showed significant reductions in the 5xFAD group compared to controls. Deficits in spatial memory, along with increases in Aβ load, were detectable at older ages, allowing us to test for temporal associations with the onset of Ca^{2+} dysregulation. Our results provide evidence that reduced, rather than elevated, neuronal Ca^{2+} is identified in this 5xFAD model and suggests that this surprising result may be a novel biomarker of AD.

4.2 Introduction

The rise in Alzheimer's disease (AD) cases is predicted to reach exponential numbers by the year 2050, yet few, if any, new effective therapeutic drugs are currently available. Further, the cost of care is burdensome for families and healthcare providers [185], resulting in an urgent need for the development of new treatment strategies. While several cellular alterations have been identified as key contributors to the onset and progression of AD, including amyloid-β (Aβ) deposits, apolipoprotein E status, tau tangles, oxidative stress, neuroinflammation, and synaptic loss [496-502], it is imperative to look beyond these for new biomarkers. One target that has received considerable interest is neuronal Ca^{2+} dysregulation.

The hypothesis of brain aging and AD has provided evidence that neuronal Ca^{2+} is dysregulated and can negatively impact neuronal health, network communication, and synaptic plasticity [1-4, 503-506]. In the hippocampus, a structure necessary for spatial mapping and short-term memory, an altered network fraught with reduced synaptic plasticity [18, 507, 508], increased pruning [509-512], and recent evidence of hyperactivity [336, 513] is likely to mediate cognitive and memory impairments [338, 514-523]. The role that neuronal Ca^{2+} assumes with respect to these processes is unclear, as Ca^{2+} dysregulation may occur when Ca^{2+} is elevated or decreased, during states of rest or during synaptic activation, or as the consequence of alterations in synaptic communication. Given the variability in Ca^{2+} homeostasis measures in normal aging, it is important to measure Ca^{2+} in models of AD as well.

Critical mechanistic insights regarding Ca^{2+} dysregulation have been gained in AD animal models [183, 274, 345, 393, 502, 524-527]; however, few studies have investigated

this AD-associated Ca^{2+} dysregulation alongside aging. Initial studies of the associations between Aβ and Ca^{2+} homeostasis, including the impact of Ca^{2+} on Aβ production, were mostly conducted *in vitro* (*i.e.* human cell lines or animal cell culture) [reviewed in 284]. With the exception of a few culture studies conducted in adult tissues [275, 282, 528-530], most of this early work used primary neuronal cultures derived from neonatal pups, which prevented the inclusion of the aging component. When investigating Ca^{2+} dysregulation and its physiological impact either directly (using Ca^{2+} imaging techniques) or indirectly (using electrophysiological techniques), nearly all measures were obtained from AD animals at single timepoints between the ages of 4 weeks and 12 months [281, 289-300, 512]. Although these studies highlighted increases in resting or stimulated Ca^{2+} levels, triggered either synaptically or via the activation of inositol 1,4,5-trisphosphate or ryanodine receptors, few have specifically investigated the impact of AD-associated Ca^{2+} dysregulation during the progress of aging [127, 241].

Stutzmann and colleagues examined Ca^{2+} changes across age (1.5, 6, and 18 months) in three transgenic mouse models (PS1KI, 3xTg, and APPSweTauP301L). While enhanced endoplasmic reticulum (ER) Ca^{2+} signaling was observed in the PS1KI and 3xTg models, presumably due to the PS1 mutation, this effect was not found to be age-dependent [127]. However, similar to early aging studies [2, 9, 182], the Ca^{2+}-mediated afterhyperpolarization (AHP) was larger with aging, but remained unaltered across genotype. In another study, L-type voltage-gated Ca^{2+} channel (L-VGCC) density was measured across age (1, 6-9, and 12-16 months) in wild-type (WT) and 3xTg mice [241]. L-VGCC density was significantly increased at 12-16 months in the transgenic mice compared to WT littermates. Surprisingly, however, no significant increase in these

75

measures were found across age in WT animals at 12-16 months. This contradicts previous findings in the F344 rat model of aging, which showed elevations at 23-26 months of age [97].

The paucity of direct Ca^{2+} measures in aged AD animal models is partly due to the identification of human amyloid β precursor protein and presenilin (PS) mutations, which increase production of amyloidogenic proteins from birth, resulting in the development of a very aggressive phenotype, precluding studies in older animals. Further, besides humans and dogs, other animal models do not develop AD phenotypes (*e.g.* Aβ deposition, tau tangles). Additionally, it has been difficult to draw comparisons between pathological aging and AD, as the former lacks clear biomarkers (*i.e.* Aβ plaques, tau tangles, "leaky channels" of the ER, and enhanced neuronal death) that differentiate the disease from normal brain aging. Furthermore, recapitulating these phenotypes in transgenic animals does not necessarily clarify whether Ca^{2+} dysregulation impacts AD pathology or vice versa.

These difficulties, together with recent evidence that Ca^{2+} signals appear to decrease in two animal models of AD [242, 348], highlight the possibility that methodological differences may mediate these discrepancies. Interestingly, previous work by our group has shown a significant *reduction* in L-VGCC density in 14-month-old 2xTg mice compared to WT using the dissociated "zipper" hippocampal slice technique [242]. Using the same methods, however, a two-fold *increase* in L-VGCC density was found in aged F344 rats compared to young animals [97]. In a more recent study, we identified a significant decrease in the AHP of 2-month-old 5xFAD mice on a C57BL/6 genetic background compared to WT [348]. Further, in a 2008 comprehensive review of Ca^{2+}

76

dysregulation in AD across 32 studies performed in both cell lines and mouse models with PS mutations [525], over 100 measures of Ca^{2+} were identified. Of these, 24 showed enhanced Ca^{2+} release from the ER while 21 exhibited decreased release. Moreover, 17 measures of plasma membrane Ca^{2+} influx were downregulated, two were upregulated, and five showed no change across genotypes. Thus, while the field has argued that Ca^{2+} dysregulation may be a unifying mechanism that impacts aging and AD in similar ways, this over-simplification may have hindered, rather than helped, the advancements made on this topic.

To better characterize these processes in AD animal models in the context of aging, we tested for the presence of Ca^{2+} dysregulation in the 5xFAD mice on a C57BL/6 genetic background at three distinct ages using two techniques that have reliably identified key biomarkers of aging across labs [2, 531, 532]. This approach allowed us to address the onset of the Ca^{2+} dysregulation using both direct (Ca^{2+} imaging) and indirect (electrophysiology) measures. Given that aging is the number one risk factor for AD, we chose to utilize this 5xFAD mouse model on a congenic C57BL/L genetic background, as these animals display a slower development of the AD phenotype [490, 533], allowing the aging processes to participate in disease progression. Sharp electrode electrophysiology and Oregon-green Bapta-1 (OGB-1) Ca^{2+} imaging were used to measure neuronal physiology and corresponding Ca^{2+} changes. Behavioral characterization using the Morris water maze (MWM) and Aβ deposition (BTA-1) was quantified to characterize phenotypic progression. Based on our prior results, we hypothesized that contrary to what is seen in normal aging, somatic Ca^{2+} would be *reduced* over time in this 5xFAD transgenic model of amyloidogenesis.

4.3 Methods

4.3.1 Animals

Young-adult (1.5 months), adult (4 months), and mid-age (10 months) male and female 5xFAD mice and their WT littermates were derived at the University of Michigan (Ann Arbor, MI) and shipped to the University of Kentucky (Lexington, KY) in several cohorts of 10-20 animals. The 5xFAD mice [495] were originally obtained from the Mutant Mouse Regional Resource Facility (MMRC) on a C57BL/6J background (stock # 034848-JAX). Hemizygous 5xFAD mice were crossed with WT C57BL/6Tac mice and maintained at the University of Michigan on this background since late 2012 (20+ generations). A recent report suggests that 5xFAD mice on a C57BL/6 background exhibit AD-related pathology and cognitive impairments approximately 2-4 months later than the mice originally described by Oakley and colleagues, which utilized mice on a hybrid B6/SJL genetic background [495, 533]. Typically, a cohort represented animals at a particular age (*e.g.* 4.5 weeks, 3.5 months, and 9.5 months). Because only one animal could be electrophysiologically recorded per day, data acquisition for each cohort was staggered across 3-5 weeks; thus, the average age of each cohort was 1.5, 4, and 10 months.

4.3.2 Housing

While at the University of Michigan, the mice were same-sex housed in groups of three to five, with a 14 h on/10 h off light/dark cycle, an ambient temperature of 20–22°C, and *ad libitum* access to food and water. Upon transfer to the University of Kentucky, mice were housed in a quarantined facility for a minimum of one week prior to experimentation. Male mice were housed individually while females were paired. All animals were

78

maintained on a 12 h on/12 h off light/dark cycle and fed a Teklad Global 18% protein rodent diet *ad libitum*. Routine assessment of animal health was performed by a veterinarian at both institutions and animals exhibiting signs of morbidity were excluded from the study. Treatment and handling of all animals were performed in accordance with each university's Institutional Animal Care and Use Committee guidelines.

4.3.3 Slice Preparation

Mice were anesthetized using aerosolized isoflurane (5%) followed by rapid decapitation. Brains were quickly removed and incubated in ice cold low Ca^{2+}, high magnesium artificial cerebrospinal fluid (ACSF) [in mM]: 114 NaCl, 3 KCl, 10 Glucose, 1.25 KH_2PO_4, 26 $NaHCO_3$, 0.096 $CaCl_2$ anhydrous, and 7.98 $MgCl_2$ anhydrous. Three-hundred and fifty µm thick slices from the dorsal hippocampus were obtained using a Vibratome® 3000 (TPI; St. Louis, MO) and incubated for at least 2 h at 32°C in a humidified (95% O_2 – 5% CO_2) interface-type chamber in normal Ca^{2+} ACSF [in mM]: 114 NaCl, 3 KCl, 10 Glucose, 1.25 KH_2PO_4, 26 $NaHCO_3$, 2 $CaCl_2$ anhydrous, and 2 $MgCl_2$ anhydrous. Slices were then placed in a recording chamber (RC-22C; Warner Instruments, Co., Hamden, CT) heated to 32°C with a $TC^2Bip/HPRE2$ in-line heating system (Cell Micro Controls; Norfolk, VA) and perfused with a continuous flow of oxygenated, normal ACSF at a rate of 1.5 mL/min. Slices were then visualized under a Nikon Eclipse E600FN microscope.

4.3.4 Electrophysiology

Sharp electrodes (~80 – 120 MΩ) were pulled from 1.0 mm diameter borosilicate glass capillaries (World Precision Instruments, Inc.; Sarasota, FL) on a Sutter Instruments P80 pipette puller (Novato, CA). Electrode tips were first backfilled with a bolus of 1.25 mM OGB-1, pH 7.4 (ThermoFisher Scientific, Catalog number: O6806; Waltham, MA), while the rest of the electrode was filled with a 1 M potassium methyl sulfate (KMeSO4) in 10 mM HEPES. A bipolar stimulating electrode was placed on the Shaffer collaterals and the recording electrode was slowly guided through *stratum pyramidale* of area CA1. An SD9K stimulator (Astro Med Inc., Grass Instruments; Warwick, RI) was used to synaptically stimulate the tissue slice. Responses were obtained through an AxoClamp-2B amplifier (Molecular Devices LLC.; San Jose, CA) and digitized at ~ 5-10 KHz using a Digidata® 1550B (Molecular Devices LLC.; San Jose, CA). Data was processed using pClamp 10.7 software (Molecular Devices LLC.; San Jose, CA).

4.3.4.1 Afterhyperpolarization

For measures of post-synaptic activation, cells were held at -65 mV. Action potential (AP) threshold was set to -55 mV, and 4 AP bursts were evoked (depolarizing 150 ms current injection) to generate the Ca^{2+}-dependent AHP every 30 s for five min. Three measures of the AHP were quantified including the medium AHP (mAHP), slow AHP (sAHP), and AHP duration. The mAHP was defined as the peak hyperpolarization observed immediately after the end of the current injection. The sAHP was measured as the change in amplitude (compared to baseline) 800 ms post-current injection. Quantification of the AHP duration was defined as the time between peak amplitude of the AHP and the return to baseline. Here, we report data from 11 neurons (♂=6, ♀=5)/7 mice

($\male$=4, $\female$=3) (1.5 months), 14 neurons ($\male$=6, $\female$=8)/10 mice ($\male$=5, $\female$=5) (4 months), and 13 neurons ($\male$=9, $\female$=4)/9 mice ($\male$=7, $\female$=2) (10 months) in the WT dataset, and 21 neurons ($\male$=14, $\female$=7)/11 mice ($\male$=6, $\female$=5) (1.5 months), 19 neurons ($\male$=12, $\female$=7)/13 mice ($\male$=8, $\female$=5) (4 months), and 15 neurons ($\male$=8, $\female$=7) /10 mice ($\male$=5, $\female$=5) (10 months) in the 5xFAD dataset.

4.3.4.2 *Input/Output*

For measures obtained during synaptic activation, cells were held at -70 mV and stimulated every 10 s. Data reported were derived from 11 neurons ($\male$=6, $\female$=5)/7 mice ($\male$=4, $\female$=3) (1.5 months), 13 neurons ($\male$=5, $\female$=8)/10 mice ($\male$=5, $\female$=5) (4 months), and 10 neurons ($\male$=7, $\female$=3)/7 mice ($\male$=5, $\female$=2) (10 months) for the WT dataset, and 19 neurons ($\male$=13, $\female$=6) /11 mice ($\male$=6, $\female$=5) (1.5 months), 16 neurons ($\male$=10, $\female$=6)/12 mice ($\male$=8, $\female$=4) (4 months), and 12 neurons ($\male$=8, $\female$=4)/9 mice ($\male$=5, $\female$=4) (10 months) in the 5xFAD dataset. Excitatory post-synaptic potential (EPSP) amplitudes determined from an increasing series of activation voltages were plotted to generate *I/O* curves and used to determine the threshold for an AP.

4.3.4.3 Repeated Synaptic Stimulation

Stimulation intensity during repeated synaptic stimulation (RSS; 10 s, 7 Hz) was set at the threshold for an AP. Outcome measures included synaptic hyperpolarization and potentiation of EPSPs in relation to measures of the first EPSP (baseline) in the train. Synaptic hyperpolarization was tabulated as the mean peak hyperpolarization amplitudes following the 6th through 9th EPSPs. The growth of the EPSP during the train was measured early (EPSPs 6 through 9) and late (last 4 EPSPs).

4.3.5 Ca^{2+} Imaging

All cells were imaged after measures of input resistance, AHP, and *I/O* slopes were taken. Data reported were taken from 8 neurons (♂=5, ♀=3)/5 mice (♂=3, ♀=2) (1.5 months), 7 neurons (♂=3, ♀=4)/6 mice (♂=3, ♀=3) (4 months), and 7 neurons (♂=5, ♀=2)/5 mice (♂=4, ♀=1) (10 months) for the WT dataset, and 13 neurons (♂=8, ♀=5)/10 mice (♂=6, ♀=4) (1.5 months), 9 neurons (♂=6, ♀=3)/8 mice (♂=5, ♀=3) (4 months), and 8 neurons (♂=5, ♀=3)/6 mice (♂=3, ♀=3) (10 months) were included for the 5xFAD dataset. Cells were visualized under a 40x objective using a filter cube (Ex: 470/40 nm; Em: 525/50; Dichroic 495 nm; Chroma Technology Corp.; Bellows Falls, VT). Imaging Workbench (INDEC BioSystems; Los Altos, CA) was used to quantify outcome measures. A Lambda DG-4 (Sutter Instruments; Novato, CA) was used as a source to activate the fluorophore with exposures in the range of 250-800 ms depending on the depth of the cell imaged. A photometrics camera (Teledyne Photometrics; Tucson, AZ) was used to image Ca^{2+} fluorescence and kinetics. Two regions of interest (ROI) were created: one around the cell body and another of similar size in tissue adjacent to the imaged cell. Background subtraction and normalization to baseline were used to quantify changes in fluorescence (% ΔF/F). For quantification of resting fluorescence, values were averaged before RSS and normalized to the depth of the recorded cell. Outcome measures also included rise time, peak amplitude, decay time, and area-under-the-curve (AUC) during RSS, and were derived using Clampfit (Molecular Devices LLC.; San Jose, CA) and SigmaPlot software (Systat Software, Inc.; San Jose, CA).

4.3.6 Morris Water Maze

Water maze experiments were performed at the University of Michigan as previously described [534-536] utilizing male and female 5xFAD mice and non-carrier littermates (WT) as controls. Three age groups were examined; 1.5 month (5xFAD: ♂=5, ♀=2; WT: ♂=2, ♀=5), 4 month (5xFAD: ♂=4, ♀=4; WT: ♂=4, ♀=3) and 10 month (5xFAD: ♂=17, ♀=19; WT: ♂=28, ♀=11). A larger cohort of 10-month animals was used to provide sufficient power to detect differences that we anticipated would be modest between genotypes at this time point. The MWM was composed of a round white acrylic pool that was 1.2 m in diameter. The pool was filled with water that was made opaque using nontoxic, white tempera paint and heated to 28°C. A round platform made of clear acrylic (10 cm in diameter) was submerged just below the surface of the water, ~ 20 cm from the edge of the pool in the northeast quadrant. Mice were tracked using a digital camera mounted above the pool in combination with Actimetrics Water Maze (V4) software. Mice were trained to find the hidden platform during 4 trials a day. Before each trial, mice were individually placed on the platform for 10 s. At the start of the trial, mice were released into the maze, facing the wall at predefined pseudo-random locations, and the time taken to reach the platform was recorded. For all trials, mice were given 60 s to find the platform, and, if unsuccessful, were then guided to the platform. Previous experience indicated that older mice (regardless of genotype) require additional training to perform above chance. Therefore, young mice (1.5-month and 4-month) received 9 days of training and the older mice (10-month) received a total of 12 days of training. Mice were tested for their long-term memory for platform location during several probe tests throughout training. All mice received probe trials on days 4, 7 and 10 (24 hrs after the last

training trial). Aged mice (10-month) received an additional probe trial on day 13 (24 hrs after the last training trial). For the probe trials, the platform was removed from the pool, and each mouse was allowed to swim for 60 s, starting at a point directly opposite to the trained platform location. To control for motivation, swimming ability, and sensory perception (elements required for spatial recognition), mice were run in the visible-platform version of the water maze on the day following the final probe trial. In this version, a distinct local cue (a flag) was fixed to the center of the hidden platform. Mice were given four visible-platform trials with a maximum of 60 s per trial.

4.3.7 Tissue Section for β-amyloid and BTA-1 Staining

Male and female 5xFAD mouse brains were harvested for β-amyloid plaque staining at 3 time points; 1.5-month (n =15 sections from 3 mice; ♂=5, ♀=10), 4-month (n = 16 sections from 3 mice; ♂=16, ♀=0) and 10-month (n = 11 sections from 2 mice; ♂=5, ♀=6). Mice were anesthetized using aerosolized isoflurane, then cardiac-perfused with 1x PBS followed by 4% paraformaldehyde. Brains were removed, further fixed in 4% paraformaldehyde overnight at 4°C, and then placed in a 30% sucrose solution at 4°C until they sank (2-3 days). Brains were then embedded in optimal cutting temperature (OCT) compound (Fisher; Maltham, MA) and frozen at -80°C. Once frozen, the embedded brains were sliced coronally at 40 μm on a cryostat (Leica; Buffalo Grove, IL) and immediately mounted on Superfrost Plus slides (Fisher). Once mounted, sections were washed three times with 1x PBS to remove any residual OCT followed by incubation in 10 μM BTA-1 (Sigma-Aldrich; St. Louis, MO) for 30 min. Sections were then washed for an additional three times with 1x PBS before being cover-slipped using VectaMount® Aqueous Mounting Media (Vector Laboratories; Burlingame, CA).

4.3.8 β-amyloid Imaging

Images were collected from two subregions of the hippocampus: the CA1 and dentate gyrus (DG) subfields. Images were obtained using an upright laser scanning confocal microscope (Olympus; Center Valley, PA) equipped with 4x and 20x air objectives. For each region, single images (1024 x 1024 pixels) were captured every 5 µm for a total of 15 um total depth. BTA-1 staining was visualized using a 405 nm laser. Imaging acquisition settings (voltage (HV), gain, and offset) in the Olympus FluoView software were consistent across samples to allow for comparison. β-amyloid images were processed using ImageJ software (FIJI) and quantified using maximum projections of images at a depth of 15 µm. The images were then background subtracted with a 50-pixel rolling-ball radius, manually thresholded, and converted into binary masks of BTA-1 positive ROIs. ROIs were then used to count individual Aβ plaques in the raw image. This value was then divided by the volume of the image to give a result of plaque density in number/μm^3. Images are presented in grayscale.

4.3.9 Cell Health and Exclusion Criteria

Only neurons that fit the following criteria were included in the electrophysiological and Ca^{2+} imaging analyses: input resistance $\geq$ 30 MΩ, holding current $\leq$ -350 pA, and AP peak $\geq$ -2 mV. These values are reported in **Table 4.1**. Additionally, if the number of APs during RSS were > 2 SD from the mean, the cell was considered an outlier and removed from the analysis.

4.3.10 Data Quantification and Statistics

The statistical significance of electrophysiological and imaging measures was calculated using SigmaPlot. Using three-way ANOVA, we report on main effects of age, sex, or genotype, as well as interaction terms using the Holm-Sidak multiple comparisons test. For behavioral analysis, significance was tested using a 2-factor repeated measures ANOVA, unpaired t-tests, and single factor t-tests. Sex differences were not investigated for behavior. All β-amyloid imaging data was analyzed and displayed using GraphPad Prism 8 and Aβ deposition between 4-month and 10-month mice was compared using a 2-tailed unpaired t-test. The 1.5-month mice were excluded from analysis due to the absence of any observable plaques. Significance for all data was set at $p < 0.05$. Data are represented as means ± standard error of the mean (SEM).

Table 4.1. Measures of Neuronal Health and Cellular Activation.

Genotype	Age (months)	Holding Current (pA)	Input Resistance (MΩ)	AP Amplitude (mV)	# of APs During Imaging
WT Male	1.5	-125 ± 65.1	91.3 ± 15.2	4.5 ± 2.3	70.2 ± 3.0
	4	-241.7 ± 16.6	48.7 ± 2.6	7.7 ± 1.5	70 ± 0.6
	10	-143.3 ± 31.6	63.3 ± 3.9	8.7 ± 1.8	66.8 ± 4.5
5xFAD Male	1.5	-76.4 ± 27.5	71.4 ± 4.8	9.2 ± 1.6	68.1 ± 2.2
	4	-208.3 ± 22.8	43.3 ± 2.1	8.8 ± 1.3	70 ± 0.7
	10	-156.3 ± 36.1	61.0 ± 4.7	7.8 ± 1.9	73.8 ± 1.2
WT Female	1.5	-120 ± 48.1	76.5 ± 10.7	10 ± 2.1	68.7 ± 0.3
	4	-120 ± 27.6	54.6 ± 4.6	9.1 ± 1.8	66.8 ± 4.3
	10	-105 ± 33.8	85.1 ± 12.2	8.8 ± 1.9	70.0 ± 0
5xFAD Female	1.5	-201.4 ± 28.1	61.5 ± 7.7	5.6 ± 2.5	68.2 ± 3.2
	4	-185.7 ± 17.6	58.7 ± 6.0	2.9 ± 2.2	70.3 ± 0.3
	10	-84.3 ± 40.1	80.0 ± 4.9	6.5 ± 1.6	70.7 ± 0.3
Significance	-	$p < 0.02$	$p < 0.001$	n.s.	n.s.

Table 4.1. Measures of Neuronal Health and Cellular Activation. Neuronal health was compared across genotype, sex, and age. The amplitude of APs during AHP data acquisition and the number of APs during RSS while imaging were recorded. Holding current and input resistance reflect cell membrane "leakiness" and integrity. Holding current and input resistance at 4 months were both significantly elevated ($p < 0.05$). No changes were detected between groups on measures of AP amplitude or number of APs during imaging ($p > 0.05$).

4.4 Results

The following results were derived from 93 cells recorded in 61 animals and from 52 imaged cells. We compared several measures of neuronal health and numbers of APs triggered during imaging protocols to confirm that the results reported here were all derived from healthy dorsal CA1 pyramidal neurons (Table 4.1). For behavioral analysis, 55 WT and 51 5xFAD mice were used. Tissue sections from eight 5xFAD mice were stained and analyzed for β-amyloid deposits. **Table 4.2** illustrates the impact of training as compared to genotype on MWM outcome measures.

4.4.1 Afterhyperpolarization

To determine if an age, sex, or genotype effect on the Ca^{2+}-dependent AHP was present, we measured the mAHP and the sAHP amplitude, as well as the AHP duration (**Figure 4.1**). These measures revealed that the amplitude of the mAHP ($F_{2,92} = 9.99$, $p < 0.001$; three-way ANOVA; Fig. 4.1B) was significantly reduced in both WT and 5xFAD mice from 6 weeks to 4 months of age. Interestingly, from 4 to 10 months, the mAHP significantly increased to levels indistinguishable from those seen at 6 weeks. Similar results were seen on measures of the sAHP amplitude ($F_{2,92} = 11.00$, $p < 0.001$; three-way ANOVA) and the AHP duration ($F_{2,92} = 10.70$, $p < 0.001$; three-way ANOVA; Fig. 4.1C). The "U" shaped aging effect seen in Fig. 4.1 is intriguing, and may reflect on the inclusion of the 1.5-month age group. In fact, most studies of aging use 3-4 months old animals as the "young" age group. Still, one prior study using patch electrodes describes a significant increase between 1.5 months and 1.5 years in similar WT and transgenic animals, but no significant genotype effect was reported at any ages [127]. Of interest, analysis of the sAHP amplitude here revealed a significant sex by genotype interaction term ($F_{1,92} = 5.47$, $p =$

0.02), where a reduction was noted in female 5xFAD compared to WT ($p < 0.05$), but not in males. Further, when analyzing the AHP duration (Fig. 4.1D), an age by sex interaction term was noted ($F_{2,92} = 3.30$, $p = 0.04$); again, this aging effect was only significant in females ($p < 0.05$). These results highlight the importance of investigating sex differences in animal models of AD.

Table 4.2. Results and Statistical Analyses of Behavioral Data.

Measure		Age (months)	F-value	p-value	Significance
Latency to Platform	Effect of Training	1.5	$F_{(8, 88)} = 11.26$	P < 0.0001	Yes
		4	$F_{(8, 96)} = 4.896$	P < 0.0001	Yes
		10	$F_{(12, 876)} = 68.14$	P < 0.0001	Yes
	Effect of Genotype	1.5	$F_{(1, 11)} = 2.395$	P = 0.15	No
		4	$F_{(1, 12)} = 0.008$	P = 0.929	No
		10	$F_{(1, 73)} = 10.53$	P = 0.0018	Yes
Time spent in target quadrant	Effect of Training	1.5	$F_{(2, 22)} = 12.21$	P = 0.0003	Yes
		4	$F_{(2, 24)} = 0.666$	P = 0.523	No
		10	$F_{(3, 228)} = 24.33$	P < 0.0001	Yes
	Effect of Genotype	1.5	$F_{(1, 11)} = 0.006$	P = 0.938	No
		4	$F_{(1, 12)} = 0.198$	P = 0.663	No
		10	$F_{(1, 76)} = 12.03$	P = 0.0009	Yes
Swim Speed	Effect of Genotype	1.5	$F_{(5, 6)} = 1.179$	P = 0.022	Yes
		4	$F_{(6, 7)} = 4.374$	P = 0.404	No
		10	$F_{(36, 36)} = 2.266$	P = 0.8725	No

Table 4.2. Results and Statistical Analyses of Behavioral Data. Latency to platform, time spent in the target quadrant, and swim speed were compared across genotype and age. Training significantly reduced the latency to platform across age ($p < 0.0001$); however, on measures of time spent in target quadrant, this was only seen in 1.5- and 10-month old animals ($p < 0.001$). Compared to WT littermates, 5xFAD mice showed significant behavioral deficits by 10 months of age ($p < 0.0018$) and spent significantly less time in the target quadrant ($p = 0.0009$). Genotype significantly influenced swim speed at 1.5 months ($p = 0.022$), but not at 4 or 10 months.
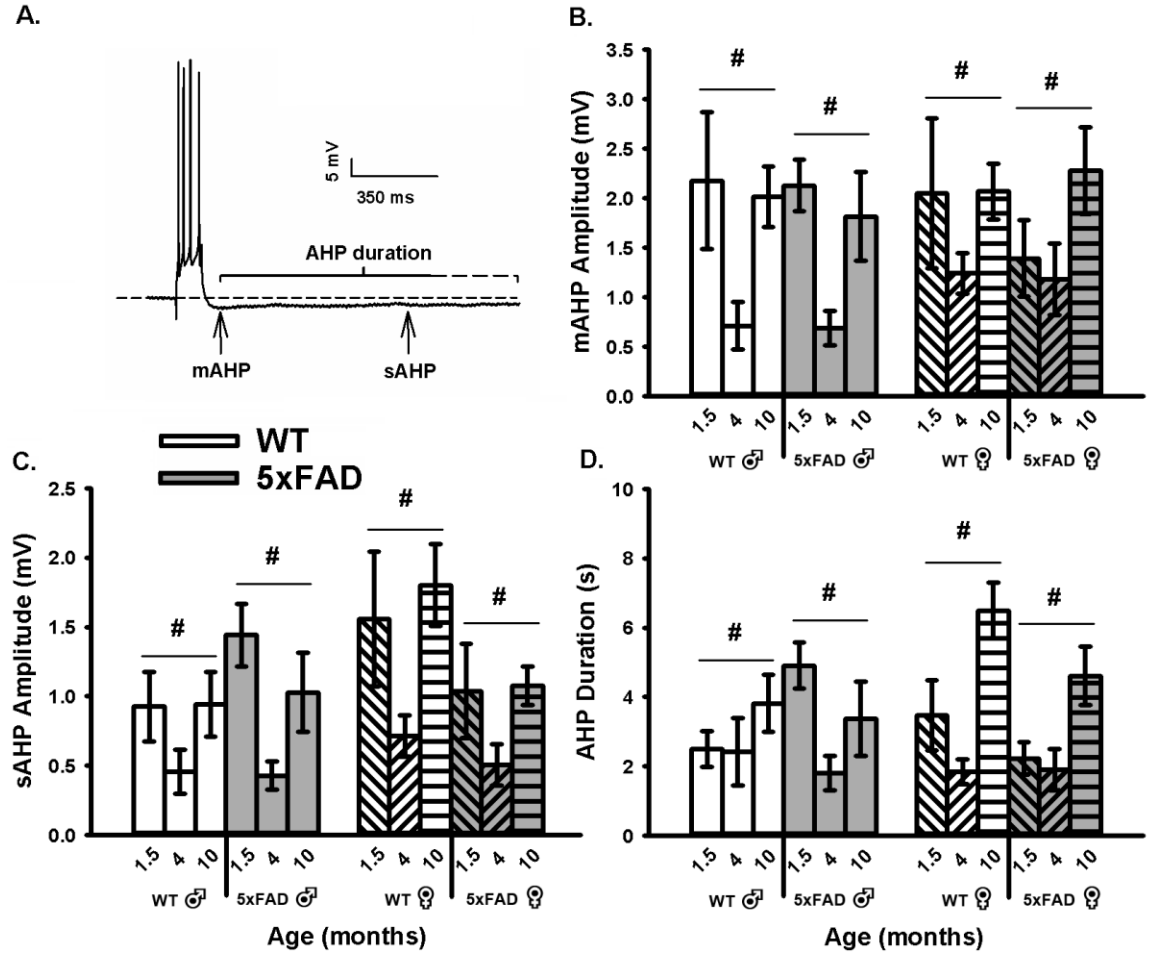
Figure 4.1. AHP Measures in WT and 5xFAD Mice Across Age and Sex.

A. Example of an AHP following post-synaptic depolarization with 4 APs. **B.** A main effect of aging ($p < 0.05$) on the mAHP was observed within each genotype and across sex. **C-D.** Similar findings were observed on the sAHP (800 ms) amplitude measures, as well as on the AHP duration. Hashes (#) represent significance in aging at $p < 0.05$.

4.4.2 Synaptic Activation

We quantified neuronal excitability during synaptic activation using measures of EPSP amplitudes and *I/O* slopes (**Figure 4.2A and B**). In alignment with the age-dependent changes in the AHP presented in Figure 4.1 where a "U" shaped curve was noted, analysis of the excitability data (*I/O* slopes) reveals inverse relationships with age, as highlighted by greater excitability at 4 months. Indeed, a main effect of age was detected ($F_{2,80} = 8.02$, $p < 0.001$; three-way ANOVA). Further, an age by sex by genotype interaction was also identified ($F_{2,80} = 5.13$, $p < 0.008$), albeit only at 1.5 and 4 months of age ($p < 0.05$ for both). Once again, this effect was more pronounced in female 5xFAD mice than in males.

We then obtained measures of RSS at 7 Hz, including synaptic hyperpolarization (**Figure 4.3A, B, and C**) as well as short-term EPSP facilitation (Fig. 4.3A, B, D, and E). While synaptic hyperpolarization has been shown to decrease with age in the F344 rats model of aging [532], no age or genotype effect was identified in the 5xFAD mice and at the ages tested here (Fig. 4.3C). However, while investigating changes in EPSP facilitation during RSS (both early and late, Fig. 4.3D and 3E), we noticed a significant increase in the late phases of EPSP facilitation as a function of age in the 5xFAD model ($F_{2,76} = 4.11$, $p = 0.02$; three-way ANOVA). This result is surprising, given prior literature reporting on depressed EPSP facilitation with aging [10, 51, 455, 537].
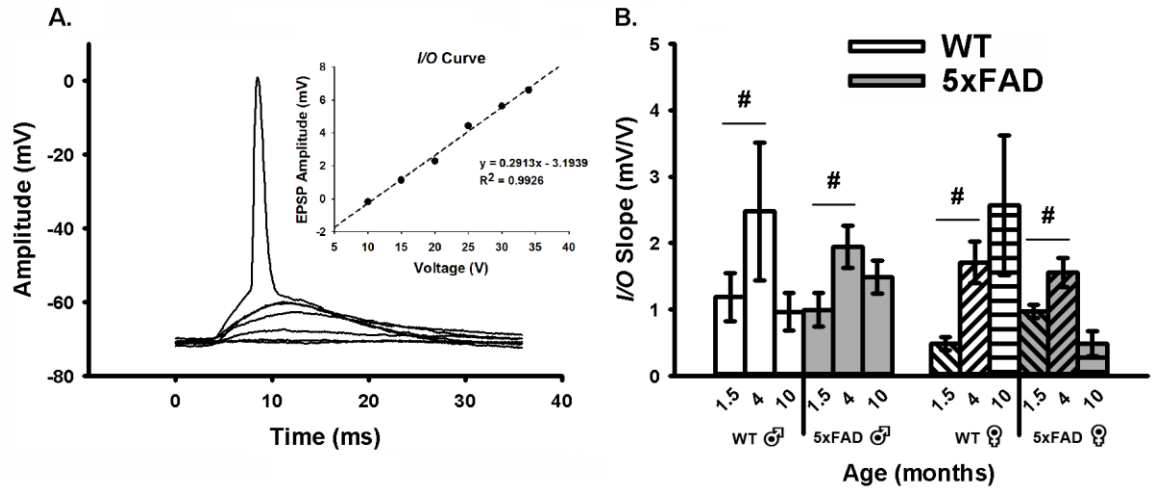
Figure 4.2. Extracellular Synaptic Activation.

    A. Example of EPSPs recorded below and at threshold of an AP. Inset shows input/output (*I/O*) plot fit from EPSP amplitudes with increasing stimulation intensity. **B.** Synaptic excitability derived from *I/O* measures (slopes) reveal a significant main effect of aging across genotypes and sex. Hashes (#) represent significance in aging at $p < 0.05$.

A.

B.

WT
5xFAD

C.

D.

E.

96
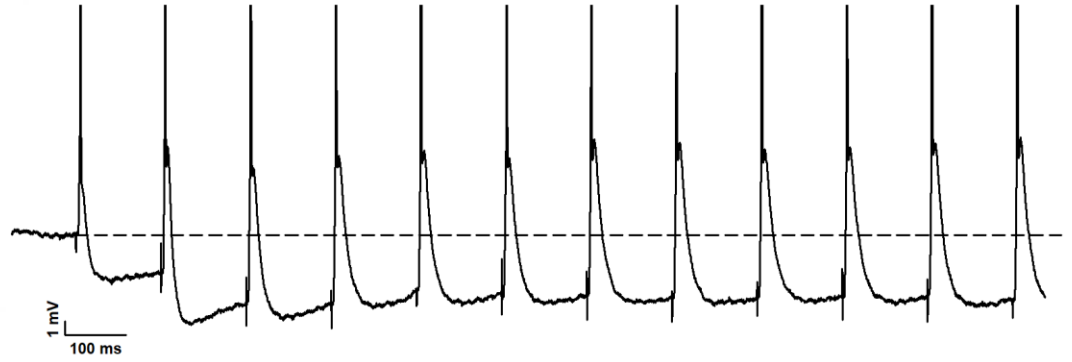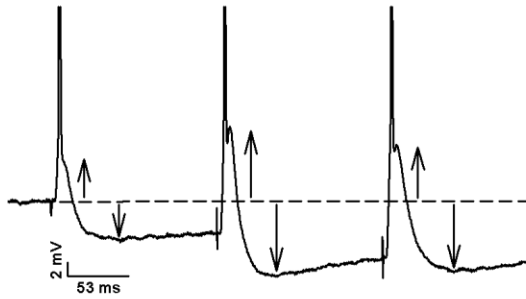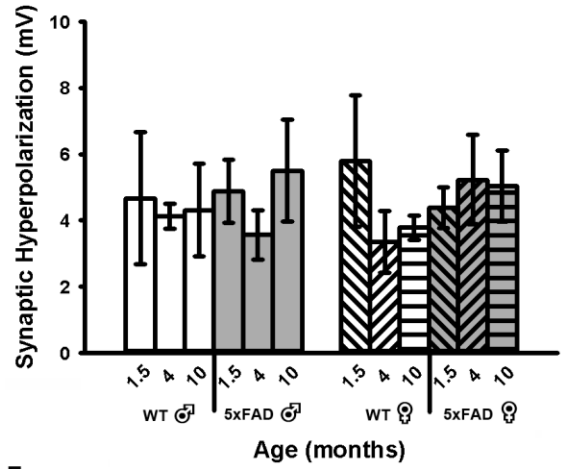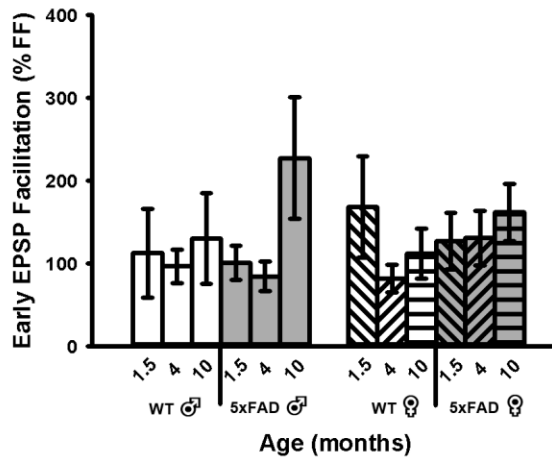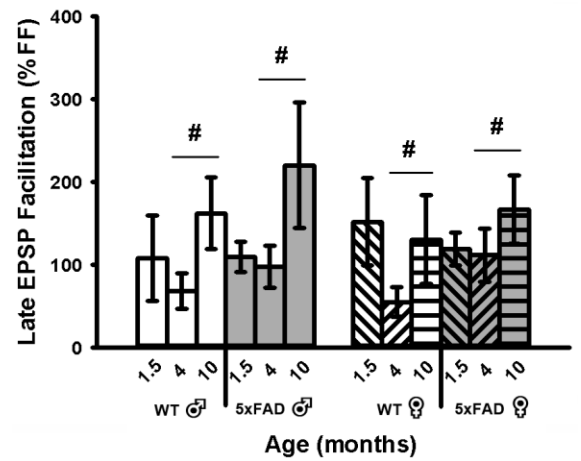
Figure 4.3. Repeated Synaptic Stimulation (RSS).

A. Example of RSS showing EPSP potentiation and synaptic hyperpolarization. Cells were repeatedly stimulated at 7 Hz for 10 s. **B.** Upward arrows illustrate growth in EPSP amplitude during RSS and downward arrows show increased amplitude in the synaptic hyperpolarization. APs are truncated for illustration in A and B. **C.** Synaptic hyperpolarization measured during RSS was not altered across aging or genotypes. **D-E.** EPSP facilitation taken during the first (early) and last (late) periods of RSS. A main effect of age was noted on measures of late EPSP facilitation displaying an increase in the older group, independent of sex. Hashes (#) represent significance in aging at $p < 0.05$.

4.4.3 Ca^{2+} Imaging

Age-, sex-, and genotype-sensitive changes in Ca^{2+} kinetics and overall somatic levels were derived from OGB-1 fluorescence before, during, and after RSS (**Figure 4.4**). Cells were synaptically-stimulated at 7 Hz for 10 s and changes in fluorescence were normalized to resting fluorescence (% $\Delta F/F$) just prior to stimulation. Results show that neither age, sex, nor genotype altered measures of Ca^{2+} kinetics based on rise time or decay time constants (Fig. 4.4D and 4E). However, measures of peak amplitude and AUC (Fig. 4.4C and 4.4F) highlighted a significant main effect of age and sex. Measures of peak amplitude and AUC revealed a main effect of age highlighted mostly by differences between the 1.5- and 4-month-old groups ($F_{1,51} = 3.71$, $p = 0.03$; $F_{1,51} = 3.54$, $p = 0.04$, respectively; three-way ANOVA). The same measures also showed an overall main effect of sex, as highlighted by reductions in fluorescence intensity during RSS in females compared to males (peak: $F_{1,51} = 6.52$, $p = 0.02$; AUC: $F_{1,51} = 6.14$, $p = 0.02$).

A main effect of genotype on mean resting fluorescence ($F_{1,49} = 8.62$, $p < 0.01$; three-way ANOVA) was seen with reductions in Ca^{2+}-dependent fluorescence in the 5xFAD compared to WT in both sexes (**Figure 4.5**). Because OGB-1 fluorescence values depend on Ca^{2+} levels, duration of exposure to the indicator, and the depth of the cell recorded, we normalized mean resting fluorescence to the depth of each cell. While a significant main effect of age on measures of recorded depth ($F_{2,49} = 3.80$, $p = 0.03$; three-way ANOVA) was noted, this was mostly mediated by an increase in depth in 4-month-old animals and was independent of genotype, and therefore unlikely to have contributed to the overall genotype effect (Fig. 4.5).

A.
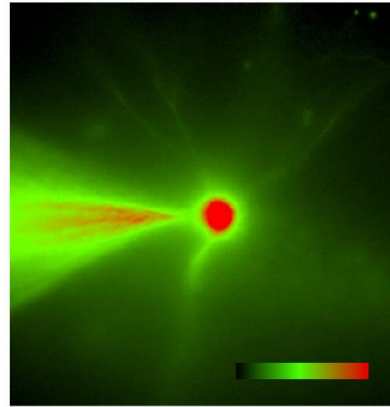
B.
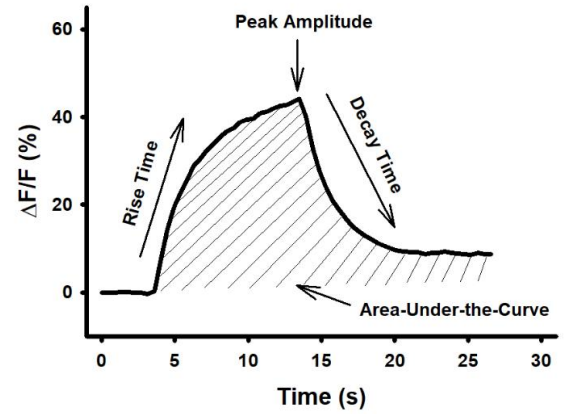
C.
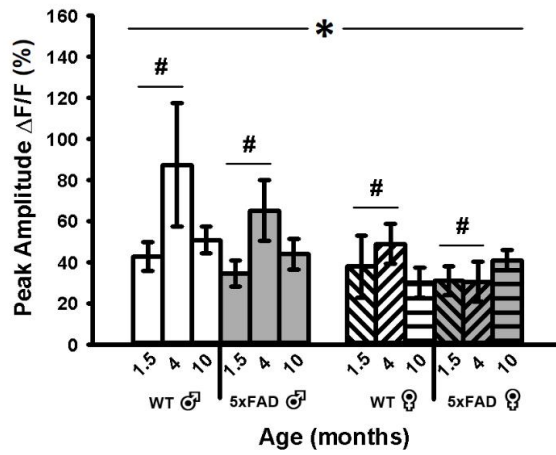
D.
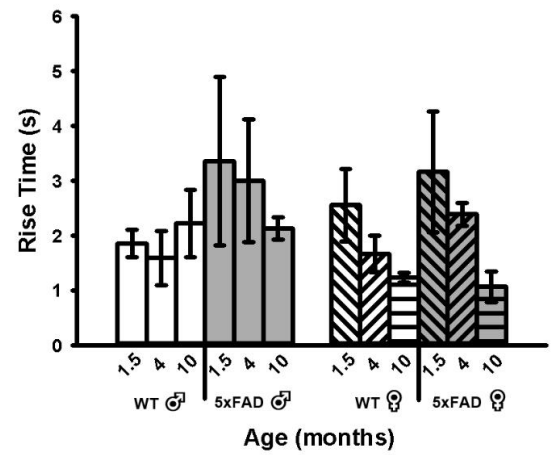
E.
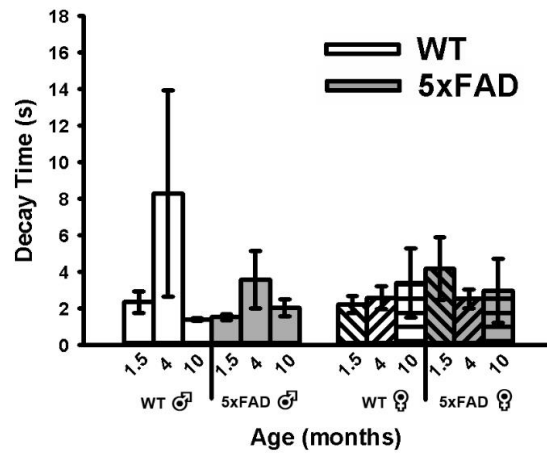
F.
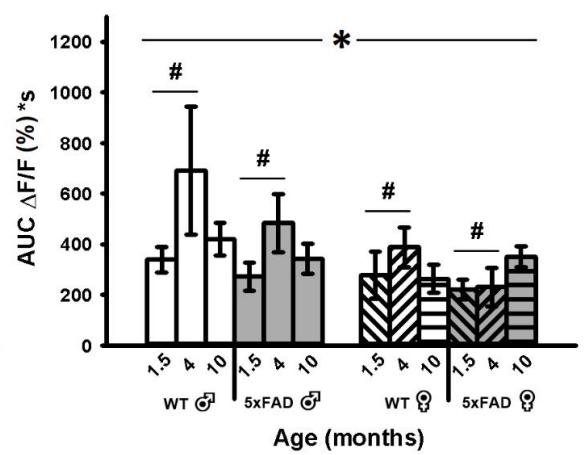
Figure 4.4. Changes in OGB-1 Fluorescence During 10 s RSS.

A. Example of an imaged OGB-1 loaded neuron. **B.** Normalized fluorescence change across time (% $\Delta F/F$) before, during, and after RSS. **C.** Peak amplitude measures show both a significant effect of age and sex. **D-E.** No significant differences were found in measures of rise or decay time constants. **F.** AUC shows significant effects of both age and sex. Hashes (#) represent significance in aging and asterisks (*) represent sex differences at $p < 0.05$.
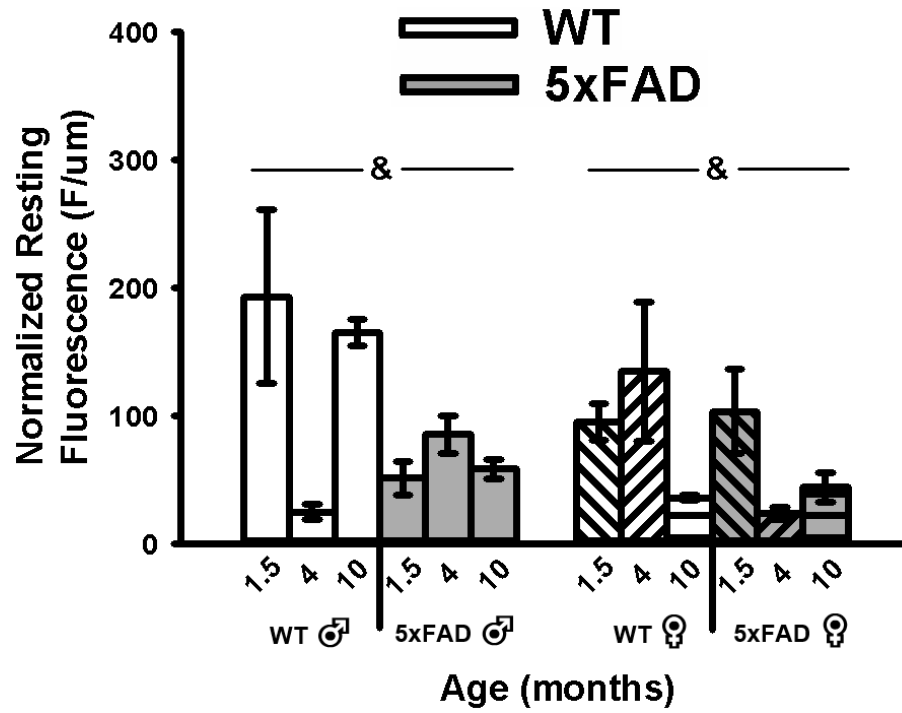
Figure 4.5. Resting Fluorescence Before RSS.

Mean resting fluorescence was normalized to the depth of each recorded cell. Significant genotype effect was detected, highlighting reduced fluorescence in the 5xFAD animals compared to WT. Ampersands (&) indicate significance for genotype at $p < 0.05$.

4.4.4 Behavior

We explored the impact of age on hippocampal-dependent learning and memory using the MWM task [538]. Analysis of latency to find the hidden platform during training revealed a significant reduction across training days at 1.5 months ($F_{8, 88} = 11.26$, $p < 0.0001$; two-way repeated measures ANOVA), 4 months ($F_{8, 96} = 4.896$, $p < 0.0001$; two-way repeated measures ANOVA), and 10 months ($F_{12, 876} = 68.14$, $p < 0.0001$; two-way repeated measures ANOVA). As expected, there were no differences between 5xFAD and WT mice in latency to platform in either the 1.5-month or 4-month groups (**Figure 4.6A₁-B₁**). However, there was a significant reduction in latency observed in the 10-month group ($F_{1, 73} = 10.53$, $p = 0.0018$; two-way repeated measures ANOVA) (Fig. 4.6C₁), indicating that the 5xFAD mice have a deficit in their ability to learn the platform location across training days.

By the final probe trial, 5xFAD mice and their WT littermates in all groups had spent a significant percentage of time in the target quadrant compared to chance ($p < 0.05$, single factor *t*-test). As expected, there was no effect of genotype in either the 1.5- or 4-month groups across probe trials ($p = 0.605$, $p = 0.938$, respectively; two-way repeated measures ANOVA) (Fig. 4.6A₂-B₂). However, the 10-month 5xFAD mice spent significantly less time across probe trials searching in the quadrant where the platform was previously located in comparison to their WT littermates ($F_{1, 76} = 12.03$, $p = 0.0009$; two-way repeated measures ANOVA) (Fig. 4.6C₂), indicating a memory deficit for platform location. No significant difference in swim speed between 5xFAD and WT mice ($p = 0.217$; unpaired *t*-test) was noted, establishing that this deficit was not due to alterations in

either motor function or motivation. Additionally, a non-spatial version of the water maze was performed in which the escape platform was clearly marked. The 5xFAD and WT mice exhibited similar escape latencies (p = 0.7114; unpaired *t*-test), suggesting that the memory deficit we observed in the 10-month 5xFAD mice was not due to a nonspecific performance issue. Similarly, no significant differences were observed in performance during the visible platform in the 1.5-month and 4-month mice (p = 0.33 and p = 0.054, respectively). With respect to potential sex differences across groups, we did not observe a statistically significant effect of sex on any of the behavioral performance variables analyzed. Finally, we did not observe a correlation between MWM performance, Ca^{2+} dynamics, and sex. Taken together, these data indicate that learning and memory deficits are present in 5xFAD mice by 10 months of age.

1.5 month

4 month

10 month

104
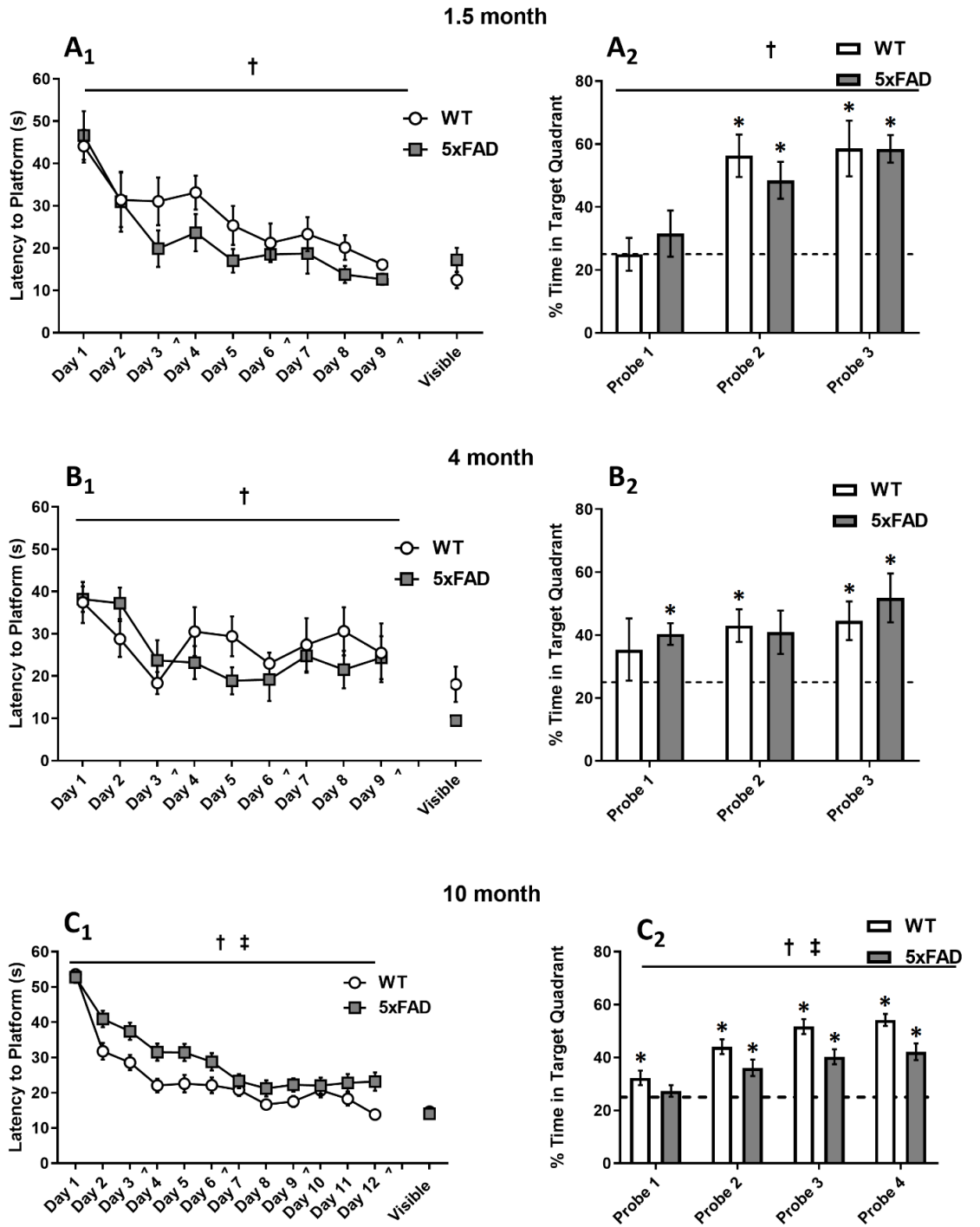
Figure 4.6. Morris Water Maze Data.

Mice were trained using 4 trials per day for 9 days (1.5- and 4-month-old animals; **A₁-B₁.**) or 12 days (10-month-old animals; **C₁.**) days on the hidden platform task. Memory performance was assessed using probe trials on days 4, 7, 10 [^] (all age groups; **A₂-C₂.**) and 13 (10-month; **C₂.**). By the final probe, all groups spent significantly more time (> 25%) in the target quadrant. 1.5- and 4-month mice exhibited a significant decline in the latency to find the hidden platform across training days, but no differences were seen between genotypes (**A₁-B₁.**). There were no significant differences between genotypes during probe trials (**A₂-B₂.**). 10-month-old 5xFAD and WT mice exhibited a significant decline in latency to find the hidden platform across training days; however, 5xFAD mice had a longer latency to reach the platform compared to the WT mice (**C₁.**). During probe trials, 5xFAD mice spent significantly less time in the target quadrant than WT littermates (**C₂.**), indicating a memory deficit. Asterisks (*), daggers (†), and double daggers (‡) represent significant values at p < 0.05.

4.4.5 β-amyloid Deposition

To measure the deposition of Aβ plaques with age, sections from 5xFAD mice at 3 time points (1.5, 4, and 10 months) were stained with BTA-1 and imaged using confocal microscopy. The plaques density (# of plaques/μm^3) within two hippocampal regions (CA1 and DG) was quantified (**Figure 4.7**). The results show a significant increase in plaque density in the 10-month mice compared to the 4-month mice in both the CA1 region ($p < 0.0001$; unpaired t-test) and DG ($p < 0.0001$; unpaired t-test). These data show an age-dependent progressive increase in β-amyloid plaque deposition in both the CA1 region and DG.
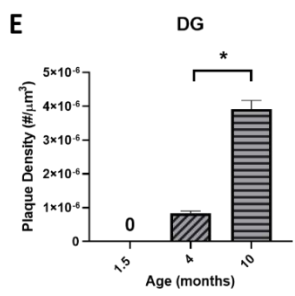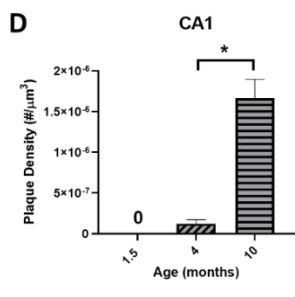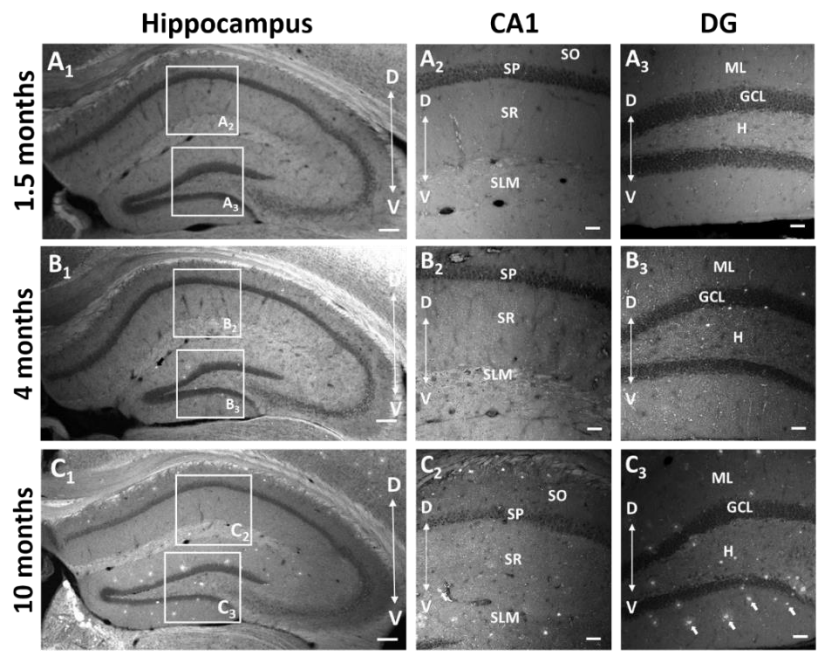
Figure 4.7. Amyloid-β (Aβ) Plaque Deposits in the Hippocampus of 5xFAD Mice.

Coronal sections (40 µm) of the dorsal hippocampus (AP, -2.0 bregma) from 1.5, 4, and 10-month-old 5xFAD mice were stained with the amyloid imaging agent BTA-1. **A$_1$-C$_1$)** Representative images of the hippocampus of 5xFAD mice demonstrating the observed age-dependent increase in Aβ plaque accumulation and the regions of interest (ROI) in CA1 and dentate gyrus (DG) that were used to quantify Aβ plaque density. **A$_{2,3}$ – C$_{2,3}$)** Representative maximum intensity projection images (20x air; 635 µm x 635 µm x 15 µm, Δz = 5 µm) of Aβ plaque deposits in CA1 and DG from 1.5, 4, and 10-month-old 5xFAD mice. Arrows in panel C$_3$ point to BTA-1 stained Aβ plaques. **D and E)** Aβ plaque density (plaque #/µm^3) was quantified in the CA1 region and DG from 20x images using the Analyze Particles plug-in in FIJI. Significant differences in Aβ plaque density were found between 4-month-old and 10-month-old 5xFAD mice. Analysis of the 1.5-month-old mice were not included because no plaques were observed. Hippocampal layers; CA1: *stratum oriens* (SO), *stratum pyramidale* (SP), *stratum radiatum* (SR), *stratum lacunosum-moleculare* (SLM) and DG: molecular layer (ML), granule cell layer (GCL) and the hilus (H). Scale bar: 4x images = 200 µm, 20x images = 50 µm. Asterisks (*) represent significance determined by a 2-tailed unpaired *t*-test with $p < 0.05$. Dorsal (D) ←→ Ventral (V).

4.5   Discussion

This study examined the relationship between neuronal Ca^{2+}-mediated variables and aging in a 5xFAD mice on a C57BL/6 genetic background. We conducted this series of experiments using electrophysiological and imaging techniques to report on changes in Ca^{2+} measures in brain aging. These experiments were conducted to test the hypothesis that, contrary to what is seen in normal aging, measures of Ca^{2+}-mediated processes are *reduced* in the 5xFAD transgenic model of amyloidogenesis. We based this on prior reports showing that L-VGCC density and the AHP are reduced in two different models of AD [242, 348]. In the current study, we show that changes in Ca^{2+}-mediated potentials and levels were identified across early age, sex, and genotype. Briefly, reductions in Ca^{2+}-mediated processes appear to be more robust in females compared to males in this animal model of AD (Fig. 4.4). While surprising, these results underscore a significant lack of alignment between normal aging processes and those initiated in pathological aging, suggesting that not only is AD not an accelerated form of aging, but that when considering Ca^{2+} dysregulation, these processes may actually diverge. Here, several discrepancies from the canonical Ca^{2+} hypothesis of brain aging and dementia were noted, including 1) the presence of a reduced AHP at 4 months compared to 1.5 and 10 months, 2) the presence of significant reductions in OGB-1 fluorescence (peak amplitude and AUC) in females irrespective of genotype, and 3) reduced resting fluorescence in 5xFAD mice compared to WT.

4.5.1 Onset of Ca^{2+} Dysregulation

The amyloidogenic 5xFAD model mimics human AD at an accelerated pace and presents with amyloid deposition by 1.5 to 2 months, cognitive deficits and synaptic impairment by 4 months, and neuronal loss by 6 months of age [495]. While this transgenic design is extremely well-suited for studies of specific phenotypes (*e.g.* Aβ deposition, behavior, Ca^{2+} dysregulation, oxidative stress), the aging component is seldom considered in the experimental design, likely due to the reduced life-span of these animals. Using 5xFAD mice on a C57BL/6 genetic background, we sought to incorporate components of aging within the context of AD. Compared to the original report [495], 5xFAD mice on a C57BL/6 genetic background presents with behavioral deficits starting at 10 months *vs.* 3 months of age (Fig. 4.6). With respect to the aging effect identified, our results are surprising, as a significant reduction in the AHP at 4 months of age (Fig. 4.1) was combined with an increase in excitability (Fig. 4.2) and a lack of change in short-term synaptic plasticity (Fig. 4.3) or OGB-1 fluorescence (Fig. 4.4). It should be noted, however, that relatively similar results in response to age were previously reported in the F344 rat model of aging, where Ca^{2+} dysregulation (measured through either the AHP or Ca^{2+} levels) did not manifest until 12 months of age [135]. One limitation of our study may be that we did not investigate animals at later time points. Also, very few prior studies have investigated the Ca^{2+}-dependent AHP at 1.5 months of age *ex vivo* (*i.e.* slices), suggesting more analyses around this age are warranted [127]. The "U" shape curve (a reduction at 4 months) presented in Fig. 4.1 is reminiscent of prior work in the retina measuring L-VGCC Ca^{2+} flux *in vivo* using manganese-enhanced MRI [539-541]. In disease models with progression of the neurodegenerative events ranging from days to weeks and months

(ischemic reperfusion, retinitis pigmentosa, or even diabetes, respectively), Berkowitz and colleagues find significant prodromal reductions in Ca^{2+} influx in response to initial stressors; over time manganese uptake/ L-type Ca^{2+} channel function appears to return to seemingly normal levels. Whether our "U" shape curve reflects on a combination of developmental/maturation processes or aging changes, or on initially competent Ca^{2+} handling processes that ultimately fail at latter stages requires further investigations.

Based on the increase in the Aβ load (Fig. 4.7) and the time course of progression, it seems clear that Ca^{2+} dysregulation does not parallel Aβ increases. Our current results cannot confirm that amyloid deposits in the dorsal hippocampus alter either neuronal physiology or Ca^{2+} kinetics; however, independent of age, a reduction in resting Ca^{2+} fluorescence was seen in the 5xFAD compared to the WT (Fig. 4.5). Therefore, in this model, no evidence of enhanced Ca^{2+} dysregulation was seen using sharp electrode recording techniques, and instead, possible reductions in Ca^{2+} processes were noted.

4.5.2 Differences in Techniques

Two prior studies have investigated differences between sharp electrode recording techniques and whole-cell recordings using patch electrodes [542, 543]. Aside from clear differences in recording stability and duration (AHPs can be recorded for hours in the same cell under sharp electrode conditions), input resistance and leak conductance, and the use of supplemented nucleotides, Ca^{2+} buffers, and K^+ salts, it is clear that under whole-cell recording conditions, a large amount of APs are needed to elicit a significant AHP [9, 127, 294, 543, 544]. Here, as previously reported in numerous studies of aging, we quantified the AHP following a series of 4 APs and observed that the Ca^{2+}-dependent potentials were smaller than those recorded from rat neurons [2, 7]. Typically, the mAHP amplitude in

young mice is approximately ~1.4 mV [242, 348], while the AHP (recorded with the same number of APs) from rat neurons is ~2.8 mV [135, 242, 532, 545]. This difference in technique is important when comparing measures of Ca^{2+} biomarkers across animal models of aging and AD and may underlie the current novel results while using sharp electrode physiology. Nevertheless, this does not necessarily negate previous work using Ca^{2+} imaging techniques in combination with patch-clamp electrophysiology, where several underlying mechanisms have been identified in the context of aging and AD [127, 160, 241, 281, 290, 292-294, 297, 299, 512, 546]. In fact, recent studies have presented compelling evidence that Ca^{2+}-dependent neuronal measures of hyperactivity are present in the amyloidogenic brain.

4.5.3 Alternative Ca^{2+}-Dependent Biomarkers in AD: Hyperactivity

Several recent studies show that a new Ca^{2+}-dependent biomarker of AD, previously unseen in *in vitro* studies, may be neuronal hyperactivity. Using *in vivo* multiphoton imaging, these studies have shown that, depending on the proximity to Aβ plaques, a significant increase in hyperactivity in several neuronal fields in the amyloidogenic brain is seen [335-337, 339, 340, 547, 548]. Moreover, hyperactivity in astrocytes adjacent to Aβ plaques has also been reported [549, 550], in some cases with concomitant increases in spontaneous vasoconstriction [551]. One suggested mechanism for increased neuronal hyperactivity in AD may be the reduction in glutamate reuptake via a reduction of glutamate transporters in the microenvironments surrounding Aβ plaques [340, 547]. Alternatively, this hyperexcitability could develop in response to failing Ca^{2+} buffering mechanisms, similar to those seen in basal forebrain neurons in aged animals [13, 16, 161]. Together, these alterations highlight the presence of increased hyperactivity in

112

neuronal circuits of AD which would likely translate into altered network communication during encoding.

As one may suspect, this increase in hyperexcitability could reflect on the presence of an epileptic-like phenotype in some models of AD [258, 552-556]. Age-dependent susceptibility to epilepsy has been well documented in the literature, with marked increases of epilepsy development reported in the elderly [557-561]. Epilepsy has long been characterized as a disease of neuronal hyperexcitability and abnormal firing with dysregulated Ca^{2+} as a key contributor [259, 562-567]. It is becoming evident that there is clear overlap between the profiles of these two diseases. A recent study performed in a rat model of epileptogenesis used bioinformatics to identify regulatory proteins in the hippocampal and parahippocampal brain regions that overlap in AD and epilepsy [513]. Among the shared dysregulated proteins of these diseases, 63 were identified to be involved with both mitochondrial function and Ca^{2+} homeostasis. At the least, these alterations certainly highlight AD as a disease of synaptic dysfunction that propagates intracellular dysregulation. Thus, it is clear that further characterization of this novel Ca^{2+}-dependent biomarker of AD is needed.

While previous work in the field of neuronal excitability in aging has mostly remarked on reduced synaptic excitability, especially with respect to the larger AHP, but also reduced synaptic connectivity [2, 8, 9, 294, 568-571], our results showing an age-dependent reduction in the AHP (at 4 months), elevations in *I/O* slope, and reductions in resting Ca^{2+} align relatively well with a potential phenotype of hyperexcitability. As expected, reductions in Ca^{2+} and Ca^{2+}-mediated cellular events (*i.e.* AHP) seem likely to

engage hyperactivity processes, increase network communication, and, perhaps, reduce the threshold for epileptogenesis in this animal model of AD.

4.6 Conclusions

While our study does not identify increases in Ca^{2+} dysregulation in the 5xFAD animals compared to WT littermates across age, it does highlight the possibility that Ca^{2+}-related processes in aging may be significantly different than those seen in AD. Further, studies investigating older animals (*i.e.* > 12 months of age) are needed to test whether Aβ accumulation induces Ca^{2+} dysregulation. It appears that neuronal hyperactivity may be a reliable reporter of Ca^{2+} dysregulation in AD; as such, further *in vivo* investigations are needed to identify new therapeutic strategies targeting anti-epileptic processes. In fact, both basic research studies and clinical trials have already been initiated to explore the efficacy of anti-epileptic drugs in the context of AD, with potentially promising results having been reported [260, 572-577]. Additional investigations will be needed as we further elucidate the precipitating factors involved with these two disease states.

4.7 Acknowledgments

4.8 Conflict of Interest/Disclosure Statement

The authors have no conflict of interest to report.

CHAPTER 5. DISCUSSION, LIMITATIONS, AND FUTURE DIRECTIONS

5.1   Discussion

5.1.1 Recap of *Aldh2*$^{-/-}$ and 5xFAD Study Results

Using sharp electrode electrophysiological and Ca^{2+} imaging techniques, direct and indirect Ca^{2+}-dependent processes were characterized in two AD mouse models at 1.5, 4, and 10 months of age. These models, the *Aldh2*$^{-/-}$ and 5xFAD, were specifically chosen to represent sporadic and familial Alzheimer's disease, respectively. Further, these models manifest similar AD phenotypes progressively, from birth, that align relatively well with the early phases of aging. The *Aldh2*$^{-/-}$ model develops high quantities of lipid peroxidation byproduct HNE through the knockdown of the *ALDH2* gene, which promotes elevated oxidative stress, morphological and quantitative atrophy to dendritic processes, Aβ monomers and oligomers, phosphorylated tau, and cognitive impairment. The 5xFAD mouse, however, develops amyloid deposits, synaptic dysfunction, and cognitive deficit phenotypes through the genetic manipulation of *APP*, *PSN1*, and *PSN2* genes. As neuronal Ca^{2+} handling has not been well characterized alongside aging in animal models of AD, it was of interest to directly measure Ca^{2+}, as well as Ca^{2+} signaling in these two very different mice.

The significant findings of these two studies illustrate that Ca^{2+}-mediated alterations differ across animal models of AD. In the *Aldh2*$^{-/-}$ study, very few neuronal alterations were observed despite the increasing levels of oxidative stress as the mice aged. Of these alterations, only an age-related decrease in the AHP, a genotype-mediated elevation in the slow AHP amplitude, and a genotype-driven decrease in LTP maintenance

were noted in the *Aldh2$^{-/-}$* knockout group. Alternatively, in addition to MWM behavioral deficits and increases in amyloid deposits with age, 5xFAD mice showed considerable changes in their neuronal physiology. Indeed, while age-related decrease (1.5 to 4 months of age) *and* increase (4 to 10 months) in amplitude were noted across 5xFAD and WT genotypes in AHP measures, a robust sex difference was present during Ca^{2+} imaging showing less Ca^{2+} in neurons of female mice during synaptic stimulation. Further, in general, 5xFAD mice had less resting Ca^{2+} compared to their WT counterparts, irrespective to age or sex. Together, these studies showed no evidence of increased neuronal Ca^{2+} to propagate the development of AD-like phenotypes in either model.

Table 5.1. Summary of *Aldh2*$^{-/-}$ and 5xFAD Results.

Outcome Measure		5xFAD Male	5xFAD Female	*Aldh2*$^{-/-}$ Male	*Aldh2*$^{-/-}$ Female
AHP	mAHP (mV)	sig. age "U"	sig. age "U"	sig. age ↓	sig. age ↓ / sig. sex ↓
	sAHP (mV)	sig. age "U"	sig. age "U"	sig. age ↓ / sig. gen. ↓	sig. age ↓ / sig. gen. ↓
	Duration (s)	sig. age "U"	sig. age "U"	n.s.	n.s.
I/O Slope (mV/V)	Synaptic Activation	sig. age "U"	sig. age "U"	n.s.	n.s.
RSS	Synaptic Hyperpolarization (mV)	n.s.	n.s.	n.s.	n.s.
	Early EPSP (% FF)	n.s.	n.s.	n.s.	n.s.
	Late EPSP (% FF)	sig. age ↑	sig. age ↑	n.s.	n.s.
Ca^{2+} Imaging (During RSS)	AUC (ΔF/F (%)*s)	sig. age ↑	sig. age ↑ / sig. sex ↓	n.s.	n.s.
	Peak Amplitude (ΔF/F (%))	sig. age ↑	sig. age ↑ / sig. sex ↓	n.s.	n.s.
	Rise Time (s)	n.s.	n.s.	n.s.	n.s.
	Decay Time (s)	n.s.	n.s.	n.s.	n.s.
Normalized Resting Fluorescence (F/um)		sig. gen. ↓	sig. gen. ↓	n.s.	n.s.

Table 5.1. Summary of *Aldh2*$^{-/-}$ and 5xFAD Results. Compilation of neuronal Ca^{2+} handling results across age, genotype, and sex in *Aldh2*$^{-/-}$ and 5xFAD mouse models. An age-mediated reduction in the AHP amplitude was observed in the mAHP and sAHP outcome measures of the *Aldh2*$^{-/-}$ mice. Additionally, a main effect of sex was present as a reduction in the mAHP, while a genotype-driven decrease in the sAHP was also identified in the *Aldh2*$^{-/-}$ group. In the 5xFAD mice, measures of the mAHP, sAHP, and AHP duration showed a decrease from 1.5 to 4 months of age, followed by an increase from 4 to 10 months. This unique "U" shaped curve is discussed in **Chapter 4.5.1**. Measures of synaptic activation via an *I/O* curve revealed an increase, then a decrease across age in the 5xFAD mice; an expected inverse of the AHP data. While no other significant alterations were identified in outcome measures of the *Aldh2*$^{-/-}$ data, significant age-related increases were observed in late EPSP, AUC, and peak amplitude measures of the 5xFAD mice. Further, a sex-mediated reduction in the AUC and peak amplitude was noted in female 5xFAD animals. A main effect of genotype was also seen in the 5xFAD group as a reduction in resting fluorescence. Significance was determined as $p < 0.05$. A main effect of age is highlighted in yellow, sex in blue, and genotype (gen.) in green. No significance is represented as "n.s.".

5.1.2 Familial vs. Sporadic AD Model Design

With inconsistencies of Ca^{2+} dysregulation (i.e. elevations *and* reductions) observed in both animal and culture models of AD (here and in previous literature), perhaps the initial hypothesis that elevated neuronal Ca^{2+} in AD progression is a gross generalization that lacks relevance across all AD models. Considering fAD only accounts for a small fraction (~5%) of total human AD cases and sAD (95%) remains more prevalent, the primary use of transgenic models with fAD gene mutations in AD research may be hindering the growth of the field. Further, it is important to note that in addition to fAD cases being less prevalent, symptoms manifest as early as 30 years of age and this type of dementia is not only more severe, but progresses faster. With sAD patients generally showing symptoms by 65 years of age and progressing more slowly, research models have not been effectively recapitulating AD phenotypes to mimic what is observed in humans. However, it should be emphasized that the focus on using fAD models in AD research is due to the poorly understood nature of sAD development, as the latter is likely due to a culmination of genetic, environmental, lifestyle, and metabolic risk factors. That being said, the understanding of sAD is still developing. Only recently was an ER and plasma membrane channel called calcium homeostasis modulation 1 (CALHM1) identified as being linked to a gene polymorphism that increases sAD risk by decreasing Ca^{2+} permeability and increases Aβ production [578, 579]. Nevertheless, as fAD and sAD have similar phenotypes, there is value in drawing comparisons between research models of each type to better understand AD development and progression as a whole. In addition to the incorporation of genetic mutations, careful consideration of an animal's genetic background should be made when selecting a research model to study.

5.1.3 Genetic Background of Research Models

Importantly, an animal's genetic background can drastically alter phenotypic expression, meaning greater emphasis must be placed on comparing animal models of like backgrounds. Indeed, early studies assessing the impact of genetic backgrounds on learning behavioral tasks and fear conditioning have squarely implicated animal strain as a participating factor in both learning enhancements and deficits [580]. In concert with gene mutations, genetic background differences can elicit staggering variability to physiological phenomena like neuronal excitability and the post-burst AHP as well [431]. Additionally, choosing whether to work with an inbred or outbred strain of an animal model is just as important. While an enhancement in the AHP has classically been shown in aged *inbred* F344 rats [182], the *outbred* Long Evans rat model seems to show a reduction in the AHP of aged animals [581]. Here, the *Aldh2$^{-/-}$* and 5xFAD mouse strains were both of a C57BL/6 genetic background in the experimental studies. Thus, genetic background variability should not have confounded data comparisons between the respective mouse models.

5.1.4 Neuronal Excitability in the Animals

In **Chapter 4.5.3** it was discussed how in the 5xFAD mice there was an observed increase in neuronal excitability accompanied by a reduction in the AHP, decreased levels of resting Ca^{2+}, and the early production of Aβ plaques by 4 months of age. As AD and epilepsy profiles seem to share many dysregulated proteins [513] and considering the growing evidence of neuronal hyperactivity in the amyloidogenic brain [335-337, 339, 340, 547, 548], we concluded that, perhaps, a reduced threshold of epileptogenesis could be the byproduct of dysregulated Ca^{2+} and Ca^{2+}-mediated processes. It is curious, however, that while Aβ promotes oxidative stress [229], synaptic deficits [230], and excitotoxicity [229,

231], we should see very little change in hyperactivity in the *Aldh2$^{-/-}$* mice. Given the well-established relationship between ROS promoting neuronal hyperexcitability [582-585], it is surprising that no increases in excitability were noted in the *Aldh2$^{-/-}$* mice, a model of excess oxidative stress. Notably in contrast to the 5xFAD, we saw no changes in resting or stimulated Ca^{2+} levels in neurons of the *Aldh2$^{-/-}$* mice. Also, while Aβ has been characterized in the *Aldh2$^{-/-}$* mice, no histochemical staining of plaques was conducted in this study, therefore the severity of plaque deposition in the *Aldh2$^{-/-}$* mice may be significantly less than in the 5xFAD. It is possible that oxidative stress alone is not enough to promote the hyperexcitability phenotype, but rather it is when oxidative stress is coupled with pronounced dysregulated Ca^{2+} or Aβ plaques that chronic excitability persists.

5.1.5 Animal Sexes

With a by and large push for sex inclusion as a variable in basic research, we decided to acquire data from both male and female mice in each study. To our surprise, sex differences were mostly absent across outcome measures. In the 5xFAD data, significant reductions in the area-under-the-curve and peak amplitude Ca^{2+} measures were observed in neurons from female mice compared to their male counterparts, regardless of genotype. Though sex differences were not shown in the *Aldh2$^{-/-}$* study (due to low n) as stated in **Chapter 2.4.2**, a significant sex-mediated reduction in the mAHP of female mice was indeed present. Upon combining sexes, an age-driven decrease in the mAHP was present in both *Aldh2$^{-/-}$* and WT mice. As past work has shown, estrogen plays an important role in the mediation of Ca^{2+}-dependent processes. As estrogen levels decrease, L-VGCC expression increases [122], while application of estrogen receptor agonists decrease the AHP amplitude [102], elevate NMDA receptor density [71], increase dendritic spines and

synaptic density [187, 509], mitigate age-mediated L-VGCC current increases [96], and reduce intracellular Ca^{2+} release [191]. Thus, our results of reduced Ca^{2+} during synaptic stimulation in neurons of female mice compared to males may align with previous literature. Considering the previously described benefits of estrogen replacement therapy to reduce AD incidence [96, 353-357], there is clearly a necessity for further measures pertaining to estrogen in future studies. Moreover, as AD prevalence is three times greater in women than men likely due to post-menopausal depletions in estrogen levels [185] and considering rodent perimenopause typically occurs between 9-12 months of age [586-589], it is also possible that our mice were not aged enough to observe estrogen-mediated declines in Ca^{2+} processes. It should be noted, however, that data pertaining to the reproductive cycle of 5xFAD and $Aldh2^{-/-}$ mice is limited.

5.2 Study Limitations

5.2.1 Animal Age

As measuring changes in neuronal Ca^{2+} handling during aging was an important aspect of these studies, it should be noted that, perhaps, our animals were not aged enough to detect more drastic alterations to the AHP, synaptic plasticity, and Ca^{2+} levels. The selected timelines were indeed favorable to account for recording outcome measures before, during, and after amyloidogenesis, however, it is possible that the extent of degeneration was not fully realized by 10 months of age. For instance, in previous work measuring the AHP in 3xTg and $PS1_{KI}$ mice at 6 weeks, 6 months, and 18 months of age, a significant age-driven increase was not identified until 18 months [127]. Similarly, in

3xTg mice of 1, 6-9, and 12-16 months of age, age-dependent increases in NMDA and L-VGCC current were only present by 12-16 months [241]. Even regarding measurements of Ca^{2+} binding proteins, previous work has shown an increase in calbindin immunoreactivity of $APP_{SWE}/PS1dE9$ at 3 months but a decrease by 12 months, suggesting an initial compensatory mechanism that is later downregulated [309]. Considering our 5xFAD design was curated to induce a slower developing amyloidogenesis, it is possible that dire alterations to Ca^{2+} kinetics are not present until a timepoint beyond 10 months of age. In the interest of time and limited resources, the truncated timeline (*i.e.* 1.5, 4, and 10 months) that was used in our studies did serve the purpose of reporting gradual changes in Ca^{2+} processes. Nevertheless, it is of interest to acquire data at later ages in future studies to further characterize a comprehensive picture of neuronal Ca^{2+} handling during aging.

5.2.2 Shipping of Animals

The inter-lab collaborations of these studies cultivated meaningful exchanges of knowledge, expertise, and resources. Further, a large component of these collaborations was the transportation of cohorts of mice from either Queens U. or the U. of Michigan to the U. of Kentucky. In carefully coordinated shipments, 20+ mice were sent to us at a time, pending inclement weather conditions were not in the immediate forecast. At times of extreme weather, transportation of animals was challenging to navigate and impactful to data acquisition. Considering animals were to be utilized at specific timepoints, during offset schedules I would have to rearrange my schedule accordingly to accommodate for these unexpected delays to assure timelines were met. More recently we had plans to measure network Ca^{2+} handling using a two-photon imaging approach. However, due to

the SARS-CoV-2 pandemic of 2020 affecting colony maintenance and shipment of animals, we had to forego these plans until a later time.

5.2.3 Alternative Brain Regions

While the experiments in **Chapters 2** and **4** were conducted using hippocampal sections, it is of interest to explore neuronal Ca^{2+} handling in alternative brain structures as well. As highlighted in **Chapter 1**, Ca^{2+} levels, kinetics, and processing seem to vary based on brain region, which may be linked to a divergence in normal brain aging and a pathogenic AD brain. In fact, early literature has illustrated significant alterations in Ca^{2+} metabolism across brain structures as rodents age [590]. For example, while it has been shown that L-VGCC density, Ca^{2+} currents, mRNA protein expression levels, and their post-translational phosphorylation state are increased in hippocampal neurons of aged rats [80, 95-102], expression patterns and function of L-VGCCs are not altered in cortical neurons [120, 121]. Further, some CBP activity has been notably decreased in hippocampal tissue [149-151], but is increased in basal forebrain neurons [16, 160, 161]. These examples are not exclusive to just animal models, however. As mentioned in **Chapter 1**, in autopsied human AD patients reductions of ER IP_3R density have been noted in hippocampal and parietal lobe tissue, but no significant alterations were present in frontal, temporal, or occipital lobes [301]. Thus, while this limitation underscores the many permutations of conducting neuronal Ca^{2+} handling research as it pertains to a brain structure of interest, it also highlights the vast amount of possibilities for future directions, especially with regard to neuronal network communication.

5.3   Future Directions

5.3.1 Imaging of Ca^{2+} Network

Indeed, there are many different future directions that this work can take. First and foremost, our lab has plans to shift the focus of recording Ca^{2+} changes in single neurons to two-photon imaging of neuronal and astrocytic networks. Through both adeno-associated virus injections and genetically modified rodents with Ca^{2+} indicator encoded neurons, we have already generated promising preliminary data. In 5xFAD mice genetically modified with GCaMP6, it seems that Ca^{2+} dysregulation may impact neuronal density, firing patterns, and distance of communication. It is of interest to assess how gradual amyloidogenesis (5xFAD) or free oxygen radicals ($Aldh2^{-/-}$) affect these important neuronal communication properties. A common concern in single-neuron recordings is that only healthy neurons are being measured while degeneration-impacted neurons are not healthy enough to be electrophysiologically recorded. While this is accounted for by acquiring neuronal health measures (see **Chapters 2.4.1** and **4.3.9**), field imaging of a network of neurons that are simultaneously stimulated provide greater insight to the widespread physiologic implications of neurodegeneration. While single-cell recordings show a piece of a puzzle, field imaging tells a comprehensive story of how those pieces fit together and should be considered for future studies.

5.3.2 Amyloid Plaques in $Aldh2^{-/-}$ Mice

Considering that amyloid plaques are widely considered a hallmark of AD and though concentrations of Aβ have been identified in the $Aldh2^{-/-}$ model, the extent of Aβ accumulation and how it compares with the 5xFAD mice across age requires more

attention. In the 5xFAD model, it was clear that by 4 months of age the amyloid deposits were starting to accumulate in region CA1 and the DG, and were substantially elevated in both of these hippocampal subregions by 10 months (**Chapter 4.4.5**). This measurement elicited valuable comparisons between amyloid load, Ca^{2+} levels, and pre-/post-synaptic events including the observation of a reduced AHP and elevated *I/O* excitability in concert with amyloid generation. As oxidative stress has been long thought to play a robust role in APP metabolism [401, 591-595], it is of utmost interest to characterize a timeline of amyloid plaque progression as it aligns with increasing oxygen radical load. Further, normalization of Aβ concentrations and neuronal Ca^{2+} levels between the 5xFAD and *Aldh2$^{-/-}$* models may provide evidence of the magnitude of impact that oxidative stress has on global cell health. Lastly, with the characterization of Aβ concentrations across age, this future direction may also lead to identifying how changes in Aβ, Ca^{2+}, synaptic communication, and oxidative stress affect intracellular regulatory factors like Ca^{2+} binding protein levels.

5.3.3 Ca^{2+} Binding Protein Measures

Another important measure that can be further investigated is the impact of the age, sex, and genotype of these models on the regulation of Ca^{2+} binding proteins (CBPs). As discussed in **Chapters 1.4.3** and **1.12.3**, CBPs have an invaluable role in Ca^{2+} ion buffering and signaling that can be compromised during aging and in AD progression. Unfortunately, measures of CBPs were not conducted in these studies. It would be fascinating to quantitate various CBPs such as calbindin or calretinin that have been shown to decrease in the hippocampus of aged and AD animals, which has led to reduced synaptic strength [149, 150, 309, 310]. Further, in the 5xFAD mouse that showed reduced resting Ca^{2+} compared

to WT, as well as a sex-mediated decrease in stimulated Ca^{2+} in females compared to males, CBP quantification may reveal additional sex- or genotype-related alterations to neuron physiology in these mice. Also, considering calcineurin has been shown to participate in the enhancement of L-VGCC function in aging [101, 159], measuring its level of activation in the context of decreased resting or stimulated Ca^{2+} may be another outcome measure worthy of attention. In conjunction with this, the application of Ca^{2+} agonists or blockers would surely help to elucidate if L-VGCCs participate in the decreases of Ca^{2+} observed in the 5xFAD model.

5.3.4 Ca^{2+} Blockers and Other Therapeutics

The use of Ca^{2+} channel agonists and blockers has provided the field with a better understanding of intra- and extracellular neuronal Ca^{2+} handling through the characterization of Ca^{2+} sources and their function. Additionally, although controversial, the translatability of Ca^{2+} channel blockers in clinical studies has helped to validate the Calcium Hypothesis of Brain Aging and ultimately Ca^{2+}'s role in AD progression. Thus, as a future direction of these studies, the inclusion of Ca^{2+}-related drugs and other therapeutics might navigate researchers to better identify the chronological order of abnormal cellular process as animal models of AD age. For instance, though reduced resting Ca^{2+} in the 5xFAD mice and overall less stimulated Ca^{2+} in females was observed in that study, it is unclear where the source of decreased Ca^{2+} originates. If the sex-mediated reduction in Ca^{2+} is related to estrogen levels, then perhaps introducing 17beta-estradiol benzoate to hippocampal slices during electrophysiological recordings might abolish the AHP amplitude [102]. However, if a reduction in L-VGCC current is present as previously observed in the 5xFAD mouse [348], as well as the 2xTg model [242], then perhaps

application of 17beta-estradiol may further reduce L-VGCC activity [96]. If indeed decreased L-VGCC channel activity is a source of reduced resting Ca^{2+} in this model, then it may be of interest to test the effect of L-VGCC agonist Bay K8644 on increasing resting Ca^{2+} in the 5xFAD mice [11]. Regarding the *Aldh2^{-/-}* study, though few phenotypic alterations were observed, the use of antioxidant or photobiomodulation interventions to buffer oxidative stress and regulate downstream alterations like Aβ production and synaptic deficits could be of interest. Overall, great insights can be made by targeting specific organelles involved in Ca^{2+} events with therapeutics and determining their impact in these two models, with respect to age, sex, and genotype.

5.4   Conclusions

Ca^{2+} is an essential ion involved in many physiologic events necessary for biological homeostasis. In the brain, Ca^{2+} is utilized by neurons when eliciting action potentials in specific patterns and frequencies to communicate neurochemical messages, as well as in the encoding and erasure of memories. It is important that Ca^{2+} is regulated at specific concentrations both inside and outside of neurons to maintain normal action potential properties. In aging and AD, it has been noted that neuron Ca^{2+} levels deviate from homeostatic concentrations, which leads to widespread physiologic impairment. This deviation, coined "calcium dysregulation", was once widely thought to manifest as *elevated* intracellular Ca^{2+} levels, as it was historically observed in models of aging. However, in addition to the work shown here, a growing body of literature suggests that intracellular neuronal Ca^{2+} concentrations and handling in AD not only deviates from normal aging, but may actually be *reduced* [242, 348, 525].

Given AD is a neurodegenerative disease that progresses in late-life, it was often assumed that 1) AD is an accelerated form of aging and 2) elevated intracellular Ca^{2+} may give rise to disease development. AD development, however, can be subdivided into two categories: fAD, which makes up 5% of total cases, and sAD, the other 95%. Basic research has implicated mutations of the *APP*, *PSN1*, and *PSN2* genes as primary promoters of fAD, which have been modeled in transgenic animals of AD. Many fAD models have shown increased intracellular Ca^{2+} due to the inclusion of the ER Ca^{2+} channel-modifying PS mutations, despite the lack of this genetic mutation in most human AD cases. In fact, many animal models of AD have shown either no changes or reduced neuronal Ca^{2+}. We sought to further investigate this by measuring Ca^{2+} and Ca^{2+}-mediated processes across age in both fAD and sAD mouse models.

Here, we showed that resting Ca^{2+} levels were reduced in neurons of a model of fAD and unaltered in sAD. There were clear AD-related deficits that developed in each model as the mice aged, but these impairments were not due to *elevated* neuronal Ca^{2+}. As Ca^{2+} dysregulation has been shown to have a robust role in disrupting many neuronal processes, it is not to say that Ca^{2+} dyshomeostasis does not warrant downstream cellular abnormalities. However, perhaps the dogma of the Calcium Hypothesis of Brain Aging has become too generally accepted and its philosophy of increased neuronal Ca^{2+} with aging has somewhat hindered growth of the field. Common factors like genetic background, sex, and gene mutations clearly impact phenotypic expression of animal models. Coupled with the fact that the AD field lacks a perfect AD surrogate that mimics human pathology progression, it is understandable that controversial findings have riddled researchers. Indeed, it is difficult to control every experimental variable in a study, however through

the careful consideration of intrinsic biological factors and the influence they may have on other variables, new doors of discovery will undoubtedly continue to open.

APPENDIX

List of Abbreviations

Aβ	amyloid-β
ACSF	artificial cerebral spinal fluid
AD	Alzheimer's disease
AHP	afterhyperpolarization
Aldh2$^{-/-}$	aldehyde dehydrogenase 2 knockout
AMPA	α-amino-3-hydroxy-5-methylisoxazole-4- propionate
AP	action potential
APP	amyloid precursor protein
ATP	adenosine triphosphate
AUC	area-under-the-curve
CA1	Cornu Ammonis-1
CBP	Calcium binding proteins
CCE	capacitive Ca^{2+} entry
CICR	calcium-induced calcium release
DG	dentate gyrus
EPSP	excitatory post-synaptic potential

ER   endoplasmic reticulum

fPSP   field post-synaptic potentials

GCL   granule cell layer

HFS   high frequency stimulation

H   hilus

HNE   4-hydroxynonenal

ICS   intracellular calcium stores

I/O   input/output

IP_3 inositol (1, 4, 5)-trisphosphate

KO   knockout

LGCC   ligand-gated calcium channel

LPx   lipid peroxidation

LTD   long-term depression

LTP   long-term potentiation

L-VGCC   L-type voltage-gated calcium channel

mAHP   medium afterhyperpolarization

MCU   mitochondrial Ca^{2+} uniporter

mNCX   mitochondrial Na^+/ Ca^{2+} exchangers

ML	molecular layer
MWM	Morris water maze
NCX	Na^+/ Ca^{2+} exchangers
NMDA	N-methyl-D-asparate
OGB-1	Oregon Green Bapta-1
PMCA	plasma membrane Ca^{2+} ATPase
PS	presenilin
p-tau	phosphorylated tau protein
ROI	region of interest
ROS	reactive oxygen species
RSS	repeated synaptic stimulation
RyR	ryanodine receptor
sAHP	slow afterhyperpolarization
SC	Schaffer collaterals
SEM	standard error of the mean
SERCA	sarco-endoplasmic reticulum Ca^{2+}-ATPase
SO	*stratum oriens*
SOCE	store-operated Ca^{2+} entry

SLM   *stratum lacunosum-moleculare*

SP   *stratum pyramidale*

SR   *stratum radiatum*

TBI   traumatic brain injury

VGCC   voltage-gated Ca^{2+} channels

WT   wild-type

REFERENCES

[1]   Landfield PW (1987) 'Increased calcium-current' hypothesis of brain aging. *Neurobiol Aging* **8**, 346-347.

[2]   Landfield PW, Pitler TA (1984) Prolonged Ca2+-dependent afterhyperpolarizations in hippocampal neurons of aged rats. *Science* **226**, 1089-1092.

[3]   Khachaturian ZS (1989) Calcium, membranes, aging, and Alzheimer's disease. Introduction and overview. *Ann N Y Acad Sci* **568**, 1-4.

[4]   Khachaturian ZS (1994) Calcium hypothesis of Alzheimer's disease and brain aging. *Ann N Y Acad Sci* **747**, 1-11.

[5]   Disterhoft JF, Moyer JR, Jr., Thompson LT (1994) The calcium rationale in aging and Alzheimer's disease. Evidence from an animal model of normal aging. *Ann N Y Acad Sci* **747**, 382-406.

[6]   Gibson GE, Peterson C (1987) Calcium and the aging nervous system. *Neurobiol Aging* **8**, 329-343.

[7]   Kerr DS, Campbell LW, Hao SY, Landfield PW (1989) Corticosteroid modulation of hippocampal potentials: increased effect with aging. *Science* **245**, 1505-1509.

[8]   Moyer JR, Jr., Thompson LT, Black JP, Disterhoft JF (1992) Nimodipine increases excitability of rabbit CA1 pyramidal neurons in an age- and concentration-dependent manner. *J Neurophysiol* **68**, 2100-2109.

[9]   Disterhoft JF, Thompson LT, Moyer JR, Jr., Mogul DJ (1996) Calcium-dependent afterhyperpolarization and learning in young and aging hippocampus. *Life Sci* **59**, 413-420.

[10]   Landfield PW, Pitler TA, Applegate MD (1986) The effects of high Mg2+-to-Ca2+ ratios on frequency potentiation in hippocampal slices of young and aged rats. *J Neurophysiol* **56**, 797-811.

[11]   Thibault O, Hadley R, Landfield PW (2001) Elevated postsynaptic [Ca2+]i and L-type calcium channel activity in aged hippocampal neurons: relationship to impaired synaptic plasticity. *J Neurosci* **21**, 9744-9756.

[12]   Verkhratsky A, Shmigol A, Kirischuk S, Pronchuk N, Kostyuk P (1994) Age-dependent changes in calcium currents and calcium homeostasis in mammalian neurons. *Ann N Y Acad Sci* **747**, 365-381.

[13]   Murchison D, Griffith WH (1999) Age-related alterations in caffeine-sensitive calcium stores and mitochondrial buffering in rat basal forebrain. *Cell Calcium* **25**, 439-452.

[14]   Pottorf WJ, Duckles SP, Buchholz JN (2002) Aging and calcium buffering in adrenergic neurons. *Auton Neurosci* **96**, 2-7.

[15]   Toescu EC, Verkhratsky A (2003) Neuronal ageing from an intraneuronal perspective: roles of endoplasmic reticulum and mitochondria. *Cell Calcium* **34**, 311-323.

[16]   Murchison D, Zawieja DC, Griffith WH (2004) Reduced mitochondrial buffering of voltage-gated calcium influx in aged rat basal forebrain neurons. *Cell Calcium* **36**, 61-75.

[17]   Clodfelter GV, Porter NM, Landfield PW, Thibault O (2002) Sustained Ca2+-induced Ca2+-release underlies the post-glutamate lethal Ca2+ plateau in older cultured hippocampal neurons. *Eur J Pharmacol* **447**, 189-200.

[18]   Foster TC, Norris CM (1997) Age-associated changes in Ca(2+)-dependent processes: relation to hippocampal synaptic plasticity. *Hippocampus* **7**, 602-612.

[19]   Verkhratsky A, Toescu EC (1998) Calcium and neuronal ageing. *Trends Neurosci* **21**, 2-7.

[20]   Xiong J, Verkhratsky A, Toescu EC (2002) Changes in mitochondrial status associated with altered Ca2+ homeostasis in aged cerebellar granule neurons in brain slices. *J Neurosci* **22**, 10761-10771.

[21]   Toescu EC, Verkhratsky A, Landfield PW (2004) Ca2+ regulation and gene expression in normal brain aging. *Trends Neurosci* **27**, 614-620.

[22]   Kumar A, Bodhinathan K, Foster TC (2009) Susceptibility to Calcium Dysregulation during Brain Aging. *Front Aging Neurosci* **1**, 2.

[23]   Mattson MP, Chan SL (2001) Dysregulation of cellular calcium homeostasis in Alzheimer's disease: bad genes and bad habits. *J Mol Neurosci* **17**, 205-224.

[24]   Berridge MJ (1998) Neuronal calcium signaling. *Neuron* **21**, 13-26.

[25]   Berridge MJ, Lipp P, Bootman MD (2000) The versatility and universality of calcium signalling. *Nat Rev Mol Cell Biol* **1**, 11-21.

[26]   Rizzuto R (2001) Intracellular Ca(2+) pools in neuronal signalling. *Curr Opin Neurobiol* **11**, 306-311.

[27]   Orrenius S, Zhivotovsky B, Nicotera P (2003) Regulation of cell death: the calcium-apoptosis link. *Nat Rev Mol Cell Biol* **4**, 552-565.

[28]   Verkhratsky A, Mattson MP, Toescu EC (2004) Aging in the mind. *Trends Neurosci* **27**, 577-578.

[29]   Bootman MD, Collins TJ, Peppiatt CM, Prothero LS, MacKenzie L, De Smet P, Travers M, Tovey SC, Seo JT, Berridge MJ, Ciccolini F, Lipp P (2001) Calcium signalling--an overview. *Semin Cell Dev Biol* **12**, 3-10.

[30]   Michaelis EK (1998) Molecular biology of glutamate receptors in the central nervous system and their role in excitotoxicity, oxidative stress and aging. *Prog Neurobiol* **54**, 369-415.

[31]   Meldrum BS (2000) Glutamate as a neurotransmitter in the brain: review of physiology and pathology. *J Nutr* **130**, 1007S-1015S.

[32]   Ghosh A, Ginty DD, Bading H, Greenberg ME (1994) Calcium regulation of gene expression in neuronal cells. *J Neurobiol* **25**, 294-303.

[33]   Geiger JR, Melcher T, Koh DS, Sakmann B, Seeburg PH, Jonas P, Monyer H (1995) Relative abundance of subunit mRNAs determines gating and Ca2+ permeability of AMPA receptors in principal neurons and interneurons in rat CNS. *Neuron* **15**, 193-204.

[34]   Moccia F, Zuccolo E, Soda T, Tanzi F, Guerra G, Mapelli L, Lodola F, D'Angelo E (2015) Stim and Orai proteins in neuronal Ca(2+) signaling and excitability. *Front Cell Neurosci* **9**, 153.

[35]   Giladi M, Shor R, Lisnyansky M, Khananshvili D (2016) Structure-Functional Basis of Ion Transport in Sodium-Calcium Exchanger (NCX) Proteins. *Int J Mol Sci* **17**.

[36]   Carafoli E (1991) Calcium pump of the plasma membrane. *Physiol Rev* **71**, 129-153.

[37]   Wang X, Zheng W (2019) Ca(2+) homeostasis dysregulation in Alzheimer's disease: a focus on plasma membrane and cell organelles. *FASEB J* **33**, 6697-6712.

[38]   Duchen MR (2000) Mitochondria and calcium: from cell signalling to cell death. *J Physiol* **529 Pt 1**, 57-68.

[39]   Nicholls DG, Budd SL (2000) Mitochondria and neuronal survival. *Physiol Rev* **80**, 315-360.

[40]   Toescu EC (2000) Mitochondria and Ca(2+) signaling. *J Cell Mol Med* **4**, 164-175.

[41]   Solovyova N, Veselovsky N, Toescu EC, Verkhratsky A (2002) Ca(2+) dynamics in the lumen of the endoplasmic reticulum in sensory neurons: direct visualization of Ca(2+)-induced Ca(2+) release triggered by physiological Ca(2+) entry. *EMBO J* **21**, 622-630.

[42]   Toescu EC, Verkhratsky A (2004) Ca2+ and mitochondria as substrates for deficits in synaptic plasticity in normal brain ageing. *J Cell Mol Med* **8**, 181-190.

[43]   McGuinness L, Bardo SJ, Emptage NJ (2007) The lysosome or lysosome-related organelle may serve as a Ca2+ store in the boutons of hippocampal pyramidal cells. *Neuropharmacology* **52**, 126-135.

[44]   Murchison D, Griffith WH (2007) Calcium buffering systems and calcium signaling in aged rat basal forebrain neurons. *Aging Cell* **6**, 297-305.

[45]   Putney JW, Jr. (2003) Capacitative calcium entry in the nervous system. *Cell Calcium* **34**, 339-344.

[46]   Bennett DL, Bootman MD, Berridge MJ, Cheek TR (1998) Ca2+ entry into PC12 cells initiated by ryanodine receptors or inositol 1,4,5-trisphosphate receptors. *Biochem J* **329 (Pt 2)**, 349-357.

[47]   Smyth JT, Hwang SY, Tomita T, DeHaven WI, Mercer JC, Putney JW (2010) Activation and regulation of store-operated calcium entry. *J Cell Mol Med* **14**, 2337-2349.

[48]   Hanley JG (2018) The Regulation of AMPA Receptor Endocytosis by Dynamic Protein-Protein Interactions. *Front Cell Neurosci* **12**, 362.

[49]   Fernandez de Sevilla D, Buno W (2010) The muscarinic long-term enhancement of NMDA and AMPA receptor-mediated transmission at Schaffer collateral synapses develop through different intracellular mechanisms. *J Neurosci* **30**, 11032-11042.

[50]   Lynch G, Granger R (1992) Variations in synaptic plasticity and types of memory in corticohippocampal networks. *J Cogn Neurosci* **4**, 189-199.

[51]   Landfield PW, McGaugh JL, Lynch G (1978) Impaired synaptic potentiation processes in the hippocampus of aged, memory-deficient rats. *Brain Res* **150**, 85-101.

[52]   Rosenzweig ES, Barnes CA (2003) Impact of aging on hippocampal function: plasticity, network dynamics, and cognition. *Prog Neurobiol* **69**, 143-179.

[53]   Behr J, Wozny C, Fidzinski P, Schmitz D (2009) Synaptic plasticity in the subiculum. *Prog Neurobiol* **89**, 334-342.

[54]   Shapiro M (2001) Plasticity, hippocampal place cells, and cognitive maps. *Arch Neurol* **58**, 874-881.

[55]   Nicoll RA, Kauer JA, Malenka RC (1988) The current excitement in long-term potentiation. *Neuron* **1**, 97-103.

[56]   Cummings JA, Mulkey RM, Nicoll RA, Malenka RC (1996) Ca2+ signaling requirements for long-term depression in the hippocampus. *Neuron* **16**, 825-833.

[57]   Bonhaus DW, Perry WB, McNamara JO (1990) Decreased density, but not number, of N-methyl-D-aspartate, glycine and phencyclidine binding sites in hippocampus of senescent rats. *Brain Res* **532**, 82-86.

[58]   Kito S, Miyoshi R, Nomoto T (1990) Influence of age on NMDA receptor complex in rat brain studied by in vitro autoradiography. *J Histochem Cytochem* **38**, 1725-1731.

[59]   Miyoshi R, Kito S, Doudou N, Nomoto T (1991) Influence of age on N-methyl-D-aspartate antagonist binding sites in the rat brain studied by in vitro autoradiography. *Synapse* **8**, 212-217.

[60]   Tamaru M, Yoneda Y, Ogita K, Shimizu J, Nagata Y (1991) Age-related decreases of the N-methyl-D-aspartate receptor complex in the rat cerebral cortex and hippocampus. *Brain Res* **542**, 83-90.

[61]   Wenk GL, Walker LC, Price DL, Cork LC (1991) Loss of NMDA, but not GABA-A, binding in the brains of aged rats and monkeys. *Neurobiol Aging* **12**, 93-98.

[62]   Magnusson KR (1995) Differential effects of aging on binding sites of the activated NMDA receptor complex in mice. *Mech Ageing Dev* **84**, 227-243.

[63]   Magnusson KR, Kresge D, Supon J (2006) Differential effects of aging on NMDA receptors in the intermediate versus the dorsal hippocampus. *Neurobiol Aging* **27**, 324-333.

[64]   Billard JM, Rouaud E (2007) Deficit of NMDA receptor activation in CA1 hippocampal area of aged rats is rescued by D-cycloserine. *Eur J Neurosci* **25**, 2260-2268.

[65]   Das SR, Magnusson KR (2008) Relationship between mRNA expression of splice forms of the zeta1 subunit of the N-methyl-D-aspartate receptor and spatial memory in aged mice. *Brain Res* **1207**, 142-154.

[66]   Liu P, Smith PF, Darlington CL (2008) Glutamate receptor subunits expression in memory-associated brain structures: regional variations and effects of aging. *Synapse* **62**, 834-841.

[67]   Zhao X, Rosenke R, Kronemann D, Brim B, Das SR, Dunah AW, Magnusson KR (2009) The effects of aging on N-methyl-D-aspartate receptor subunits in the synaptic membrane and relationships to long-term spatial memory. *Neuroscience* **162**, 933-945.

[68]   Barnes CA, Rao G, Shen J (1997) Age-related decrease in the N-methyl-D-aspartateR-mediated excitatory postsynaptic potential in hippocampal region CA1. *Neurobiol Aging* **18**, 445-452.

[69]   Eckles-Smith K, Clayton D, Bickford P, Browning MD (2000) Caloric restriction prevents age-related deficits in LTP and in NMDA receptor expression. *Brain Res Mol Brain Res* **78**, 154-162.

[70]   Mesches MH, Gemma C, Veng LM, Allgeier C, Young DA, Browning MD, Bickford PC (2004) Sulindac improves memory and increases NMDA receptor subunits in aged Fischer 344 rats. *Neurobiol Aging* **25**, 315-324.

[71]   Adams MM, Morrison JH, Gore AC (2001) N-methyl-D-aspartate receptor mRNA levels change during reproductive senescence in the hippocampus of female rats. *Exp Neurol* **170**, 171-179.

[72]   Liu F, Day M, Muniz LC, Bitran D, Arias R, Revilla-Sanchez R, Grauer S, Zhang G, Kelley C, Pulito V, Sung A, Mervis RF, Navarra R, Hirst WD, Reinhart PH, Marquis KL, Moss SJ, Pangalos MN, Brandon NJ (2008) Activation of estrogen receptor-beta regulates hippocampal synaptic plasticity and improves memory. *Nat Neurosci* **11**, 334-343.

[73]   Sonntag WE, Bennett SA, Khan AS, Thornton PL, Xu X, Ingram RL, Brunso-Bechtold JK (2000) Age and insulin-like growth factor-1 modulate N-methyl-D-aspartate receptor subtype expression in rats. *Brain Res Bull* **51**, 331-338.

[74]   Wang LY, Orser BA, Brautigan DL, MacDonald JF (1994) Regulation of NMDA receptors in cultured hippocampal neurons by protein phosphatases 1 and 2A. *Nature* **369**, 230-232.

[75]   Heidinger V, Manzerra P, Wang XQ, Strasser U, Yu SP, Choi DW, Behrens MM (2002) Metabotropic glutamate receptor 1-induced upregulation of NMDA receptor current: mediation through the Pyk2/Src-family kinase pathway in cortical neurons. *J Neurosci* **22**, 5452-5461.

[76]   Ben-Ari Y, Aniksztejn L, Bregestovski P (1992) Protein kinase C modulation of NMDA currents: an important link for LTP induction. *Trends Neurosci* **15**, 333-339.

[77]   Chen L, Huang LY (1992) Protein kinase C reduces Mg2+ block of NMDA-receptor channels as a mechanism of modulation. *Nature* **356**, 521-523.

[78]   Raman IM, Tong G, Jahr CE (1996) Beta-adrenergic regulation of synaptic NMDA receptors by cAMP-dependent protein kinase. *Neuron* **16**, 415-421.

[79]   Lieberman DN, Mody I (1994) Regulation of NMDA channel function by endogenous Ca(2+)-dependent phosphatase. *Nature* **369**, 235-239.

[80]   Norris CM, Halpain S, Foster TC (1998) Reversal of age-related alterations in synaptic plasticity by blockade of L-type Ca2+ channels. *J Neurosci* **18**, 3171-3179.

[81]   Foster TC, Sharrow KM, Masse JR, Norris CM, Kumar A (2001) Calcineurin links Ca2+ dysregulation with brain aging. *J Neurosci* **21**, 4066-4073.

[82]   Coultrap SJ, Bickford PC, Browning MD (2008) Blueberry-enriched diet ameliorates age-related declines in NMDA receptor-dependent LTP. *Age (Dordr)* **30**, 263-272.

[83]   Williams SM, Diaz CM, Macnab LT, Sullivan RK, Pow DV (2006) Immunocytochemical analysis of D-serine distribution in the mammalian brain reveals novel anatomical compartmentalizations in glia and neurons. *Glia* **53**, 401-411.

[84]   Veselovskii NS, Fedulova SA (1983) [2 types of calcium channels in the somatic membrane of spinal ganglion neurons in the rat]. *Dokl Akad Nauk SSSR* **268**, 747-750.

[85]   Carbone E, Lux HD (1984) A low voltage-activated, fully inactivating Ca channel in vertebrate sensory neurones. *Nature* **310**, 501-502.

[86]   Fedulova SA, Kostyuk PG, Veselovsky NS (1985) Two types of calcium channels in the somatic membrane of new-born rat dorsal root ganglion neurones. *J Physiol* **359**, 431-446.

[87]   Nilius B, Hess P, Lansman JB, Tsien RW (1985) A novel type of cardiac calcium channel in ventricular cells. *Nature* **316**, 443-446.

[88]   Nowycky MC, Fox AP, Tsien RW (1985) Three types of neuronal calcium channel with different calcium agonist sensitivity. *Nature* **316**, 440-443.

[89]   Bean BP (1989) Classes of calcium channels in vertebrate cells. *Annu Rev Physiol* **51**, 367-384.

[90]   Soong TW, Stea A, Hodson CD, Dubel SJ, Vincent SR, Snutch TP (1993) Structure and functional expression of a member of the low voltage-activated calcium channel family. *Science* **260**, 1133-1136.

[91]   Gamelli AE, McKinney BC, White JA, Murphy GG (2011) Deletion of the L-type calcium channel Ca(V) 1.3 but not Ca(V) 1.2 results in a diminished sAHP in mouse CA1 pyramidal neurons. *Hippocampus* **21**, 133-141.

[92]   Roehm PC, Xu N, Woodson EA, Green SH, Hansen MR (2008) Membrane depolarization inhibits spiral ganglion neurite growth via activation of multiple types of voltage sensitive calcium channels and calpain. *Mol Cell Neurosci* **37**, 376-387.

[93]   Vandael DH, Mahapatra S, Calorio C, Marcantoni A, Carbone E (2013) Cav1.3 and Cav1.2 channels of adrenal chromaffin cells: emerging views on cAMP/cGMP-mediated phosphorylation and role in pacemaking. *Biochim Biophys Acta* **1828**, 1608-1618.

[94]   Buraei Z, Yang J (2015) Inhibition of Voltage-Gated Calcium Channels by RGK Proteins. *Curr Mol Pharmacol* **8**, 180-187.

[95]   Campbell LW, Hao SY, Thibault O, Blalock EM, Landfield PW (1996) Aging changes in voltage-gated calcium currents in hippocampal CA1 neurons. *J Neurosci* **16**, 6286-6295.

[96]   Brewer LD, Dowling AL, Curran-Rauhut MA, Landfield PW, Porter NM, Blalock EM (2009) Estradiol reverses a calcium-related biomarker of brain aging in female rats. *J Neurosci* **29**, 6058-6067.

[97]   Thibault O, Landfield PW (1996) Increase in single L-type calcium channels in hippocampal neurons during aging. *Science* **272**, 1017-1020.

[98]   Herman JP, Chen KC, Booze R, Landfield PW (1998) Up-regulation of alpha1D Ca2+ channel subunit mRNA expression in the hippocampus of aged F344 rats. *Neurobiol Aging* **19**, 581-587.

[99]   Chen KC, Blalock EM, Thibault O, Kaminker P, Landfield PW (2000) Expression of alpha 1D subunit mRNA is correlated with L-type Ca2+ channel activity in single neurons of hippocampal "zipper" slices. *Proc Natl Acad Sci U S A* **97**, 4357-4362.

[100]   Veng LM, Mesches MH, Browning MD (2003) Age-related working memory impairment is correlated with increases in the L-type calcium channel protein alpha1D (Cav1.3) in area CA1 of the hippocampus and both are ameliorated by chronic nimodipine treatment. *Brain Res Mol Brain Res* **110**, 193-202.

[101]   Norris CM, Blalock EM, Chen KC, Porter NM, Landfield PW (2002) Calcineurin enhances L-type Ca(2+) channel activity in hippocampal neurons: increased effect with age in culture. *Neuroscience* **110**, 213-225.

[102]   Kumar A, Foster TC (2002) 17beta-estradiol benzoate decreases the AHP amplitude in CA1 pyramidal neurons. *J Neurophysiol* **88**, 621-626.

[103]   Disterhoft JF, Moyer JR, Jr., Thompson LT, Kowalska M (1993) Functional aspects of calcium-channel modulation. *Clin Neuropharmacol* **16 Suppl 1**, S12-24.

[104]   Thibault O, Porter NM, Chen KC, Blalock EM, Kaminker PG, Clodfelter GV, Brewer LD, Landfield PW (1998) Calcium dysregulation in neuronal aging and Alzheimer's disease: history and new directions. *Cell Calcium* **24**, 417-433.

[105]   Shankar S, Teyler TJ, Robbins N (1998) Aging differentially alters forms of long-term potentiation in rat hippocampal area CA1. *J Neurophysiol* **79**, 334-341.

[106]   Deyo RA, Straube KT, Moyer JR, Jr., Disterhoft JF (1989) Nimodipine ameliorates aging-related changes in open-field behaviors of the rabbit. *Exp Aging Res* **15**, 169-175.

[107]   Straube KT, Deyo RA, Moyer JR, Jr., Disterhoft JF (1990) Dietary nimodipine improves associative learning in aging rabbits. *Neurobiol Aging* **11**, 659-661.

[108]   Thompson LT, Deyo RA, Disterhoft JF (1990) Nimodipine enhances spontaneous activity of hippocampal pyramidal neurons in aging rabbits at a dose that facilitates associative learning. *Brain Res* **535**, 119-130.

[109]   Levy A, Kong RM, Stillman MJ, Shukitt-Hale B, Kadar T, Rauch TM, Lieberman HR (1991) Nimodipine improves spatial working memory and elevates hippocampal acetylcholine in young rats. *Pharmacol Biochem Behav* **39**, 781-786.

[110]   Levere TE, Walker A (1992) Old age and cognition: enhancement of recent memory in aged rats by the calcium channel blocker nimodipine. *Neurobiol Aging* **13**, 63-66.

[111]   Quartermain D, Hawxhurst A, Ermita B, Puente J (1993) Effect of the calcium channel blocker amlodipine on memory in mice. *Behav Neural Biol* **60**, 211-219.

[112]   Kowalska M, Disterhoft JF (1994) Relation of nimodipine dose and serum concentration to learning enhancement in aging rabbits. *Exp Neurol* **127**, 159-166.

[113]   Solomon PR, Wood MS, Groccia-Ellison ME, Yang BY, Fanelli RJ, Mervis RF (1995) Nimodipine facilitates retention of the classically conditioned nictitating membrane response in aged rabbits over long retention intervals. *Neurobiol Aging* **16**, 791-796.

[114]   Woodruff-Pak DS, Chi J, Li YT, Pak MH, Fanelli RJ (1997) Nimodipine ameliorates impaired eyeblink classical conditioning in older rabbits in the long-delay paradigm. *Neurobiol Aging* **18**, 641-649.

[115]   Quevedo J, Vianna M, Daroit D, Born AG, Kuyven CR, Roesler R, Quillfeldt JA (1998) L-type voltage-dependent calcium channel blocker nifedipine enhances memory retention when infused into the hippocampus. *Neurobiol Learn Mem* **69**, 320-325.

[116]   Rose GM, Ong VS, Woodruff-Pak DS (2007) Efficacy of MEM 1003, a novel calcium channel blocker, in delay and trace eyeblink conditioning in older rabbits. *Neurobiol Aging* **28**, 766-773.

[117]	Ban TA, Morey L, Aguglia E, Azzarelli O, Balsano F, Marigliano V, Caglieris N, Sterlicchio M, Capurso A, Tomasi NA, et al. (1990) Nimodipine in the treatment of old age dementias. *Prog Neuropsychopharmacol Biol Psychiatry* **14**, 525-551.

[118]	Lopez de Armentia M, Sah P (2004) Firing properties and connectivity of neurons in the rat lateral central nucleus of the amygdala. *J Neurophysiol* **92**, 1285-1294.

[119]	Trompet S, Westendorp RG, Kamper AM, de Craen AJ (2008) Use of calcium antagonists and cognitive decline in old age. The Leiden 85-plus study. *Neurobiol Aging* **29**, 306-308.

[120]	Tanaka Y, Ando S (2001) Age-related changes in the subtypes of voltage-dependent calcium channels in rat brain cortical synapses. *Neurosci Res* **39**, 213-220.

[121]	Iwamoto M, Hagishita T, Shoji-Kasai Y, Ando S, Tanaka Y (2004) Age-related changes in the levels of voltage-dependent calcium channels and other synaptic proteins in rat brain cortices. *Neurosci Lett* **366**, 277-281.

[122]	Foster TC (2005) Interaction of rapid signal transduction cascades and gene expression in mediating estrogen effects on memory over the life span. *Front Neuroendocrinol* **26**, 51-64.

[123]	Martini A, Battaini F, Govoni S, Volpe P (1994) Inositol 1,4,5-trisphosphate receptor and ryanodine receptor in the aging brain of Wistar rats. *Neurobiol Aging* **15**, 203-206.

[124]	Burnett DM, Daniell LC, Zahniser NR (1990) Decreased efficacy of inositol 1,4,5-trisphosphate to elicit calcium mobilization from cerebrocortical microsomes of aged rats. *Mol Pharmacol* **37**, 566-571.

[125]	Igwe OJ, Ning L (1993) Inositol 1,4,5-trisphosphate arm of the phosphatidylinositide signal transduction pathway in the rat cerebellum during aging. *Neurosci Lett* **164**, 167-170.

[126]	Simonyi A, Xia J, Igbavboa U, Wood WG, Sun GY (1998) Age differences in the expression of metabotropic glutamate receptor 1 and inositol 1,4,5-trisphosphate receptor in mouse cerebellum. *Neurosci Lett* **244**, 29-32.

[127]	Stutzmann GE, Smith I, Caccamo A, Oddo S, Laferla FM, Parker I (2006) Enhanced ryanodine receptor recruitment contributes to Ca2+ disruptions in young, adult, and aged Alzheimer's disease mice. *J Neurosci* **26**, 5180-5189.

[128]	Hidalgo C, Bull R, Behrens MI, Donoso P (2004) Redox regulation of RyR-mediated Ca2+ release in muscle and neurons. *Biol Res* **37**, 539-552.

[129]	Bull R, Finkelstein JP, Humeres A, Behrens MI, Hidalgo C (2007) Effects of ATP, Mg2+, and redox agents on the Ca2+ dependence of RyR channels from rat brain cortex. *Am J Physiol Cell Physiol* **293**, C162-171.

[130]	Gokulrangan G, Zaidi A, Michaelis ML, Schoneich C (2007) Proteomic analysis of protein nitration in rat cerebellum: effect of biological aging. *J Neurochem* **100**, 1494-1504.

[131]	Peuchen S, Duchen MR, Clark JB (1996) Energy metabolism of adult astrocytes in vitro. *Neuroscience* **71**, 855-870.

[132]	Long LH, Liu J, Liu RL, Wang F, Hu ZL, Xie N, Fu H, Chen JG (2009) Differential effects of methionine and cysteine oxidation on [Ca2+] i in cultured hippocampal neurons. *Cell Mol Neurobiol* **29**, 7-15.

[133]	Kumar A, Foster TC (2004) Enhanced long-term potentiation during aging is masked by processes involving intracellular calcium stores. *J Neurophysiol* **91**, 2437-2444.

[134]	Kumar A, Foster TC (2005) Intracellular calcium stores contribute to increased susceptibility to LTD induction during aging. *Brain Res* **1031**, 125-128.

[135]	Gant JC, Sama MM, Landfield PW, Thibault O (2006) Early and simultaneous emergence of multiple hippocampal biomarkers of aging is mediated by Ca2+-induced Ca2+ release. *J Neurosci* **26**, 3482-3490.

[136] Danial NN, Korsmeyer SJ (2004) Cell death: critical control points. *Cell* **116**, 205-219.

[137] Green DR, Kroemer G (2004) The pathophysiology of mitochondrial cell death. *Science* **305**, 626-629.

[138] Rizzuto R, De Stefani D, Raffaello A, Mammucari C (2012) Mitochondria as sensors and regulators of calcium signalling. *Nat Rev Mol Cell Biol* **13**, 566-578.

[139] Williams GS, Boyman L, Chikando AC, Khairallah RJ, Lederer WJ (2013) Mitochondrial calcium uptake. *Proc Natl Acad Sci U S A* **110**, 10479-10486.

[140] Carafoli E, Lehninger AL (1971) A survey of the interaction of calcium ions with mitochondria from different tissues and species. *Biochem J* **122**, 681-690.

[141] Fernandez-Morales JC, Arranz-Tagarro JA, Calvo-Gallardo E, Maroto M, Padin JF, Garcia AG (2012) Stabilizers of neuronal and mitochondrial calcium cycling as a strategy for developing a medicine for Alzheimer's disease. *ACS Chem Neurosci* **3**, 873-883.

[142] Leslie SW, Chandler LJ, Barr EM, Farrar RP (1985) Reduced calcium uptake by rat brain mitochondria and synaptosomes in response to aging. *Brain Res* **329**, 177-183.

[143] Brustovetsky N, Brustovetsky T, Purl KJ, Capano M, Crompton M, Dubinsky JM (2003) Increased susceptibility of striatal mitochondria to calcium-induced permeability transition. *J Neurosci* **23**, 4858-4867.

[144] Jiang D, Sullivan PG, Sensi SL, Steward O, Weiss JH (2001) Zn(2+) induces permeability transition pore opening and release of pro-apoptotic peptides from neuronal mitochondria. *J Biol Chem* **276**, 47524-47529.

[145] Beckman KB, Ames BN (1998) The free radical theory of aging matures. *Physiol Rev* **78**, 547-581.

[146] Carafoli E (1986) Membrane transport in the cellular homeostasis of calcium. *J Cardiovasc Pharmacol* **8 Suppl 8**, S3-6.

[147] Gattoni G, Bernocchi G (2019) Calcium-Binding Proteins in the Nervous System during Hibernation: Neuroprotective Strategies in Hypometabolic Conditions? *Int J Mol Sci* **20**.

[148] Jin YH, Wu XS, Shi B, Zhang Z, Guo X, Gan L, Chen Z, Wu LG (2019) Protein Kinase C and Calmodulin Serve As Calcium Sensors for Calcium-Stimulated Endocytosis at Synapses. *J Neurosci* **39**, 9478-9490.

[149] Villa A, Podini P, Panzeri MC, Racchetti G, Meldolesi J (1994) Cytosolic Ca2+ binding proteins during rat brain ageing: loss of calbindin and calretinin in the hippocampus, with no change in the cerebellum. *Eur J Neurosci* **6**, 1491-1499.

[150] Potier B, Krzywkowski P, Lamour Y, Dutar P (1994) Loss of calbindin-immunoreactivity in CA1 hippocampal stratum radiatum and stratum lacunosum-moleculare interneurons in the aged rat. *Brain Res* **661**, 181-188.

[151] de Jong GI, Naber PA, Van der Zee EA, Thompson LT, Disterhoft JF, Luiten PG (1996) Age-related loss of calcium binding proteins in rabbit hippocampus. *Neurobiol Aging* **17**, 459-465.

[152] Krzywkowski P, De Bilbao F, Senut MC, Lamour Y (1995) Age-related changes in parvalbumin- and GABA-immunoreactive cells in the rat septum. *Neurobiol Aging* **16**, 29-40.

[153] Michaelis ML, Johe K, Kitos TE (1984) Age-dependent alterations in synaptic membrane systems for Ca2+ regulation. *Mech Ageing Dev* **25**, 215-225.

[154] Michaelis ML, Bigelow DJ, Schoneich C, Williams TD, Ramonda L, Yin D, Huhmer AF, Yao Y, Gao J, Squier TC (1996) Decreased plasma membrane calcium transport activity in aging brain. *Life Sci* **59**, 405-412.

[155] Zaidi A, Gao J, Squier TC, Michaelis ML (1998) Age-related decrease in brain synaptic membrane Ca2+-ATPase in F344/BNF1 rats. *Neurobiol Aging* **19**, 487-495.

[156] Hanahisa Y, Yamaguchi M (2001) Decrease in Ca2+-ATPase activity in the brain plasma membrane of rats with increasing age: involvement of brain calcium accumulation. *Int J Mol Med* **7**, 407-411.

[157] Pottorf WJ, De Leon DD, Hessinger DA, Buchholz JN (2001) Function of SERCA mediated calcium uptake and expression of SERCA3 in cerebral cortex from young and old rats. *Brain Res* **914**, 57-65.

[158] Gomez-Villafuertes R, Mellstrom B, Naranjo JR (2007) Searching for a role of NCX/NCKX exchangers in neurodegeneration. *Mol Neurobiol* **35**, 195-202.

[159] Norris CM, Blalock EM, Chen KC, Porter NM, Thibault O, Kraner SD, Landfield PW (2010) Hippocampal 'zipper' slice studies reveal a necessary role for calcineurin in the increased activity of L-type Ca(2+) channels with aging. *Neurobiol Aging* **31**, 328-338.

[160] Murchison D, Griffith WH (1996) High-voltage-activated calcium currents in basal forebrain neurons during aging. *J Neurophysiol* **76**, 158-174.

[161] Murchison D, Griffith WH (1998) Increased calcium buffering in basal forebrain neurons during aging. *J Neurophysiol* **80**, 350-364.

[162] Bliss TV, Lomo T (1973) Long-lasting potentiation of synaptic transmission in the dentate area of the anaesthetized rabbit following stimulation of the perforant path. *J Physiol* **232**, 331-356.

[163] Foster TC, Kumar A (2002) Calcium dysregulation in the aging brain. *Neuroscientist* **8**, 297-301.

[164] Norris CM, Korol DL, Foster TC (1996) Increased susceptibility to induction of long-term depression and long-term potentiation reversal during aging. *J Neurosci* **16**, 5382-5392.

[165] Foster TC (2007) Calcium homeostasis and modulation of synaptic plasticity in the aged brain. *Aging Cell* **6**, 319-325.

[166] Madison DV, Nicoll RA (1984) Control of the repetitive discharge of rat CA 1 pyramidal neurones in vitro. *J Physiol* **354**, 319-331.

[167] Coulter DA, Lo Turco JJ, Kubota M, Disterhoft JF, Moore JW, Alkon DL (1989) Classical conditioning reduces amplitude and duration of calcium-dependent afterhyperpolarization in rabbit hippocampal pyramidal cells. *J Neurophysiol* **61**, 971-981.

[168] Wu WW, Chan CS, Disterhoft JF (2004) Slow afterhyperpolarization governs the development of NMDA receptor-dependent afterdepolarization in CA1 pyramidal neurons during synaptic stimulation. *J Neurophysiol* **92**, 2346-2356.

[169] Sah P, Faber ES (2002) Channels underlying neuronal calcium-activated potassium currents. *Prog Neurobiol* **66**, 345-353.

[170] Disterhoft JF, Oh MM (2006) Learning, aging and intrinsic neuronal plasticity. *Trends Neurosci* **29**, 587-599.

[171] Moyer JR, Jr., Power JM, Thompson LT, Disterhoft JF (2000) Increased excitability of aged rabbit CA1 neurons after trace eyeblink conditioning. *J Neurosci* **20**, 5476-5482.

[172] Matthews EA, Weible AP, Shah S, Disterhoft JF (2008) The BK-mediated fAHP is modulated by learning a hippocampus-dependent task. *Proc Natl Acad Sci U S A* **105**, 15154-15159.

[173] Moyer JR, Jr., Thompson LT, Disterhoft JF (1996) Trace eyeblink conditioning increases CA1 excitability in a transient and learning-specific manner. *J Neurosci* **16**, 5536-5546.

[174] McKay BM, Matthews EA, Oliveira FA, Disterhoft JF (2009) Intrinsic neuronal excitability is reversibly altered by a single experience in fear conditioning. *J Neurophysiol* **102**, 2763-2770.

[175]   Saar D, Barkai E (2003) Long-term modifications in intrinsic neuronal properties and rule learning in rats. *Eur J Neurosci* **17**, 2727-2734.

[176]   Saar D, Grossman Y, Barkai E (1998) Reduced after-hyperpolarization in rat piriform cortex pyramidal neurons is associated with increased learning capability during operant conditioning. *Eur J Neurosci* **10**, 1518-1523.

[177]   Oh MM, Kuo AG, Wu WW, Sametsky EA, Disterhoft JF (2003) Watermaze learning enhances excitability of CA1 pyramidal neurons. *J Neurophysiol* **90**, 2171-2179.

[178]   Davies PJ, Ireland DR, Martinez-Pinna J, McLachlan EM (1999) Electrophysiological roles of L-type channels in different classes of guinea pig sympathetic neuron. *J Neurophysiol* **82**, 818-828.

[179]   Nedergaard S, Flatman JA, Engberg I (1993) Nifedipine- and omega-conotoxin-sensitive Ca2+ conductances in guinea-pig substantia nigra pars compacta neurones. *J Physiol* **466**, 727-747.

[180]   Viana F, Bayliss DA, Berger AJ (1993) Multiple potassium conductances and their role in action potential repolarization and repetitive firing behavior of neonatal rat hypoglossal motoneurons. *J Neurophysiol* **69**, 2150-2163.

[181]   Brewer LD, Porter NM, Kerr DS, Landfield PW, Thibault O (2006) Chronic 1alpha,25-(OH)2 vitamin D3 treatment reduces Ca2+ -mediated hippocampal biomarkers of aging. *Cell Calcium* **40**, 277-286.

[182]   Thibault O, Mazzanti ML, Blalock EM, Porter NM, Landfield PW (1995) Single-channel and whole-cell studies of calcium currents in young and aged rat hippocampal slice neurons. *J Neurosci Methods* **59**, 77-83.

[183]   Thibault O, Gant JC, Landfield PW (2007) Expansion of the calcium hypothesis of brain aging and Alzheimer's disease: minding the store. *Aging Cell* **6**, 307-317.

[184]   Power JM, Wu WW, Sametsky E, Oh MM, Disterhoft JF (2002) Age-related enhancement of the slow outward calcium-activated potassium current in hippocampal CA1 pyramidal neurons in vitro. *J Neurosci* **22**, 7234-7243.

[185]   Alzheimer's A (2016) 2016 Alzheimer's disease facts and figures. *Alzheimers Dement* **12**, 459-509.

[186]   Adams MM, Morrison JH (2003) Estrogen and the aging hippocampal synapse. *Cereb Cortex* **13**, 1271-1275.

[187]   McEwen B (2002) Estrogen actions throughout the brain. *Recent Prog Horm Res* **57**, 357-384.

[188]   Rapp PR, Morrison JH, Roberts JA (2003) Cyclic estrogen replacement improves cognitive function in aged ovariectomized rhesus monkeys. *J Neurosci* **23**, 5708-5714.

[189]   Hao J, Janssen WG, Tang Y, Roberts JA, McKay H, Lasley B, Allen PB, Greengard P, Rapp PR, Kordower JH, Hof PR, Morrison JH (2003) Estrogen increases the number of spinophilin-immunoreactive spines in the hippocampus of young and aged female rhesus monkeys. *J Comp Neurol* **465**, 540-550.

[190]   Grassi S, Scarduzio M, Panichi R, Dall'Aglio C, Boiti C, Pettorossi VE (2013) Opposite long-term synaptic effects of 17beta-estradiol and 5alpha-dihydrotestosterone and localization of their receptors in the medial vestibular nucleus of rats. *Brain Res Bull* **97**, 1-7.

[191]   Chen J, Adachi N, Liu K, Arai T (1998) The effects of 17beta-estradiol on ischemia-induced neuronal damage in the gerbil hippocampus. *Neuroscience* **87**, 817-822.

[192]   Chu Z, Andrade J, Shupnik MA, Moenter SM (2009) Differential regulation of gonadotropin-releasing hormone neuron activity and membrane properties by acutely

applied estradiol: dependence on dose and estrogen receptor subtype. *J Neurosci* **29**, 5616-5627.

[193]   West MJ (1993) Regionally specific loss of neurons in the aging human hippocampus. *Neurobiol Aging* **14**, 287-293.

[194]   Peters A, Rosene DL, Moss MB, Kemper TL, Abraham CR, Tigges J, Albert MS (1996) Neurobiological bases of age-related cognitive decline in the rhesus monkey. *J Neuropathol Exp Neurol* **55**, 861-874.

[195]   Rapp PR, Gallagher M (1996) Preserved neuron number in the hippocampus of aged rats with spatial learning deficits. *Proc Natl Acad Sci U S A* **93**, 9926-9930.

[196]   Rasmussen T, Schliemann T, Sorensen JC, Zimmer J, West MJ (1996) Memory impaired aged rats: no loss of principal hippocampal and subicular neurons. *Neurobiol Aging* **17**, 143-147.

[197]   Calhoun ME, Kurth D, Phinney AL, Long JM, Hengemihle J, Mouton PR, Ingram DK, Jucker M (1998) Hippocampal neuron and synaptophysin-positive bouton number in aging C57BL/6 mice. *Neurobiol Aging* **19**, 599-606.

[198]   Dickstein DL, Kabaso D, Rocher AB, Luebke JI, Wearne SL, Hof PR (2007) Changes in the structural complexity of the aged brain. *Aging Cell* **6**, 275-284.

[199]   Geinisman Y, Ganeshina O, Yoshida R, Berry RW, Disterhoft JF, Gallagher M (2004) Aging, spatial learning, and total synapse number in the rat CA1 stratum radiatum. *Neurobiol Aging* **25**, 407-416.

[200]   Smith TD, Adams MM, Gallagher M, Morrison JH, Rapp PR (2000) Circuit-specific alterations in hippocampal synaptophysin immunoreactivity predict spatial learning impairment in aged rats. *J Neurosci* **20**, 6587-6593.

[201]   Potier B, Poindessous-Jazat F, Dutar P, Billard JM (2000) NMDA receptor activation in the aged rat hippocampus. *Exp Gerontol* **35**, 1185-1199.

[202]   Disterhoft JF, Oh MM (2007) Alterations in intrinsic neuronal excitability during normal aging. *Aging Cell* **6**, 327-336.

[203]   Parnetti L, Senin U, Carosi M, Baasch H (1993) Mental deterioration in old age: results of two multicenter, clinical trials with nimodipine. The Nimodipine Study Group. *Clin Ther* **15**, 394-406.

[204]   Tollefson GD (1990) Short-term effects of the calcium channel blocker nimodipine (Bay-e-9736) in the management of primary degenerative dementia. *Biol Psychiatry* **27**, 1133-1142.

[205]   Lopez-Arrieta JM, Birks J (2002) Nimodipine for primary degenerative, mixed and vascular dementia. *Cochrane Database Syst Rev*, CD000147.

[206]   Nimmrich V, Eckert A (2013) Calcium channel blockers and dementia. *Br J Pharmacol* **169**, 1203-1210.

[207]   Forette F, Seux ML, Staessen JA, Thijs L, Birkenhager WH, Babarskiene MR, Babeanu S, Bossini A, Gil-Extremera B, Girerd X, Laks T, Lilov E, Moisseyev V, Tuomilehto J, Vanhanen H, Webster J, Yodfat Y, Fagard R (1998) Prevention of dementia in randomised double-blind placebo-controlled Systolic Hypertension in Europe (Syst-Eur) trial. *Lancet* **352**, 1347-1351.

[208]   Forette F, Seux ML, Staessen JA, Thijs L, Babarskiene MR, Babeanu S, Bossini A, Fagard R, Gil-Extremera B, Laks T, Kobalava Z, Sarti C, Tuomilehto J, Vanhanen H, Webster J, Yodfat Y, Birkenhager WH, Systolic Hypertension in Europe I (2002) The prevention of dementia with antihypertensive treatment: new evidence from the Systolic Hypertension in Europe (Syst-Eur) study. *Arch Intern Med* **162**, 2046-2052.

[209] Salomone S, Caraci F, Leggio GM, Fedotova J, Drago F (2012) New pharmacological strategies for treatment of Alzheimer's disease: focus on disease modifying drugs. *Br J Clin Pharmacol* **73**, 504-517.

[210] Webber KM, Raina AK, Marlatt MW, Zhu X, Prat MI, Morelli L, Casadesus G, Perry G, Smith MA (2005) The cell cycle in Alzheimer disease: a unique target for neuropharmacology. *Mech Ageing Dev* **126**, 1019-1025.

[211] Holscher C (2005) Development of beta-amyloid-induced neurodegeneration in Alzheimer's disease and novel neuroprotective strategies. *Rev Neurosci* **16**, 181-212.

[212] Steiner H, Winkler E, Edbauer D, Prokop S, Basset G, Yamasaki A, Kostka M, Haass C (2002) PEN-2 is an integral component of the gamma-secretase complex required for coordinated expression of presenilin and nicastrin. *J Biol Chem* **277**, 39062-39065.

[213] Hardy J, Selkoe DJ (2002) The amyloid hypothesis of Alzheimer's disease: progress and problems on the road to therapeutics. *Science* **297**, 353-356.

[214] Beyreuther K, Masters CL (1991) Amyloid precursor protein (APP) and beta A4 amyloid in the etiology of Alzheimer's disease: precursor-product relationships in the derangement of neuronal function. *Brain Pathol* **1**, 241-251.

[215] Hardy J, Allsop D (1991) Amyloid deposition as the central event in the aetiology of Alzheimer's disease. *Trends Pharmacol Sci* **12**, 383-388.

[216] Selkoe DJ (1991) Amyloid protein and Alzheimer's disease. *Sci Am* **265**, 68-71, 74-66, 78.

[217] Hardy JA, Higgins GA (1992) Alzheimer's disease: the amyloid cascade hypothesis. *Science* **256**, 184-185.

[218] Arispe N, Pollard HB, Rojas E (1993) Giant multilevel cation channels formed by Alzheimer disease amyloid beta-protein [A beta P-(1-40)] in bilayer membranes. *Proc Natl Acad Sci U S A* **90**, 10573-10577.

[219] Mirzabekov TA, Lin MC, Kagan BL (1996) Pore formation by the cytotoxic islet amyloid peptide amylin. *J Biol Chem* **271**, 1988-1992.

[220] Goodman Y, Mattson MP (1994) Secreted forms of beta-amyloid precursor protein protect hippocampal neurons against amyloid beta-peptide-induced oxidative injury. *Exp Neurol* **128**, 1-12.

[221] Mattson MP, Barger SW, Cheng B, Lieberburg I, Smith-Swintosky VL, Rydel RE (1993) beta-Amyloid precursor protein metabolites and loss of neuronal Ca2+ homeostasis in Alzheimer's disease. *Trends Neurosci* **16**, 409-414.

[222] Hensley K, Butterfield DA, Mattson M, Aksenova M, Harris M, Wu JF, Floyd R, Carney J (1995) A model for beta-amyloid aggregation and neurotoxicity based on the free radical generating capacity of the peptide: implications of "molecular shrapnel" for Alzheimer's disease. *Proc West Pharmacol Soc* **38**, 113-120.

[223] Ishida A, Furukawa K, Keller JN, Mattson MP (1997) Secreted form of beta-amyloid precursor protein shifts the frequency dependency for induction of LTD, and enhances LTP in hippocampal slices. *Neuroreport* **8**, 2133-2137.

[224] Snyder EM, Nong Y, Almeida CG, Paul S, Moran T, Choi EY, Nairn AC, Salter MW, Lombroso PJ, Gouras GK, Greengard P (2005) Regulation of NMDA receptor trafficking by amyloid-beta. *Nat Neurosci* **8**, 1051-1058.

[225] Lambert MP, Barlow AK, Chromy BA, Edwards C, Freed R, Liosatos M, Morgan TE, Rozovsky I, Trommer B, Viola KL, Wals P, Zhang C, Finch CE, Krafft GA, Klein WL (1998) Diffusible, nonfibrillar ligands derived from Abeta1-42 are potent central nervous system neurotoxins. *Proc Natl Acad Sci U S A* **95**, 6448-6453.

[226]   Townsend M, Shankar GM, Mehta T, Walsh DM, Selkoe DJ (2006) Effects of secreted oligomers of amyloid beta-protein on hippocampal synaptic plasticity: a potent role for trimers. *J Physiol* **572**, 477-492.

[227]   Walsh DM, Klyubin I, Fadeeva JV, Cullen WK, Anwyl R, Wolfe MS, Rowan MJ, Selkoe DJ (2002) Naturally secreted oligomers of amyloid beta protein potently inhibit hippocampal long-term potentiation in vivo. *Nature* **416**, 535-539.

[228]   Wang HW, Pasternak JF, Kuo H, Ristic H, Lambert MP, Chromy B, Viola KL, Klein WL, Stine WB, Krafft GA, Trommer BL (2002) Soluble oligomers of beta amyloid (1-42) inhibit long-term potentiation but not long-term depression in rat dentate gyrus. *Brain Res* **924**, 133-140.

[229]   De Felice FG, Velasco PT, Lambert MP, Viola K, Fernandez SJ, Ferreira ST, Klein WL (2007) Abeta oligomers induce neuronal oxidative stress through an N-methyl-D-aspartate receptor-dependent mechanism that is blocked by the Alzheimer drug memantine. *J Biol Chem* **282**, 11590-11601.

[230]   Shankar GM, Bloodgood BL, Townsend M, Walsh DM, Selkoe DJ, Sabatini BL (2007) Natural oligomers of the Alzheimer amyloid-beta protein induce reversible synapse loss by modulating an NMDA-type glutamate receptor-dependent signaling pathway. *J Neurosci* **27**, 2866-2875.

[231]   Guo Q, Fu W, Sopher BL, Miller MW, Ware CB, Martin GM, Mattson MP (1999) Increased vulnerability of hippocampal neurons to excitotoxic necrosis in presenilin-1 mutant knock-in mice. *Nat Med* **5**, 101-106.

[232]   Querfurth HW, Selkoe DJ (1994) Calcium ionophore increases amyloid beta peptide production by cultured cells. *Biochemistry* **33**, 4550-4561.

[233]   Querfurth HW, Jiang J, Geiger JD, Selkoe DJ (1997) Caffeine stimulates amyloid beta-peptide release from beta-amyloid precursor protein-transfected HEK293 cells. *J Neurochem* **69**, 1580-1591.

[234]   Pierrot N, Ghisdal P, Caumont AS, Octave JN (2004) Intraneuronal amyloid-beta1-42 production triggered by sustained increase of cytosolic calcium concentration induces neuronal death. *J Neurochem* **88**, 1140-1150.

[235]   Pierrot N, Santos SF, Feyt C, Morel M, Brion JP, Octave JN (2006) Calcium-mediated transient phosphorylation of tau and amyloid precursor protein followed by intraneuronal amyloid-beta accumulation. *J Biol Chem* **281**, 39907-39914.

[236]   Fu H, Li W, Lao Y, Luo J, Lee NT, Kan KK, Tsang HW, Tsim KW, Pang Y, Li Z, Chang DC, Li M, Han Y (2006) Bis(7)-tacrine attenuates beta amyloid-induced neuronal apoptosis by regulating L-type calcium channels. *J Neurochem* **98**, 1400-1410.

[237]   Ueda K, Shinohara S, Yagami T, Asakura K, Kawasaki K (1997) Amyloid beta protein potentiates Ca2+ influx through L-type voltage-sensitive Ca2+ channels: a possible involvement of free radicals. *J Neurochem* **68**, 265-271.

[238]   MacManus A, Ramsden M, Murray M, Henderson Z, Pearson HA, Campbell VA (2000) Enhancement of (45)Ca(2+) influx and voltage-dependent Ca(2+) channel activity by beta-amyloid-(1-40) in rat cortical synaptosomes and cultured cortical neurons. Modulation by the proinflammatory cytokine interleukin-1beta. *J Biol Chem* **275**, 4713-4718.

[239]   Daschil N, Geisler S, Obermair GJ, Humpel C (2014) Short- and long-term treatment of mouse cortical primary astrocytes with beta-amyloid differentially regulates the mRNA expression of L-type calcium channels. *Pharmacology* **93**, 24-31.

[240]   Kim S, Rhim H (2011) Effects of amyloid-beta peptides on voltage-gated L-type Ca(V)1.2 and Ca(V)1.3 Ca(2+) channels. *Mol Cells* **32**, 289-294.

[241]   Wang Y, Mattson MP (2014) L-type Ca2+ currents at CA1 synapses, but not CA3 or dentate granule neuron synapses, are increased in 3xTgAD mice in an age-dependent manner. *Neurobiol Aging* **35**, 88-95.

[242]   Thibault O, Pancani T, Landfield PW, Norris CM (2012) Reduction in neuronal L-type calcium channel activity in a double knock-in mouse model of Alzheimer's disease. *Biochim Biophys Acta* **1822**, 546-549.

[243]   Min D, Guo F, Zhu S, Xu X, Mao X, Cao Y, Lv X, Gao Q, Wang L, Chen T, Shaw C, Hao L, Cai J (2013) The alterations of Ca2+/calmodulin/CaMKII/CaV1.2 signaling in experimental models of Alzheimer's disease and vascular dementia. *Neurosci Lett* **538**, 60-65.

[244]   Espana J, Valero J, Minano-Molina AJ, Masgrau R, Martin E, Guardia-Laguarta C, Lleo A, Gimenez-Llort L, Rodriguez-Alvarez J, Saura CA (2010) beta-Amyloid disrupts activity-dependent gene transcription required for memory through the CREB coactivator CRTC1. *J Neurosci* **30**, 9402-9410.

[245]   Saura CA (2012) CREB-regulated transcription coactivator 1-dependent transcription in Alzheimer's disease mice. *Neurodegener Dis* **10**, 250-252.

[246]   Wu CL, Wen SH (2016) A 10-year follow-up study of the association between calcium channel blocker use and the risk of dementia in elderly hypertensive patients. *Medicine (Baltimore)* **95**, e4593.

[247]   Hwang D, Kim S, Choi H, Oh IH, Kim BS, Choi HR, Kim SY, Won CW (2016) Calcium-Channel Blockers and Dementia Risk in Older Adults- National Health Insurance Service - Senior Cohort (2002-2013). *Circ J* **80**, 2336-2342.

[248]   Kennelly S, Abdullah L, Kenny RA, Mathura V, Luis CA, Mouzon B, Crawford F, Mullan M, Lawlor B (2012) Apolipoprotein E genotype-specific short-term cognitive benefits of treatment with the antihypertensive nilvadipine in Alzheimer's patients--an open-label trial. *Int J Geriatr Psychiatry* **27**, 415-422.

[249]   Lawlor B, Segurado R, Kennelly S, Olde Rikkert MGM, Howard R, Pasquier F, Borjesson-Hanson A, Tsolaki M, Lucca U, Molloy DW, Coen R, Riepe MW, Kalman J, Kenny RA, Cregg F, O'Dwyer S, Walsh C, Adams J, Banzi R, Breuilh L, Daly L, Hendrix S, Aisen P, Gaynor S, Sheikhi A, Taekema DG, Verhey FR, Nemni R, Nobili F, Franceschi M, Frisoni G, Zanetti O, Konsta A, Anastasios O, Nenopoulou S, Tsolaki-Tagaraki F, Pakaski M, Dereeper O, de la Sayette V, Senechal O, Lavenu I, Devendeville A, Calais G, Crawford F, Mullan M, Group NS (2018) Nilvadipine in mild to moderate Alzheimer disease: A randomised controlled trial. *PLoS Med* **15**, e1002660.

[250]   Lopez A, Birks J (2001) Nimodipine for primary degenerative, mixed and vascular dementia. *Cochrane Database Syst Rev*, CD000147.

[251]   Liu J, Chang L, Roselli F, Almeida OF, Gao X, Wang X, Yew DT, Wu Y (2010) Amyloid-beta induces caspase-dependent loss of PSD-95 and synaptophysin through NMDA receptors. *J Alzheimers Dis* **22**, 541-556.

[252]   Ronicke R, Mikhaylova M, Ronicke S, Meinhardt J, Schroder UH, Fandrich M, Reiser G, Kreutz MR, Reymann KG (2011) Early neuronal dysfunction by amyloid beta oligomers depends on activation of NR2B-containing NMDA receptors. *Neurobiol Aging* **32**, 2219-2228.

[253]   Hu R, Wei P, Jin L, Zheng T, Chen WY, Liu XY, Shi XD, Hao JR, Sun N, Gao C (2017) Overexpression of EphB2 in hippocampus rescues impaired NMDA receptors trafficking and cognitive dysfunction in Alzheimer model. *Cell Death Dis* **8**, e2717.

[254]   Gotz J, Probst A, Spillantini MG, Schafer T, Jakes R, Burki K, Goedert M (1995) Somatodendritic localization and hyperphosphorylation of tau protein in transgenic mice expressing the longest human brain tau isoform. *EMBO J* **14**, 1304-1313.

[255]   Kowall NW, Kosik KS (1987) Axonal disruption and aberrant localization of tau protein characterize the neuropil pathology of Alzheimer's disease. *Ann Neurol* **22**, 639-643.

[256]   Kobayashi S, Tanaka T, Soeda Y, Almeida OFX, Takashima A (2017) Local Somatodendritic Translation and Hyperphosphorylation of Tau Protein Triggered by AMPA and NMDA Receptor Stimulation. *EBioMedicine* **20**, 120-126.

[257]   Palop JJ, Chin J, Roberson ED, Wang J, Thwin MT, Bien-Ly N, Yoo J, Ho KO, Yu GQ, Kreitzer A, Finkbeiner S, Noebels JL, Mucke L (2007) Aberrant excitatory neuronal activity and compensatory remodeling of inhibitory hippocampal circuits in mouse models of Alzheimer's disease. *Neuron* **55**, 697-711.

[258]   Romanelli MF, Morris JC, Ashkin K, Coben LA (1990) Advanced Alzheimer's disease is a risk factor for late-onset seizures. *Arch Neurol* **47**, 847-850.

[259]   Meyer FB (1989) Calcium, neuronal hyperexcitability and ischemic injury. *Brain Res Brain Res Rev* **14**, 227-243.

[260]   Hommet C, Mondon K, Camus V, De Toffol B, Constans T (2008) Epilepsy and dementia in the elderly. *Dement Geriatr Cogn Disord* **25**, 293-300.

[261]   Hoover BR, Reed MN, Su J, Penrod RD, Kotilinek LA, Grant MK, Pitstick R, Carlson GA, Lanier LM, Yuan LL, Ashe KH, Liao D (2010) Tau mislocalization to dendritic spines mediates synaptic dysfunction independently of neurodegeneration. *Neuron* **68**, 1067-1081.

[262]   Boehm J (2013) A 'danse macabre': tau and Fyn in STEP with amyloid beta to facilitate induction of synaptic depression and excitotoxicity. *Eur J Neurosci* **37**, 1925-1930.

[263]   Quednau BD, Nicoll DA, Philipson KD (1997) Tissue specificity and alternative splicing of the Na+/Ca2+ exchanger isoforms NCX1, NCX2, and NCX3 in rat. *Am J Physiol* **272**, C1250-1261.

[264]   Colvin RA, Bennett JW, Colvin SL (1991) Na(+)-Ca2+ exchange activity is increased in Alzheimer's disease brain tissues. *Ann N Y Acad Sci* **639**, 325-327.

[265]   Sokolow S, Luu SH, Headley AJ, Hanson AY, Kim T, Miller CA, Vinters HV, Gylys KH (2011) High levels of synaptosomal Na(+)-Ca(2+) exchangers (NCX1, NCX2, NCX3) co-localized with amyloid-beta in human cerebral cortex affected by Alzheimer's disease. *Cell Calcium* **49**, 208-216.

[266]   Atherton J, Kurbatskaya K, Bondulich M, Croft CL, Garwood CJ, Chhabra R, Wray S, Jeromin A, Hanger DP, Noble W (2014) Calpain cleavage and inactivation of the sodium calcium exchanger-3 occur downstream of Abeta in Alzheimer's disease. *Aging Cell* **13**, 49-59.

[267]   Minelli A, Castaldo P, Gobbi P, Salucci S, Magi S, Amoroso S (2007) Cellular and subcellular localization of Na+-Ca2+ exchanger protein isoforms, NCX1, NCX2, and NCX3 in cerebral cortex and hippocampus of adult rat. *Cell Calcium* **41**, 221-234.

[268]   Moriguchi S, Kita S, Fukaya M, Osanai M, Inagaki R, Sasaki Y, Izumi H, Horie K, Takeda J, Saito T, Sakagami H, Saido TC, Iwamoto T, Fukunaga K (2018) Reduced expression of Na(+)/Ca(2+) exchangers is associated with cognitive deficits seen in Alzheimer's disease model mice. *Neuropharmacology* **131**, 291-303.

[269]   Mata AM (2018) Functional interplay between plasma membrane Ca(2+)-ATPase, amyloid beta-peptide and tau. *Neurosci Lett* **663**, 55-59.

[270]   Zaidi A (2010) Plasma membrane Ca-ATPases: Targets of oxidative stress in brain aging and neurodegeneration. *World J Biol Chem* **1**, 271-280.

[271]   Hardy J, Gwinn-Hardy K (1998) Genetic classification of primary neurodegenerative disease. *Science* **282**, 1075-1079.

[272]   Ito E, Oka K, Etcheberrigaray R, Nelson TJ, McPhie DL, Tofel-Grehl B, Gibson GE, Alkon DL (1994) Internal Ca2+ mobilization is altered in fibroblasts from patients with Alzheimer disease. *Proc Natl Acad Sci U S A* **91**, 534-538.

[273]   Yu JT, Chang RC, Tan L (2009) Calcium dysregulation in Alzheimer's disease: from mechanisms to therapeutic opportunities. *Prog Neurobiol* **89**, 240-255.

[274]   LaFerla FM (2002) Calcium dyshomeostasis and intracellular signalling in Alzheimer's disease. *Nat Rev Neurosci* **3**, 862-872.

[275]   Etcheberrigaray R, Hirashima N, Nee L, Prince J, Govoni S, Racchi M, Tanzi RE, Alkon DL (1998) Calcium responses in fibroblasts from asymptomatic members of Alzheimer's disease families. *Neurobiol Dis* **5**, 37-45.

[276]   Hirashima N, Etcheberrigaray R, Bergamaschi S, Racchi M, Battaini F, Binetti G, Govoni S, Alkon DL (1996) Calcium responses in human fibroblasts: a diagnostic molecular profile for Alzheimer's disease. *Neurobiol Aging* **17**, 549-555.

[277]   Leissring MA, Akbari Y, Fanger CM, Cahalan MD, Mattson MP, LaFerla FM (2000) Capacitative calcium entry deficits and elevated luminal calcium content in mutant presenilin-1 knockin mice. *J Cell Biol* **149**, 793-798.

[278]   Barrow PA, Empson RM, Gladwell SJ, Anderson CM, Killick R, Yu X, Jefferys JG, Duff K (2000) Functional phenotype in transgenic mice expressing mutant human presenilin-1. *Neurobiol Dis* **7**, 119-126.

[279]   Mattson MP, Zhu H, Yu J, Kindy MS (2000) Presenilin-1 mutation increases neuronal vulnerability to focal ischemia in vivo and to hypoxia and glucose deprivation in cell culture: involvement of perturbed calcium homeostasis. *J Neurosci* **20**, 1358-1364.

[280]   Schneider I, Reverse D, Dewachter I, Ris L, Caluwaerts N, Kuiperi C, Gilis M, Geerts H, Kretzschmar H, Godaux E, Moechars D, Van Leuven F, Herms J (2001) Mutant presenilins disturb neuronal calcium homeostasis in the brain of transgenic mice, decreasing the threshold for excitotoxicity and facilitating long-term potentiation. *J Biol Chem* **276**, 11539-11544.

[281]   Stutzmann GE, Caccamo A, LaFerla FM, Parker I (2004) Dysregulated IP3 signaling in cortical neurons of knock-in mice expressing an Alzheimer's-linked mutation in presenilin1 results in exaggerated Ca2+ signals and altered membrane excitability. *J Neurosci* **24**, 508-513.

[282]   Lopez JR, Lyckman A, Oddo S, Laferla FM, Querfurth HW, Shtifman A (2008) Increased intraneuronal resting [Ca2+] in adult Alzheimer's disease mice. *J Neurochem* **105**, 262-271.

[283]   Stutzmann GE (2005) Calcium dysregulation, IP3 signaling, and Alzheimer's disease. *Neuroscientist* **11**, 110-115.

[284]   Mattson MP, Chan SL (2003) Neuronal and glial calcium signaling in Alzheimer's disease. *Cell Calcium* **34**, 385-397.

[285]   Giacomello M, Barbiero L, Zatti G, Squitti R, Binetti G, Pozzan T, Fasolato C, Ghidoni R, Pizzo P (2005) Reduction of Ca2+ stores and capacitative Ca2+ entry is associated with the familial Alzheimer's disease presenilin-2 T122R mutation and anticipates the onset of dementia. *Neurobiol Dis* **18**, 638-648.

[286]   Lessard CB, Lussier MP, Cayouette S, Bourque G, Boulay G (2005) The overexpression of presenilin2 and Alzheimer's-disease-linked presenilin2 variants influences TRPC6-enhanced Ca2+ entry into HEK293 cells. *Cell Signal* **17**, 437-445.

[287]   Zatti G, Ghidoni R, Barbiero L, Binetti G, Pozzan T, Fasolato C, Pizzo P (2004) The presenilin 2 M239I mutation associated with familial Alzheimer's disease reduces Ca2+ release from intracellular stores. *Neurobiol Dis* **15**, 269-278.

[288] Kasri NN, Kocks SL, Verbert L, Hebert SS, Callewaert G, Parys JB, Missiaen L, De Smedt H (2006) Up-regulation of inositol 1,4,5-trisphosphate receptor type 1 is responsible for a decreased endoplasmic-reticulum Ca2+ content in presenilin double knock-out cells. *Cell Calcium* **40**, 41-51.

[289] Bruno AM, Huang JY, Bennett DA, Marr RA, Hastings ML, Stutzmann GE (2012) Altered ryanodine receptor expression in mild cognitive impairment and Alzheimer's disease. *Neurobiol Aging* **33**, 1001 e1001-1006.

[290] Chakroborty S, Hill ES, Christian DT, Helfrich R, Riley S, Schneider C, Kapecki N, Mustaly-Kalimi S, Seiler FA, Peterson DA, West AR, Vertel BM, Frost WN, Stutzmann GE (2019) Reduced presynaptic vesicle stores mediate cellular and network plasticity defects in an early-stage mouse model of Alzheimer's disease. *Mol Neurodegener* **14**, 7.

[291] Chakroborty S, Kim J, Schneider C, West AR, Stutzmann GE (2015) Nitric oxide signaling is recruited as a compensatory mechanism for sustaining synaptic plasticity in Alzheimer's disease mice. *J Neurosci* **35**, 6893-6902.

[292] Goussakov I, Chakroborty S, Stutzmann GE (2011) Generation of dendritic Ca2+ oscillations as a consequence of altered ryanodine receptor function in AD neurons. *Channels (Austin)* **5**, 9-13.

[293] Goussakov I, Miller MB, Stutzmann GE (2010) NMDA-mediated Ca(2+) influx drives aberrant ryanodine receptor activation in dendrites of young Alzheimer's disease mice. *J Neurosci* **30**, 12128-12137.

[294] Kaczorowski CC, Sametsky E, Shah S, Vassar R, Disterhoft JF (2011) Mechanisms underlying basal and learning-related intrinsic excitability in a mouse model of Alzheimer's disease. *Neurobiol Aging* **32**, 1452-1465.

[295] Liu J, Supnet C, Sun S, Zhang H, Good L, Popugaeva E, Bezprozvanny I (2014) The role of ryanodine receptor type 3 in a mouse model of Alzheimer disease. *Channels (Austin)* **8**, 230-242.

[296] Overk CR, Rockenstein E, Florio J, Cheng Q, Masliah E (2015) Differential calcium alterations in animal models of neurodegenerative disease: Reversal by FK506. *Neuroscience* **310**, 549-560.

[297] Shilling D, Muller M, Takano H, Mak DO, Abel T, Coulter DA, Foskett JK (2014) Suppression of InsP3 receptor-mediated Ca2+ signaling alleviates mutant presenilin-linked familial Alzheimer's disease pathogenesis. *J Neurosci* **34**, 6910-6923.

[298] Tsigelny IF, Crews L, Desplats P, Shaked GM, Sharikov Y, Mizuno H, Spencer B, Rockenstein E, Trejo M, Platoshyn O, Yuan JX, Masliah E (2008) Mechanisms of hybrid oligomer formation in the pathogenesis of combined Alzheimer's and Parkinson's diseases. *PLoS One* **3**, e3135.

[299] Zhang H, Liu J, Sun S, Pchitskaya E, Popugaeva E, Bezprozvanny I (2015) Calcium signaling, excitability, and synaptic plasticity defects in a mouse model of Alzheimer's disease. *J Alzheimers Dis* **45**, 561-580.

[300] Zhang H, Sun S, Herreman A, De Strooper B, Bezprozvanny I (2010) Role of presenilins in neuronal calcium homeostasis. *J Neurosci* **30**, 8566-8580.

[301] Young LT, Kish SJ, Li PP, Warsh JJ (1988) Decreased brain [3H]inositol 1,4,5-trisphosphate binding in Alzheimer's disease. *Neurosci Lett* **94**, 198-202.

[302] Choi B, Lee HW, Mo S, Kim JY, Kim HW, Rhyu IJ, Hong E, Lee YK, Choi JS, Kim CH, Kim H (2018) Inositol 1,4,5-trisphosphate 3-kinase A overexpressed in mouse forebrain modulates synaptic transmission and mGluR-LTD of CA1 pyramidal neurons. *PLoS One* **13**, e0193859.

[303] Windhorst S, Minge D, Bahring R, Huser S, Schob C, Blechner C, Lin HY, Mayr GW, Kindler S (2012) Inositol-1,4,5-trisphosphate 3-kinase A regulates dendritic morphology and shapes synaptic Ca2+ transients. *Cell Signal* **24**, 750-757.

[304] Kuchibhotla KV, Goldman ST, Lattarulo CR, Wu HY, Hyman BT, Bacskai BJ (2008) Abeta plaques lead to aberrant regulation of calcium homeostasis in vivo resulting in structural and functional disruption of neuronal networks. *Neuron* **59**, 214-225.

[305] Iacopino AM, Christakos S (1990) Specific reduction of calcium-binding protein (28-kilodalton calbindin-D) gene expression in aging and neurodegenerative diseases. *Proc Natl Acad Sci U S A* **87**, 4078-4082.

[306] Guo Q, Christakos S, Robinson N, Mattson MP (1998) Calbindin D28k blocks the proapoptotic actions of mutant presenilin 1: reduced oxidative stress and preserved mitochondrial function. *Proc Natl Acad Sci U S A* **95**, 3227-3232.

[307] Buxbaum JD, Choi EK, Luo Y, Lilliehook C, Crowley AC, Merriam DE, Wasco W (1998) Calsenilin: a calcium-binding protein that interacts with the presenilins and regulates the levels of a presenilin fragment. *Nat Med* **4**, 1177-1181.

[308] Leissring MA, Yamasaki TR, Wasco W, Buxbaum JD, Parker I, LaFerla FM (2000) Calsenilin reverses presenilin-mediated enhancement of calcium signaling. *Proc Natl Acad Sci U S A* **97**, 8590-8593.

[309] Verdaguer E, Brox S, Petrov D, Olloquequi J, Romero R, de Lemos ML, Camins A, Auladell C (2015) Vulnerability of calbindin, calretinin and parvalbumin in a transgenic/knock-in APPswe/PS1dE9 mouse model of Alzheimer disease together with disruption of hippocampal neurogenesis. *Exp Gerontol* **69**, 176-188.

[310] Kook SY, Jeong H, Kang MJ, Park R, Shin HJ, Han SH, Son SM, Song H, Baik SH, Moon M, Yi EC, Hwang D, Mook-Jung I (2014) Crucial role of calbindin-D28k in the pathogenesis of Alzheimer's disease mouse model. *Cell Death Differ* **21**, 1575-1587.

[311] Manczak M, Anekonda TS, Henson E, Park BS, Quinn J, Reddy PH (2006) Mitochondria are a direct site of A beta accumulation in Alzheimer's disease neurons: implications for free radical generation and oxidative damage in disease progression. *Hum Mol Genet* **15**, 1437-1449.

[312] Reddy PH, McWeeney S, Park BS, Manczak M, Gutala RV, Partovi D, Jung Y, Yau V, Searles R, Mori M, Quinn J (2004) Gene expression profiles of transcripts in amyloid precursor protein transgenic mice: up-regulation of mitochondrial metabolism and apoptotic genes is an early cellular change in Alzheimer's disease. *Hum Mol Genet* **13**, 1225-1240.

[313] Schulz KL, Eckert A, Rhein V, Mai S, Haase W, Reichert AS, Jendrach M, Muller WE, Leuner K (2012) A new link to mitochondrial impairment in tauopathies. *Mol Neurobiol* **46**, 205-216.

[314] Manczak M, Reddy PH (2012) Abnormal interaction between the mitochondrial fission protein Drp1 and hyperphosphorylated tau in Alzheimer's disease neurons: implications for mitochondrial dysfunction and neuronal damage. *Hum Mol Genet* **21**, 2538-2547.

[315] Quintanilla RA, von Bernhardi R, Godoy JA, Inestrosa NC, Johnson GV (2014) Phosphorylated tau potentiates Abeta-induced mitochondrial damage in mature neurons. *Neurobiol Dis* **71**, 260-269.

[316] Rhein V, Song X, Wiesner A, Ittner LM, Baysang G, Meier F, Ozmen L, Bluethmann H, Drose S, Brandt U, Savaskan E, Czech C, Gotz J, Eckert A (2009) Amyloid-beta and tau synergistically impair the oxidative phosphorylation system in triple transgenic Alzheimer's disease mice. *Proc Natl Acad Sci U S A* **106**, 20057-20062.

[317] Haass C, Selkoe DJ (2007) Soluble protein oligomers in neurodegeneration: lessons from the Alzheimer's amyloid beta-peptide. *Nat Rev Mol Cell Biol* **8**, 101-112.

[318] Shankar GM, Li S, Mehta TH, Garcia-Munoz A, Shepardson NE, Smith I, Brett FM, Farrell MA, Rowan MJ, Lemere CA, Regan CM, Walsh DM, Sabatini BL, Selkoe DJ (2008) Amyloid-beta protein dimers isolated directly from Alzheimer's brains impair synaptic plasticity and memory. *Nat Med* **14**, 837-842.

[319] Ma T, Hoeffer CA, Capetillo-Zarate E, Yu F, Wong H, Lin MT, Tampellini D, Klann E, Blitzer RD, Gouras GK (2010) Dysregulation of the mTOR pathway mediates impairment of synaptic plasticity in a mouse model of Alzheimer's disease. *PLoS One* **5**.

[320] Querfurth HW, LaFerla FM (2010) Alzheimer's disease. *N Engl J Med* **362**, 329-344.

[321] Terry RD (2000) Cell death or synaptic loss in Alzheimer disease. *J Neuropathol Exp Neurol* **59**, 1118-1119.

[322] Chapman PF, White GL, Jones MW, Cooper-Blacketer D, Marshall VJ, Irizarry M, Younkin L, Good MA, Bliss TV, Hyman BT, Younkin SG, Hsiao KK (1999) Impaired synaptic plasticity and learning in aged amyloid precursor protein transgenic mice. *Nat Neurosci* **2**, 271-276.

[323] Larson J, Lynch G, Games D, Seubert P (1999) Alterations in synaptic transmission and long-term potentiation in hippocampal slices from young and aged PDAPP mice. *Brain Res* **840**, 23-35.

[324] Moechars D, Dewachter I, Lorent K, Reverse D, Baekelandt V, Naidu A, Tesseur I, Spittaels K, Haute CV, Checler F, Godaux E, Cordell B, Van Leuven F (1999) Early phenotypic changes in transgenic mice that overexpress different mutants of amyloid precursor protein in brain. *J Biol Chem* **274**, 6483-6492.

[325] Oddo S, Caccamo A, Shepherd JD, Murphy MP, Golde TE, Kayed R, Metherate R, Mattson MP, Akbari Y, LaFerla FM (2003) Triple-transgenic model of Alzheimer's disease with plaques and tangles: intracellular Abeta and synaptic dysfunction. *Neuron* **39**, 409-421.

[326] Trinchese F, Liu S, Battaglia F, Walter S, Mathews PM, Arancio O (2004) Progressive age-related development of Alzheimer-like pathology in APP/PS1 mice. *Ann Neurol* **55**, 801-814.

[327] Rosenmann H, Grigoriadis N, Eldar-Levy H, Avital A, Rozenstein L, Touloumi O, Behar L, Ben-Hur T, Avraham Y, Berry E, Segal M, Ginzburg I, Abramsky O (2008) A novel transgenic mouse expressing double mutant tau driven by its natural promoter exhibits tauopathy characteristics. *Exp Neurol* **212**, 71-84.

[328] Gahtan E, Auerbach JM, Groner Y, Segal M (1998) Reversible impairment of long-term potentiation in transgenic Cu/Zn-SOD mice. *Eur J Neurosci* **10**, 538-544.

[329] Thiels E, Urban NN, Gonzalez-Burgos GR, Kanterewicz BI, Barrionuevo G, Chu CT, Oury TD, Klann E (2000) Impairment of long-term potentiation and associative memory in mice that overexpress extracellular superoxide dismutase. *J Neurosci* **20**, 7631-7639.

[330] Thiels E, Klann E (2002) Hippocampal memory and plasticity in superoxide dismutase mutant mice. *Physiol Behav* **77**, 601-605.

[331] Kamsler A, Segal M (2003) Paradoxical actions of hydrogen peroxide on long-term potentiation in transgenic superoxide dismutase-1 mice. *J Neurosci* **23**, 10359-10367.

[332] Levin ED, Christopher NC, Lateef S, Elamir BM, Patel M, Liang LP, Crapo JD (2002) Extracellular superoxide dismutase overexpression protects against aging-induced cognitive impairment in mice. *Behav Genet* **32**, 119-125.

[333]   Ma T, Hoeffer CA, Wong H, Massaad CA, Zhou P, Iadecola C, Murphy MP, Pautler RG, Klann E (2011) Amyloid beta-induced impairments in hippocampal synaptic plasticity are rescued by decreasing mitochondrial superoxide. *J Neurosci* **31**, 5589-5595.

[334]   Bindokas VP, Jordan J, Lee CC, Miller RJ (1996) Superoxide production in rat hippocampal neurons: selective imaging with hydroethidine. *J Neurosci* **16**, 1324-1336.

[335]   Busche MA, Eichhoff G, Adelsberger H, Abramowski D, Wiederhold KH, Haass C, Staufenbiel M, Konnerth A, Garaschuk O (2008) Clusters of hyperactive neurons near amyloid plaques in a mouse model of Alzheimer's disease. *Science* **321**, 1686-1689.

[336]   Busche MA, Chen X, Henning HA, Reichwald J, Staufenbiel M, Sakmann B, Konnerth A (2012) Critical role of soluble amyloid-beta for early hippocampal hyperactivity in a mouse model of Alzheimer's disease. *Proc Natl Acad Sci U S A* **109**, 8740-8745.

[337]   Busche MA (2018) In Vivo Two-Photon Calcium Imaging of Hippocampal Neurons in Alzheimer Mouse Models. *Methods Mol Biol* **1750**, 341-351.

[338]   Busche MA, Konnerth A (2015) Neuronal hyperactivity--A key defect in Alzheimer's disease? *Bioessays* **37**, 624-632.

[339]   Lerdkrai C, Asavapanumas N, Brawek B, Kovalchuk Y, Mojtahedi N, Olmedillas Del Moral M, Garaschuk O (2018) Intracellular Ca(2+) stores control in vivo neuronal hyperactivity in a mouse model of Alzheimer's disease. *Proc Natl Acad Sci U S A* **115**, E1279-E1288.

[340]   Zott B, Simon MM, Hong W, Unger F, Chen-Engerer HJ, Frosch MP, Sakmann B, Walsh DM, Konnerth A (2019) A vicious cycle of beta amyloid-dependent neuronal hyperactivation. *Science* **365**, 559-565.

[341]   Hamilton A, Zamponi GW, Ferguson SS (2015) Glutamate receptors function as scaffolds for the regulation of beta-amyloid and cellular prion protein signaling complexes. *Mol Brain* **8**, 18.

[342]   Renner M, Lacor PN, Velasco PT, Xu J, Contractor A, Klein WL, Triller A (2010) Deleterious effects of amyloid beta oligomers acting as an extracellular scaffold for mGluR5. *Neuron* **66**, 739-754.

[343]   Masliah E, Alford M, DeTeresa R, Mallory M, Hansen L (1996) Deficient glutamate transport is associated with neurodegeneration in Alzheimer's disease. *Ann Neurol* **40**, 759-766.

[344]   Li S, Hong S, Shepardson NE, Walsh DM, Shankar GM, Selkoe D (2009) Soluble oligomers of amyloid Beta protein facilitate hippocampal long-term depression by disrupting neuronal glutamate uptake. *Neuron* **62**, 788-801.

[345]   Supnet C, Bezprozvanny I (2010) The dysregulation of intracellular calcium in Alzheimer disease. *Cell Calcium* **47**, 183-189.

[346]   Del Vecchio RA, Gold LH, Novick SJ, Wong G, Hyde LA (2004) Increased seizure threshold and severity in young transgenic CRND8 mice. *Neurosci Lett* **367**, 164-167.

[347]   Wang Y, Zhang G, Zhou H, Barakat A, Querfurth H (2009) Opposite effects of low and high doses of Abeta42 on electrical network and neuronal excitability in the rat prefrontal cortex. *PLoS One* **4**, e8366.

[348]   Berkowitz BA, Lenning J, Khetarpal N, Tran C, Wu JY, Berri AM, Dernay K, Haacke EM, Shafie-Khorassani F, Podolsky RH, Gant JC, Maimaiti S, Thibault O, Murphy GG, Bennett BM, Roberts R (2017) In vivo imaging of prodromal hippocampus CA1 subfield oxidative stress in models of Alzheimer disease and Angelman syndrome. *FASEB J* **31**, 4179-4186.

[349]   Bonomo SM, Rigamonti AE, Giunta M, Galimberti D, Guaita A, Gagliano MG, Muller EE, Cella SG (2009) Menopausal transition: a possible risk factor for brain pathologic events. *Neurobiol Aging* **30**, 71-80.

[350] Pike CJ, Carroll JC, Rosario ER, Barron AM (2009) Protective actions of sex steroid hormones in Alzheimer's disease. *Front Neuroendocrinol* **30**, 239-258.

[351] Vest RS, Pike CJ (2013) Gender, sex steroid hormones, and Alzheimer's disease. *Horm Behav* **63**, 301-307.

[352] Srivastava DP, Woolfrey KM, Penzes P (2013) Insights into rapid modulation of neuroplasticity by brain estrogens. *Pharmacol Rev* **65**, 1318-1350.

[353] Henderson VW, Paganini-Hill A, Emanuel CK, Dunn ME, Buckwalter JG (1994) Estrogen replacement therapy in older women. Comparisons between Alzheimer's disease cases and nondemented control subjects. *Arch Neurol* **51**, 896-900.

[354] Kawas C, Resnick S, Morrison A, Brookmeyer R, Corrada M, Zonderman A, Bacal C, Lingle DD, Metter E (1997) A prospective study of estrogen replacement therapy and the risk of developing Alzheimer's disease: the Baltimore Longitudinal Study of Aging. *Neurology* **48**, 1517-1521.

[355] Paganini-Hill A, Henderson VW (1994) Estrogen deficiency and risk of Alzheimer's disease in women. *Am J Epidemiol* **140**, 256-261.

[356] Tang MX, Jacobs D, Stern Y, Marder K, Schofield P, Gurland B, Andrews H, Mayeux R (1996) Effect of oestrogen during menopause on risk and age at onset of Alzheimer's disease. *Lancet* **348**, 429-432.

[357] Waring SC, Rocca WA, Petersen RC, O'Brien PC, Tangalos EG, Kokmen E (1999) Postmenopausal estrogen replacement therapy and risk of AD: a population-based study. *Neurology* **52**, 965-970.

[358] Fillit H, Weinreb H, Cholst I, Luine V, McEwen B, Amador R, Zabriskie J (1986) Observations in a preliminary open trial of estradiol therapy for senile dementia-Alzheimer's type. *Psychoneuroendocrinology* **11**, 337-345.

[359] Honjo H, Ogino Y, Naitoh K, Urabe M, Kitawaki J, Yasuda J, Yamamoto T, Ishihara S, Okada H, Yonezawa T, et al. (1989) In vivo effects by estrone sulfate on the central nervous system-senile dementia (Alzheimer's type). *J Steroid Biochem* **34**, 521-525.

[360] Ohkura T, Isse K, Akazawa K, Hamamoto M, Yaoi Y, Hagino N (1994) Evaluation of estrogen treatment in female patients with dementia of the Alzheimer type. *Endocr J* **41**, 361-371.

[361] Ohkura T, Isse K, Akazawa K, Hamamoto M, Yaoi Y, Hagino N (1995) Long-term estrogen replacement therapy in female patients with dementia of the Alzheimer type: 7 case reports. *Dementia* **6**, 99-107.

[362] Cai B, Ye S, Wang Y, Hua RP, Wang TT, Lix LJ, Jiang AJ, Shen GM (2018) [Protective effects of genistein on Abeta(2)(5)(-)(3)(5)-induced PC12 cell injury via regulating CaM-CaMKIV signaling pathway]. *Zhongguo Zhong Yao Za Zhi* **43**, 571-576.

[363] Xi YD, Zhang DD, Ding J, Yu HL, Yuan LH, Ma WW, Han J, Xiao R (2016) Genistein Inhibits Abeta25-35-Induced Synaptic Toxicity and Regulates CaMKII/CREB Pathway in SH-SY5Y Cells. *Cell Mol Neurobiol* **36**, 1151-1159.

[364] Luo S, Lan T, Liao W, Zhao M, Yang H (2012) Genistein inhibits Abeta(2)(5)(-)(3)(5) - induced neurotoxicity in PC12 cells via PKC signaling pathway. *Neurochem Res* **37**, 2787-2794.

[365] Zeng H, Chen Q, Zhao B (2004) Genistein ameliorates beta-amyloid peptide (25-35)-induced hippocampal neuronal apoptosis. *Free Radic Biol Med* **36**, 180-188.

[366] Dong Y, Li R, Jiang A, Xu Z, Wang Y (2017) Phytoestrogen alpha-zearalanol attenuate endoplasmic reticulum stress to against cultured rat hippocampal neurons apoptotic death induced by amyloid beta25-35. *Neuro Endocrinol Lett* **38**, 353-359.

[367]   Hwang SL, Yen GC (2011) Effect of hesperetin against oxidative stress via ER- and TrkA-mediated actions in PC12 cells. *J Agric Food Chem* **59**, 5779-5785.

[368]   Ma ZG, Wang J, Jiang H, Xie JX, Chen L (2005) C31 enhances voltage-gated calcium channel currents in undifferentiated PC12 cells. *Neurosci Lett* **382**, 102-105.

[369]   Larson EB, Kukull WA, Katzman RL (1992) Cognitive impairment: dementia and Alzheimer's disease. *Annu Rev Public Health* **13**, 431-449.

[370]   Tyas SL, Manfreda J, Strain LA, Montgomery PR (2001) Risk factors for Alzheimer's disease: a population-based, longitudinal study in Manitoba, Canada. *Int J Epidemiol* **30**, 590-597.

[371]   Lopez OL (2011) The growing burden of Alzheimer's disease. *Am J Manag Care* **17 Suppl 13**, S339-345.

[372]   Tanzi RE (2012) The genetics of Alzheimer disease. *Cold Spring Harb Perspect Med* **2**.

[373]   Bates K, Vink R, Martins R, Harvey A (2014) Aging, cortical injury and Alzheimer's disease-like pathology in the guinea pig brain. *Neurobiol Aging* **35**, 1345-1351.

[374]   Li H, Zhu H, Wallack M, Mwamburi M, Abdul-Hay SO, Leissring MA, Qiu WQ (2016) Age and its association with low insulin and high amyloid-beta peptides in blood. *J Alzheimers Dis* **49**, 129-137.

[375]   Chen YH, Lo RY (2017) Alzheimer's disease and osteoporosis. *Ci Ji Yi Xue Za Zhi* **29**, 138-142.

[376]   D'Souza Y, Elharram A, Soon-Shiong R, Andrew RD, Bennett BM (2015) Characterization of Aldh2 (-/-) mice as an age-related model of cognitive impairment and Alzheimer's disease. *Mol Brain* **8**, 27.

[377]   Mehder RH, Bennett BM, Andrew RD (2020) Morphometric Analysis of Hippocampal and Neocortical Pyramidal Neurons in a Mouse Model of Late Onset Alzheimer's Disease. *J Alzheimers Dis*.

[378]   D'Souza Y, Kawamoto T, Bennett BM (2014) Role of the lipid peroxidation product, 4-hydroxynonenal, in the development of nitrate tolerance. *Chem Res Toxicol* **27**, 663-673.

[379]   Abner EL, Neltner JH, Jicha GA, Patel E, Anderson SL, Wilcock DM, Van Eldik LJ, Nelson PT (2018) Diffuse Amyloid-beta Plaques, Neurofibrillary Tangles, and the Impact of APOE in Elderly Persons' Brains Lacking Neuritic Amyloid Plaques. *J Alzheimers Dis* **64**, 1307-1324.

[380]   Mathias JL, Morphett K (2010) Neurobehavioral differences between Alzheimer's disease and frontotemporal dementia: a meta-analysis. *J Clin Exp Neuropsychol* **32**, 682-698.

[381]   Pasqualetti G, Brooks DJ, Edison P (2015) The role of neuroinflammation in dementias. *Curr Neurol Neurosci Rep* **15**, 17.

[382]   Spires-Jones TL, Attems J, Thal DR (2017) Interactions of pathological proteins in neurodegenerative diseases. *Acta Neuropathol* **134**, 187-205.

[383]   Rockenstein E, Crews L, Masliah E (2007) Transgenic animal models of neurodegenerative diseases and their application to treatment development. *Adv Drug Deliv Rev* **59**, 1093-1102.

[384]   Van Dam D, De Deyn PP (2006) Drug discovery in dementia: the role of rodent models. *Nat Rev Drug Discov* **5**, 956-970.

[385]   Dodart JC, May P (2005) Overview on rodent models of Alzheimer's disease. *Curr Protoc Neurosci* **Chapter 9**, Unit 9 22.

[386]   Woodruff-Pak DS (2008) Animal models of Alzheimer's disease: therapeutic implications. *J Alzheimers Dis* **15**, 507-521.

[387]   Manzano S, Gonzalez J, Marcos A, Payno M, Villanueva C, Matias-Guiu J (2009) [Experimental models in Alzheimer's disease]. *Neurologia* **24**, 255-262.

[388]   Obulesu M, Rao DM (2010) Animal models of Alzheimer's disease: an understanding of pathology and therapeutic avenues. *Int J Neurosci* **120**, 531-537.

[389]   Braidy N, Munoz P, Palacios AG, Castellano-Gonzalez G, Inestrosa NC, Chung RS, Sachdev P, Guillemin GJ (2012) Recent rodent models for Alzheimer's disease: clinical implications and basic research. *J Neural Transm (Vienna)* **119**, 173-195.

[390]   Mattson MP, Pedersen WA, Duan W, Culmsee C, Camandola S (1999) Cellular and molecular mechanisms underlying perturbed energy metabolism and neuronal degeneration in Alzheimer's and Parkinson's diseases. *Ann N Y Acad Sci* **893**, 154-175.

[391]   Sun KH, de Pablo Y, Vincent F, Shah K (2008) Deregulated Cdk5 promotes oxidative stress and mitochondrial dysfunction. *J Neurochem* **107**, 265-278.

[392]   von Bernhardi R, Eugenin J (2012) Alzheimer's disease: redox dysregulation as a common denominator for diverse pathogenic mechanisms. *Antioxid Redox Signal* **16**, 974-1031.

[393]   Magi S, Castaldo P, Macri ML, Maiolino M, Matteucci A, Bastioli G, Gratteri S, Amoroso S, Lariccia V (2016) Intracellular Calcium Dysregulation: Implications for Alzheimer's Disease. *Biomed Res Int* **2016**, 6701324.

[394]   Foster TC, Kyritsopoulos C, Kumar A (2017) Central role for NMDA receptors in redox mediated impairment of synaptic function during aging and Alzheimer's disease. *Behav Brain Res* **322**, 223-232.

[395]   Connolly NM, Prehn JH (2015) The metabolic response to excitotoxicity - lessons from single-cell imaging. *J Bioenerg Biomembr* **47**, 75-88.

[396]   Alzheimer's Association Calcium Hypothesis W (2017) Calcium Hypothesis of Alzheimer's disease and brain aging: A framework for integrating new evidence into a comprehensive theory of pathogenesis. *Alzheimers Dement* **13**, 178-182 e117.

[397]   Gibson GE, Zhang H, Xu H, Park LC, Jeitner TM (2002) Oxidative stress increases internal calcium stores and reduces a key mitochondrial enzyme. *Biochim Biophys Acta* **1586**, 177-189.

[398]   Tosun D, Schuff N, Shaw LM, Trojanowski JQ, Weiner MW, Alzheimer's Disease NeuroImaging I (2011) Relationship between CSF biomarkers of Alzheimer's disease and rates of regional cortical thinning in ADNI data. *J Alzheimers Dis* **26 Suppl 3**, 77-90.

[399]   Thurfjell L, Lotjonen J, Lundqvist R, Koikkalainen J, Soininen H, Waldemar G, Brooks DJ, Vandenberghe R (2012) Combination of biomarkers: PET [18F]flutemetamol imaging and structural MRI in dementia and mild cognitive impairment. *Neurodegener Dis* **10**, 246-249.

[400]   Stricker NH, Dodge HH, Dowling NM, Han SD, Erosheva EA, Jagust WJ, Alzheimer's Disease Neuroimaging I (2012) CSF biomarker associations with change in hippocampal volume and precuneus thickness: implications for the Alzheimer's pathological cascade. *Brain Imaging Behav* **6**, 599-609.

[401]   Markesbery WR (1997) Oxidative stress hypothesis in Alzheimer's disease. *Free Radic Biol Med* **23**, 134-147.

[402]   Butterfield DA (1997) beta-Amyloid-associated free radical oxidative stress and neurotoxicity: implications for Alzheimer's disease. *Chem Res Toxicol* **10**, 495-506.

[403]   Pratico D (2008) Oxidative stress hypothesis in Alzheimer's disease: a reappraisal. *Trends Pharmacol Sci* **29**, 609-615.

[404] Lovell MA, Ehmann WD, Butler SM, Markesbery WR (1995) Elevated thiobarbituric acid-reactive substances and antioxidant enzyme activity in the brain in Alzheimer's disease. *Neurology* **45**, 1594-1601.

[405] Hensley K, Maidt ML, Yu Z, Sang H, Markesbery WR, Floyd RA (1998) Electrochemical analysis of protein nitrotyrosine and dityrosine in the Alzheimer brain indicates region-specific accumulation. *J Neurosci* **18**, 8126-8132.

[406] Markesbery WR, Lovell MA (1998) Four-hydroxynonenal, a product of lipid peroxidation, is increased in the brain in Alzheimer's disease. *Neurobiol Aging* **19**, 33-36.

[407] Lovell MA, Ehmann WD, Mattson MP, Markesbery WR (1997) Elevated 4-hydroxynonenal in ventricular fluid in Alzheimer's disease. *Neurobiol Aging* **18**, 457-461.

[408] Halliwell B (2006) Oxidative stress and neurodegeneration: where are we now? *J Neurochem* **97**, 1634-1658.

[409] Markesbery WR, Carney JM (1999) Oxidative alterations in Alzheimer's disease. *Brain Pathol* **9**, 133-146.

[410] Montine KS, Olson SJ, Amarnath V, Whetsell WO, Jr., Graham DG, Montine TJ (1997) Immunohistochemical detection of 4-hydroxy-2-nonenal adducts in Alzheimer's disease is associated with inheritance of APOE4. *Am J Pathol* **150**, 437-443.

[411] Reed TT, Pierce WM, Markesbery WR, Butterfield DA (2009) Proteomic identification of HNE-bound proteins in early Alzheimer disease: Insights into the role of lipid peroxidation in the progression of AD. *Brain Res* **1274**, 66-76.

[412] Sultana R, Perluigi M, Butterfield DA (2013) Lipid peroxidation triggers neurodegeneration: a redox proteomics view into the Alzheimer disease brain. *Free Radic Biol Med* **62**, 157-169.

[413] Mattson MP, Fu W, Waeg G, Uchida K (1997) 4-Hydroxynonenal, a product of lipid peroxidation, inhibits dephosphorylation of the microtubule-associated protein tau. *Neuroreport* **8**, 2275-2281.

[414] Floyd RA, Hensley K (2002) Oxidative stress in brain aging. Implications for therapeutics of neurodegenerative diseases. *Neurobiol Aging* **23**, 795-807.

[415] Siegel SJ, Bieschke J, Powers ET, Kelly JW (2007) The oxidative stress metabolite 4-hydroxynonenal promotes Alzheimer protofibril formation. *Biochemistry* **46**, 1503-1510.

[416] Kruman I, Bruce-Keller AJ, Bredesen D, Waeg G, Mattson MP (1997) Evidence that 4-hydroxynonenal mediates oxidative stress-induced neuronal apoptosis. *J Neurosci* **17**, 5089-5100.

[417] Butterfield DA, Reed T, Newman SF, Sultana R (2007) Roles of amyloid beta-peptide-associated oxidative stress and brain protein modifications in the pathogenesis of Alzheimer's disease and mild cognitive impairment. *Free Radic Biol Med* **43**, 658-677.

[418] Matsuoka Y, Picciano M, La Francois J, Duff K (2001) Fibrillar beta-amyloid evokes oxidative damage in a transgenic mouse model of Alzheimer's disease. *Neuroscience* **104**, 609-613.

[419] Mohmmad Abdul H, Sultana R, Keller JN, St Clair DK, Markesbery WR, Butterfield DA (2006) Mutations in amyloid precursor protein and presenilin-1 genes increase the basal oxidative stress in murine neuronal cells and lead to increased sensitivity to oxidative stress mediated by amyloid beta-peptide (1-42), HO and kainic acid: implications for Alzheimer's disease. *J Neurochem* **96**, 1322-1335.

[420] Nunomura A, Perry G, Aliev G, Hirai K, Takeda A, Balraj EK, Jones PK, Ghanbari H, Wataya T, Shimohama S, Chiba S, Atwood CS, Petersen RB, Smith MA (2001) Oxidative damage is the earliest event in Alzheimer disease. *J Neuropathol Exp Neurol* **60**, 759-767.

[421] Nunomura A, Perry G, Pappolla MA, Friedland RP, Hirai K, Chiba S, Smith MA (2000) Neuronal oxidative stress precedes amyloid-beta deposition in Down syndrome. *J Neuropathol Exp Neurol* **59**, 1011-1017.

[422] Pratico D, Uryu K, Leight S, Trojanoswki JQ, Lee VM (2001) Increased lipid peroxidation precedes amyloid plaque formation in an animal model of Alzheimer amyloidosis. *J Neurosci* **21**, 4183-4187.

[423] Resende R, Moreira PI, Proenca T, Deshpande A, Busciglio J, Pereira C, Oliveira CR (2008) Brain oxidative stress in a triple-transgenic mouse model of Alzheimer disease. *Free Radic Biol Med* **44**, 2051-2057.

[424] Watson JB, Arnold MM, Ho YS, O'Dell TJ (2006) Age-dependent modulation of hippocampal long-term potentiation by antioxidant enzymes. *J Neurosci Res* **84**, 1564-1574.

[425] Vereker E, O'Donnell E, Lynch MA (2000) The inhibitory effect of interleukin-1beta on long-term potentiation is coupled with increased activity of stress-activated protein kinases. *J Neurosci* **20**, 6811-6819.

[426] Bellinger FP, Madamba S, Siggins GR (1993) Interleukin 1 beta inhibits synaptic strength and long-term potentiation in the rat CA1 hippocampus. *Brain Res* **628**, 227-234.

[427] Kitagawa K, Kawamoto T, Kunugita N, Tsukiyama T, Okamoto K, Yoshida A, Nakayama K, Nakayama K (2000) Aldehyde dehydrogenase (ALDH) 2 associates with oxidation of methoxyacetaldehyde; in vitro analysis with liver subcellular fraction derived from human and Aldh2 gene targeting mouse. *FEBS Lett* **476**, 306-311.

[428] Isse T, Oyama T, Kitagawa K, Matsuno K, Matsumoto A, Yoshida A, Nakayama K, Nakayama K, Kawamoto T (2002) Diminished alcohol preference in transgenic mice lacking aldehyde dehydrogenase activity. *Pharmacogenetics* **12**, 621-626.

[429] Luo J, Lee SH, VandeVrede L, Qin Z, Ben Aissa M, Larson J, Teich AF, Arancio O, D'Souza Y, Elharram A, Koster K, Tai LM, LaDu MJ, Bennett BM, Thatcher GR (2016) A multifunctional therapeutic approach to disease modification in multiple familial mouse models and a novel sporadic model of Alzheimer's disease. *Mol Neurodegener* **11**, 35.

[430] Moore SJ, Murphy GG (2020) The Role of L-Type Calcium Channels in Neuronal Excitability and Aging. *Neurobiol Learn Mem*, 107230.

[431] Murphy GG, Fedorov NB, Giese KP, Ohno M, Friedman E, Chen R, Silva AJ (2004) Increased neuronal excitability, synaptic plasticity, and learning in aged Kvbeta1.1 knockout mice. *Curr Biol* **14**, 1907-1915.

[432] Gallagher M, Bizon JL, Hoyt EC, Helm KA, Lund PK (2003) Effects of aging on the hippocampal formation in a naturally occurring animal model of mild cognitive impairment. *Exp Gerontol* **38**, 71-77.

[433] Nicolle MM, Gallagher M, McKinney M (1999) No loss of synaptic proteins in the hippocampus of aged, behaviorally impaired rats. *Neurobiol Aging* **20**, 343-348.

[434] Smith DR, Gallagher M, Stanton ME (2007) Genetic background differences and nonassociative effects in mouse trace fear conditioning. *Learn Mem* **14**, 597-605.

[435] Sung JY, Goo JS, Lee DE, Jin DQ, Bizon JL, Gallagher M, Han JS (2008) Learning strategy selection in the water maze and hippocampal CREB phosphorylation differ in two inbred strains of mice. *Learn Mem* **15**, 183-188.

[436] Scheff SW, Anderson KJ, DeKosky ST (1985) Strain comparison of synaptic density in hippocampal CA1 of aged rats. *Neurobiol Aging* **6**, 29-34.

[437] Cheng JS, Craft R, Yu GQ, Ho K, Wang X, Mohan G, Mangnitsky S, Ponnusamy R, Mucke L (2014) Tau reduction diminishes spatial learning and memory deficits after mild repetitive traumatic brain injury in mice. *PLoS One* **9**, e115765.

[438] Chen J, Wang Z, Li M (2011) Multiple 'hits' during postnatal and early adulthood periods disrupt the normal development of sensorimotor gating ability in rats. *J Psychopharmacol* **25**, 379-392.

[439] Lim AL, Taylor DA, Malone DT (2012) A two-hit model: behavioural investigation of the effect of combined neonatal MK-801 administration and isolation rearing in the rat. *J Psychopharmacol* **26**, 1252-1264.

[440] Gao HM, Zhang F, Zhou H, Kam W, Wilson B, Hong JS (2011) Neuroinflammation and alpha-synuclein dysfunction potentiate each other, driving chronic progression of neurodegeneration in a mouse model of Parkinson's disease. *Environ Health Perspect* **119**, 807-814.

[441] Knopp RC, Lee SH, Hollas M, Nepomuceno E, Gonzalez D, Tam K, Aamir D, Wang Y, Pierce E, BenAissa M, Thatcher GRJ (2020) Interaction of oxidative stress and neurotrauma in ALDH2(-/-) mice causes significant and persistent behavioral and pro-inflammatory effects in a tractable model of mild traumatic brain injury. *Redox Biol* **32**, 101486.

[442] Ikegaya Y, Saito H, Abe K (1994) Attenuated hippocampal long-term potentiation in basolateral amygdala-lesioned rats. *Brain Res* **656**, 157-164.

[443] Yaniv D, Vouimba RM, Diamond DM, Richter-Levin G (2003) Simultaneous induction of long-term potentiation in the hippocampus and the amygdala by entorhinal cortex activation: mechanistic and temporal profiles. *Neuroscience* **120**, 1125-1135.

[444] Vigot R, Batini C, Kado RT, Yamamori T (2002) Synaptic long-term depression (LTD) in vivo recorded on the rat cerebellar cortex. *Arch Ital Biol* **140**, 1-12.

[445] Zhang W, Linden DJ (2006) Long-term depression at the mossy fiber-deep cerebellar nucleus synapse. *J Neurosci* **26**, 6935-6944.

[446] Arruda-Carvalho M, Clem RL (2014) Pathway-selective adjustment of prefrontal-amygdala transmission during fear encoding. *J Neurosci* **34**, 15601-15609.

[447] Child ND, Benarroch EE (2014) Differential distribution of voltage-gated ion channels in cortical neurons: implications for epilepsy. *Neurology* **82**, 989-999.

[448] Sah P (1996) Ca(2+)-activated K+ currents in neurones: types, physiological roles and modulation. *Trends Neurosci* **19**, 150-154.

[449] Jaffe DB, Ross WN, Lisman JE, Lasser-Ross N, Miyakawa H, Johnston D (1994) A model for dendritic Ca2+ accumulation in hippocampal pyramidal neurons based on fluorescence imaging measurements. *J Neurophysiol* **71**, 1065-1077.

[450] Traub RD, Wong RK, Miles R, Michelson H (1991) A model of a CA3 hippocampal pyramidal neuron incorporating voltage-clamp data on intrinsic conductances. *J Neurophysiol* **66**, 635-650.

[451] Stocker M, Pedarzani P (2000) Differential distribution of three Ca(2+)-activated K(+) channel subunits, SK1, SK2, and SK3, in the adult rat central nervous system. *Mol Cell Neurosci* **15**, 476-493.

[452] Barnes CA, Rao G, McNaughton BL (1996) Functional integrity of NMDA-dependent LTP induction mechanisms across the lifespan of F-344 rats. *Learn Mem* **3**, 124-137.

[453] Deupree DL, Bradley J, Turner DA (1993) Age-related alterations in potentiation in the CA1 region in F344 rats. *Neurobiol Aging* **14**, 249-258.

[454] Moore CI, Browning MD, Rose GM (1993) Hippocampal plasticity induced by primed burst, but not long-term potentiation, stimulation is impaired in area CA1 of aged Fischer 344 rats. *Hippocampus* **3**, 57-66.

[455] Landfield PW, Lynch G (1977) Impaired monosynaptic potentiation in in vitro hippocampal slices from aged, memory-deficient rats. *J Gerontol* **32**, 523-533.

[456] McGrath LT, McGleenon BM, Brennan S, McColl D, Mc IS, Passmore AP (2001) Increased oxidative stress in Alzheimer's disease as assessed with 4-hydroxynonenal but not malondialdehyde. *QJM* **94**, 485-490.

[457] Sayre LM, Zelasko DA, Harris PL, Perry G, Salomon RG, Smith MA (1997) 4-Hydroxynonenal-derived advanced lipid peroxidation end products are increased in Alzheimer's disease. *J Neurochem* **68**, 2092-2097.

[458] Fukuda M, Kanou F, Shimada N, Sawabe M, Saito Y, Murayama S, Hashimoto M, Maruyama N, Ishigami A (2009) Elevated levels of 4-hydroxynonenal-histidine Michael adduct in the hippocampi of patients with Alzheimer's disease. *Biomed Res* **30**, 227-233.

[459] Butterfield DA, Bader Lange ML, Sultana R (2010) Involvements of the lipid peroxidation product, HNE, in the pathogenesis and progression of Alzheimer's disease. *Biochim Biophys Acta* **1801**, 924-929.

[460] Mark RJ, Lovell MA, Markesbery WR, Uchida K, Mattson MP (1997) A role for 4-hydroxynonenal, an aldehydic product of lipid peroxidation, in disruption of ion homeostasis and neuronal death induced by amyloid beta-peptide. *J Neurochem* **68**, 255-264.

[461] Gellerich FN, Gizatullina Z, Trumbekaite S, Korzeniewski B, Gaynutdinov T, Seppet E, Vielhaber S, Heinze HJ, Striggow F (2012) Cytosolic Ca2+ regulates the energization of isolated brain mitochondria by formation of pyruvate through the malate-aspartate shuttle. *Biochem J* **443**, 747-755.

[462] Denton RM, Randle PJ, Martin BR (1972) Stimulation by calcium ions of pyruvate dehydrogenase phosphate phosphatase. *Biochem J* **128**, 161-163.

[463] Siess EA, Wieland OH (1972) Purification and characterization of pyruvate-dehydrogenase phosphatase from pig-heart muscle. *Eur J Biochem* **26**, 96-105.

[464] Keller JN, Pang Z, Geddes JW, Begley JG, Germeyer A, Waeg G, Mattson MP (1997) Impairment of glucose and glutamate transport and induction of mitochondrial oxidative stress and dysfunction in synaptosomes by amyloid beta-peptide: role of the lipid peroxidation product 4-hydroxynonenal. *J Neurochem* **69**, 273-284.

[465] Blanc EM, Keller JN, Fernandez S, Mattson MP (1998) 4-hydroxynonenal, a lipid peroxidation product, impairs glutamate transport in cortical astrocytes. *Glia* **22**, 149-160.

[466] Mark RJ, Pang Z, Geddes JW, Uchida K, Mattson MP (1997) Amyloid beta-peptide impairs glucose transport in hippocampal and cortical neurons: involvement of membrane lipid peroxidation. *J Neurosci* **17**, 1046-1054.

[467] Yoshimura Y, Ichinose T, Yamauchi T (2003) Phosphorylation of tau protein to sites found in Alzheimer's disease brain is catalyzed by Ca2+/calmodulin-dependent protein kinase II as demonstrated tandem mass spectrometry. *Neurosci Lett* **353**, 185-188.

[468] Chen X, Huang T, Zhang J, Song J, Chen L, Zhu Y (2008) Involvement of calpain and p25 of CDK5 pathway in ginsenoside Rb1's attenuation of beta-amyloid peptide25-35-induced tau hyperphosphorylation in cortical neurons. *Brain Res* **1200**, 99-106.

[469] Fleming LM, Johnson GV (1995) Modulation of the phosphorylation state of tau in situ: the roles of calcium and cyclic AMP. *Biochem J* **309 (Pt 1)**, 41-47.

[470] Gulick J, Robbins J (2009) Cell-type-specific transgenesis in the mouse. *Methods Mol Biol* **561**, 91-104.

[471] Platt TL, Reeves VL, Murphy MP (2013) Transgenic models of Alzheimer's disease: better utilization of existing models through viral transgenesis. *Biochim Biophys Acta* **1832**, 1437-1448.

161

[472]   Cho A, Haruyama N, Kulkarni AB (2009) Generation of transgenic mice. *Curr Protoc Cell Biol* **Chapter 19**, Unit 19 11.

[473]   Glenner GG, Wong CW (1984) Alzheimer's disease: initial report of the purification and characterization of a novel cerebrovascular amyloid protein. *Biochem Biophys Res Commun* **120**, 885-890.

[474]   Masters CL, Simms G, Weinman NA, Multhaup G, McDonald BL, Beyreuther K (1985) Amyloid plaque core protein in Alzheimer disease and Down syndrome. *Proc Natl Acad Sci U S A* **82**, 4245-4249.

[475]   Kang J, Lemaire HG, Unterbeck A, Salbaum JM, Masters CL, Grzeschik KH, Multhaup G, Beyreuther K, Muller-Hill B (1987) The precursor of Alzheimer's disease amyloid A4 protein resembles a cell-surface receptor. *Nature* **325**, 733-736.

[476]   Goldgaber D, Lerman MI, McBride OW, Saffiotti U, Gajdusek DC (1987) Characterization and chromosomal localization of a cDNA encoding brain amyloid of Alzheimer's disease. *Science* **235**, 877-880.

[477]   Levitan D, Greenwald I (1995) Facilitation of lin-12-mediated signalling by sel-12, a Caenorhabditis elegans S182 Alzheimer's disease gene. *Nature* **377**, 351-354.

[478]   Jankowsky JL, Zheng H (2017) Practical considerations for choosing a mouse model of Alzheimer's disease. *Mol Neurodegener* **12**, 89.

[479]   Games D, Adams D, Alessandrini R, Barbour R, Berthelette P, Blackwell C, Carr T, Clemens J, Donaldson T, Gillespie F, et al. (1995) Alzheimer-type neuropathology in transgenic mice overexpressing V717F beta-amyloid precursor protein. *Nature* **373**, 523-527.

[480]   Drummond E, Wisniewski T (2017) Alzheimer's disease: experimental models and reality. *Acta Neuropathol* **133**, 155-175.

[481]   Pfeifer A, Hofmann A (2009) Lentiviral transgenesis. *Methods Mol Biol* **530**, 391-405.

[482]   Flotte TR, Trapnell BC, Humphries M, Carey B, Calcedo R, Rouhani F, Campbell-Thompson M, Yachnis AT, Sandhaus RA, McElvaney NG, Mueller C, Messina LM, Wilson JM, Brantly M, Knop DR, Ye GJ, Chulay JD (2011) Phase 2 clinical trial of a recombinant adeno-associated viral vector expressing alpha1-antitrypsin: interim results. *Hum Gene Ther* **22**, 1239-1247.

[483]   Daya S, Berns KI (2008) Gene therapy using adeno-associated virus vectors. *Clin Microbiol Rev* **21**, 583-593.

[484]   Nagy Z, Esiri MM, Jobst KA, Morris JH, King EM, McDonald B, Litchfield S, Smith A, Barnetson L, Smith AD (1995) Relative roles of plaques and tangles in the dementia of Alzheimer's disease: correlations using three sets of neuropathological criteria. *Dementia* **6**, 21-31.

[485]   Dournaud P, Delaere P, Hauw JJ, Epelbaum J (1995) Differential correlation between neurochemical deficits, neuropathology, and cognitive status in Alzheimer's disease. *Neurobiol Aging* **16**, 817-823.

[486]   Caramelli P, Robitaille Y, Laroche-Cholette A, Nitrini R, Gauvreau D, Joanette Y, Lecours AR (1998) Structural correlates of cognitive deficits in a selected group of patients with Alzheimer's disease. *Neuropsychiatry Neuropsychol Behav Neurol* **11**, 184-190.

[487]   Gold G, Bouras C, Kovari E, Canuto A, Glaria BG, Malky A, Hof PR, Michel JP, Giannakopoulos P (2000) Clinical validity of Braak neuropathological staging in the oldest-old. *Acta Neuropathol* **99**, 579-582; discussion 583-574.

[488]   Wilcock GK, Esiri MM (1982) Plaques, tangles and dementia. A quantitative study. *J Neurol Sci* **56**, 343-356.

[489]   Arriagada PV, Growdon JH, Hedley-Whyte ET, Hyman BT (1992) Neurofibrillary tangles but not senile plaques parallel duration and severity of Alzheimer's disease. *Neurology* **42**, 631-639.

[490]   Richard BC, Kurdakova A, Baches S, Bayer TA, Weggen S, Wirths O (2015) Gene Dosage Dependent Aggravation of the Neurological Phenotype in the 5XFAD Mouse Model of Alzheimer's Disease. *J Alzheimers Dis* **45**, 1223-1236.

[491]   Buskila Y, Crowe SE, Ellis-Davies GC (2013) Synaptic deficits in layer 5 neurons precede overt structural decay in 5xFAD mice. *Neuroscience* **254**, 152-159.

[492]   Jawhar S, Trawicka A, Jenneckens C, Bayer TA, Wirths O (2012) Motor deficits, neuron loss, and reduced anxiety coinciding with axonal degeneration and intraneuronal Abeta aggregation in the 5XFAD mouse model of Alzheimer's disease. *Neurobiol Aging* **33**, 196 e129-140.

[493]   Giesers NK, Wirths O (2020) Loss of Hippocampal Calretinin and Parvalbumin Interneurons in the 5XFAD Mouse Model of Alzheimer's Disease. *ASN Neuro* **12**, 1759091420925356.

[494]   Sompol P, Furman JL, Pleiss MM, Kraner SD, Artiushin IA, Batten SR, Quintero JE, Simmerman LA, Beckett TL, Lovell MA, Murphy MP, Gerhardt GA, Norris CM (2017) Calcineurin/NFAT Signaling in Activated Astrocytes Drives Network Hyperexcitability in Abeta-Bearing Mice. *J Neurosci* **37**, 6132-6148.

[495]   Oakley H, Cole SL, Logan S, Maus E, Shao P, Craft J, Guillozet-Bongaarts A, Ohno M, Disterhoft J, Van Eldik L, Berry R, Vassar R (2006) Intraneuronal beta-amyloid aggregates, neurodegeneration, and neuron loss in transgenic mice with five familial Alzheimer's disease mutations: potential factors in amyloid plaque formation. *J Neurosci* **26**, 10129-10140.

[496]   Mandelkow EM, Mandelkow E (1993) Tau as a marker for Alzheimer's disease. *Trends Biochem Sci* **18**, 480-483.

[497]   Lassmann H, Fischer P, Jellinger K (1993) Synaptic pathology of Alzheimer's disease. *Ann N Y Acad Sci* **695**, 59-64.

[498]   De-Paula VJ, Radanovic M, Diniz BS, Forlenza OV (2012) Alzheimer's disease. *Subcell Biochem* **65**, 329-352.

[499]   Takeda S (2019) Progression of Alzheimer's disease, tau propagation, and its modifiable risk factors. *Neurosci Res* **141**, 36-42.

[500]   Arranz AM, De Strooper B (2019) The role of astroglia in Alzheimer's disease: pathophysiology and clinical implications. *Lancet Neurol* **18**, 406-414.

[501]   Long JM, Holtzman DM (2019) Alzheimer Disease: An Update on Pathobiology and Treatment Strategies. *Cell* **179**, 312-339.

[502]   Mattson MP, Arumugam TV (2018) Hallmarks of Brain Aging: Adaptive and Pathological Modification by Metabolic States. *Cell Metab* **27**, 1176-1199.

[503]   Landfield PW, Thibault O, Mazzanti ML, Porter NM, Kerr DS (1992) Mechanisms of neuronal death in brain aging and Alzheimer's disease: role of endocrine-mediated calcium dyshomeostasis. *J Neurobiol* **23**, 1247-1260.

[504]   Kerr DS, Campbell LW, Thibault O, Landfield PW (1992) Hippocampal glucocorticoid receptor activation enhances voltage-dependent Ca2+ conductances: relevance to brain aging. *Proc Natl Acad Sci U S A* **89**, 8527-8531.

[505]   Khachaturian ZS (1987) Hypothesis on the regulation of cytosol calcium concentration and the aging brain. *Neurobiol Aging* **8**, 345-346.

[506] Murchison D, McDermott AN, Lasarge CL, Peebles KA, Bizon JL, Griffith WH (2009) Enhanced calcium buffering in F344 rat cholinergic basal forebrain neurons is associated with age-related cognitive impairment. *J Neurophysiol* **102**, 2194-2207.

[507] Bertoni-Freddari C, Meier-Ruge W, Ulrich J (1988) Quantitative morphology of synaptic plasticity in the aging brain. *Scanning Microsc* **2**, 1027-1034.

[508] Barnes CA, Rao G, Foster TC, McNaughton BL (1992) Region-specific age effects on AMPA sensitivity: electrophysiological evidence for loss of synaptic contacts in hippocampal field CA1. *Hippocampus* **2**, 457-468.

[509] McEwen BS, Woolley CS (1994) Estradiol and progesterone regulate neuronal structure and synaptic connectivity in adult as well as developing brain. *Exp Gerontol* **29**, 431-436.

[510] Koffie RM, Hyman BT, Spires-Jones TL (2011) Alzheimer's disease: synapses gone cold. *Mol Neurodegener* **6**, 63.

[511] Spires TL, Meyer-Luehmann M, Stern EA, McLean PJ, Skoch J, Nguyen PT, Bacskai BJ, Hyman BT (2005) Dendritic spine abnormalities in amyloid precursor protein transgenic mice demonstrated by gene transfer and intravital multiphoton microscopy. *J Neurosci* **25**, 7278-7287.

[512] Popugaeva E, Chernyuk D, Zhang H, Postnikova TY, Pats K, Fedorova E, Poroikov V, Zaitsev AV, Bezprozvanny I (2019) Derivatives of Piperazines as Potential Therapeutic Agents for Alzheimer's Disease. *Mol Pharmacol* **95**, 337-348.

[513] von Ruden EL, Zellinger C, Gedon J, Walker A, Bierling V, Deeg CA, Hauck SM, Potschka H (2019) Regulation of Alzheimer's Disease-Associated Proteins During the Course of Epileptogenesis: Differential Proteomic Analysis in a Rat Model. *Neuroscience*.

[514] Rodriguez JJ, Verkhratsky A (2011) Neurogenesis in Alzheimer's disease. *J Anat* **219**, 78-89.

[515] Santos SF, Pierrot N, Octave JN (2010) Network excitability dysfunction in Alzheimer's disease: insights from in vitro and in vivo models. *Rev Neurosci* **21**, 153-171.

[516] Crews L, Masliah E (2010) Molecular mechanisms of neurodegeneration in Alzheimer's disease. *Hum Mol Genet* **19**, R12-20.

[517] Ondrejcak T, Klyubin I, Hu NW, Barry AE, Cullen WK, Rowan MJ (2010) Alzheimer's disease amyloid beta-protein and synaptic function. *Neuromolecular Med* **12**, 13-26.

[518] Lamour Y, Bassant MH, Potier B, Billard JM, Dutar P (1994) [Aging of memory mechanisms]. *C R Seances Soc Biol Fil* **188**, 469-486.

[519] Rowan MJ, Klyubin I, Cullen WK, Anwyl R (2003) Synaptic plasticity in animal models of early Alzheimer's disease. *Philos Trans R Soc Lond B Biol Sci* **358**, 821-828.

[520] Honer WG (2003) Pathology of presynaptic proteins in Alzheimer's disease: more than simple loss of terminals. *Neurobiol Aging* **24**, 1047-1062.

[521] Sun S, Zhang H, Liu J, Popugaeva E, Xu NJ, Feske S, White CL, 3rd, Bezprozvanny I (2014) Reduced synaptic STIM2 expression and impaired store-operated calcium entry cause destabilization of mature spines in mutant presenilin mice. *Neuron* **82**, 79-93.

[522] Selkoe DJ (2008) Soluble oligomers of the amyloid beta-protein impair synaptic plasticity and behavior. *Behav Brain Res* **192**, 106-113.

[523] Selkoe DJ (2002) Alzheimer's disease is a synaptic failure. *Science* **298**, 789-791.

[524] Hermes M, Eichhoff G, Garaschuk O (2010) Intracellular calcium signalling in Alzheimer's disease. *J Cell Mol Med* **14**, 30-41.

[525] Bojarski L, Herms J, Kuznicki J (2008) Calcium dysregulation in Alzheimer's disease. *Neurochem Int* **52**, 621-633.

[526] Chakroborty S, Stutzmann GE (2011) Early calcium dysregulation in Alzheimer's disease: setting the stage for synaptic dysfunction. *Sci China Life Sci* **54**, 752-762.

[527]   Popugaeva E, Pchitskaya E, Bezprozvanny I (2017) Dysregulation of neuronal calcium homeostasis in Alzheimer's disease - A therapeutic opportunity? *Biochem Biophys Res Commun* **483**, 998-1004.

[528]   Michaelis ML (1994) Ion transport systems and Ca2+ regulation in aging neurons. *Ann N Y Acad Sci* **747**, 407-418.

[529]   Peterson C, Gibson GE, Blass JP (1985) Altered calcium uptake in cultured skin fibroblasts from patients with Alzheimer's disease. *N Engl J Med* **312**, 1063-1065.

[530]   Saito K, Elce JS, Hamos JE, Nixon RA (1993) Widespread activation of calcium-activated neutral proteinase (calpain) in the brain in Alzheimer disease: a potential molecular basis for neuronal degeneration. *Proc Natl Acad Sci U S A* **90**, 2628-2632.

[531]   Disterhoft JF, Coulter DA, Alkon DL (1986) Conditioning-specific membrane changes of rabbit hippocampal neurons measured in vitro. *Proc Natl Acad Sci U S A* **83**, 2733-2737.

[532]   Gant JC, Thibault O (2009) Action potential throughput in aged rat hippocampal neurons: regulation by selective forms of hyperpolarization. *Neurobiol Aging* **30**, 2053-2064.

[533]   Neuner SM, Heuer SE, Huentelman MJ, O'Connell KMS, Kaczorowski CC (2019) Harnessing Genetic Complexity to Enhance Translatability of Alzheimer's Disease Mouse Models: A Path toward Precision Medicine. *Neuron* **101**, 399-411 e395.

[534]   McKinney BC, Murphy GG (2006) The L-Type voltage-gated calcium channel Cav1.3 mediates consolidation, but not extinction, of contextually conditioned fear in mice. *Learn Mem* **13**, 584-589.

[535]   Temme SJ, Bell RZ, Fisher GL, Murphy GG (2016) Deletion of the Mouse Homolog of CACNA1C Disrupts Discrete Forms of Hippocampal-Dependent Memory and Neurogenesis within the Dentate Gyrus. *eNeuro* **3**.

[536]   White JA, McKinney BC, John MC, Powers PA, Kamp TJ, Murphy GG (2008) Conditional forebrain deletion of the L-type calcium channel Ca V 1.2 disrupts remote spatial memories in mice. *Learn Mem* **15**, 1-5.

[537]   Froc DJ, Eadie B, Li AM, Wodtke K, Tse M, Christie BR (2003) Reduced synaptic plasticity in the lateral perforant path input to the dentate gyrus of aged C57BL/6 mice. *J Neurophysiol* **90**, 32-38.

[538]   Morris R (1984) Developments of a water-maze procedure for studying spatial learning in the rat. *J Neurosci Methods* **11**, 47-60.

[539]   Berkowitz BA, Gradianu M, Bissig D, Kern TS, Roberts R (2009) Retinal ion regulation in a mouse model of diabetic retinopathy: natural history and the effect of Cu/Zn superoxide dismutase overexpression. *Invest Ophthalmol Vis Sci* **50**, 2351-2358.

[540]   Berkowitz BA, Gradianu M, Schafer S, Jin Y, Porchia A, Iezzi R, Roberts R (2008) Ionic dysregulatory phenotyping of pathologic retinal thinning with manganese-enhanced MRI. *Invest Ophthalmol Vis Sci* **49**, 3178-3184.

[541]   Berkowitz BA, Bissig D, Dutczak O, Corbett S, North R, Roberts R (2013) MRI biomarkers for evaluation of treatment efficacy in preclinical diabetic retinopathy. *Expert Opin Med Diagn* **7**, 393-403.

[542]   Staley KJ, Otis TS, Mody I (1992) Membrane properties of dentate gyrus granule cells: comparison of sharp microelectrode and whole-cell recordings. *J Neurophysiol* **67**, 1346-1358.

[543]   Zhang L, Weiner JL, Valiante TA, Velumian AA, Watson PL, Jahromi SS, Schertzer S, Pennefather P, Carlen PL (1994) Whole-cell recording of the Ca(2+)-dependent slow afterhyperpolarization in hippocampal neurones: effects of internally applied anions. *Pflugers Arch* **426**, 247-253.

[544]   Oh MM, McKay BM, Power JM, Disterhoft JF (2009) Learning-related postburst afterhyperpolarization reduction in CA1 pyramidal neurons is mediated by protein kinase A. *Proc Natl Acad Sci U S A* **106**, 1620-1625.

[545]   Blalock EM, Phelps JT, Pancani T, Searcy JL, Anderson KL, Gant JC, Popovic J, Avdiushko MG, Cohen DA, Chen KC, Porter NM, Thibault O (2010) Effects of long-term pioglitazone treatment on peripheral and central markers of aging. *PLoS ONE* **5**, e10405.

[546]   Han SH, Murchison D, Griffith WH (2005) Low voltage-activated calcium and fast tetrodotoxin-resistant sodium currents define subtypes of cholinergic and noncholinergic neurons in rat basal forebrain. *Brain Res Mol Brain Res* **134**, 226-238.

[547]   Hefendehl JK, LeDue J, Ko RW, Mahler J, Murphy TH, MacVicar BA (2016) Mapping synaptic glutamate transporter dysfunction in vivo to regions surrounding Abeta plaques by iGluSnFR two-photon imaging. *Nat Commun* **7**, 13441.

[548]   Liebscher S, Keller GB, Goltstein PM, Bonhoeffer T, Hubener M (2016) Selective Persistence of Sensorimotor Mismatch Signals in Visual Cortex of Behaving Alzheimer's Disease Mice. *Curr Biol* **26**, 956-964.

[549]   Reichenbach N, Delekate A, Breithausen B, Keppler K, Poll S, Schulte T, Peter J, Plescher M, Hansen JN, Blank N, Keller A, Fuhrmann M, Henneberger C, Halle A, Petzold GC (2018) P2Y1 receptor blockade normalizes network dysfunction and cognition in an Alzheimer's disease model. *J Exp Med* **215**, 1649-1663.

[550]   Kuchibhotla KV, Lattarulo CR, Hyman BT, Bacskai BJ (2009) Synchronous hyperactivity and intercellular calcium waves in astrocytes in Alzheimer mice. *Science* **323**, 1211-1215.

[551]   Delekate A, Fuchtemeier M, Schumacher T, Ulbrich C, Foddis M, Petzold GC (2014) Metabotropic P2Y1 receptor signalling mediates astrocytic hyperactivity in vivo in an Alzheimer's disease mouse model. *Nat Commun* **5**, 5422.

[552]   Ziyatdinova S, Gurevicius K, Kutchiashvili N, Bolkvadze T, Nissinen J, Tanila H, Pitkanen A (2011) Spontaneous epileptiform discharges in a mouse model of Alzheimer's disease are suppressed by antiepileptic drugs that block sodium channels. *Epilepsy Res* **94**, 75-85.

[553]   Risse SC, Lampe TH, Bird TD, Nochlin D, Sumi SM, Keenan T, Cubberley L, Peskind E, Raskind MA (1990) Myoclonus, seizures, and paratonia in Alzheimer disease. *Alzheimer Dis Assoc Disord* **4**, 217-225.

[554]   Mendez MF, Catanzaro P, Doss RC, R AR, Frey WH, 2nd (1994) Seizures in Alzheimer's disease: clinicopathologic study. *J Geriatr Psychiatry Neurol* **7**, 230-233.

[555]   Amatniek JC, Hauser WA, DelCastillo-Castaneda C, Jacobs DM, Marder K, Bell K, Albert M, Brandt J, Stern Y (2006) Incidence and predictors of seizures in patients with Alzheimer's disease. *Epilepsia* **47**, 867-872.

[556]   Scarmeas N, Honig LS, Choi H, Cantero J, Brandt J, Blacker D, Albert M, Amatniek JC, Marder K, Bell K, Hauser WA, Stern Y (2009) Seizures in Alzheimer disease: who, when, and how common? *Arch Neurol* **66**, 992-997.

[557]   Cockerell OC, Eckle I, Goodridge DM, Sander JW, Shorvon SD (1995) Epilepsy in a population of 6000 re-examined: secular trends in first attendance rates, prevalence, and prognosis. *J Neurol Neurosurg Psychiatry* **58**, 570-576.

[558]   Scheuer ML, Cohen J (1993) Seizures and epilepsy in the elderly. *Neurol Clin* **11**, 787-804.

[559]   Hauser WA, Annegers JF, Kurland LT (1993) Incidence of epilepsy and unprovoked seizures in Rochester, Minnesota: 1935-1984. *Epilepsia* **34**, 453-468.

[560]   Kelly KM, Kharlamov A, Hentosz TM, Kharlamova EA, Williamson JM, Bertram EH, 3rd, Kapur J, Armstrong DM (2001) Photothrombotic brain infarction results in seizure activity in aging Fischer 344 and Sprague Dawley rats. *Epilepsy Res* **47**, 189-203.

[561] Hauser WA, Morris ML, Heston LL, Anderson VE (1986) Seizures and myoclonus in patients with Alzheimer's disease. *Neurology* **36**, 1226-1230.

[562] Cain SM, Snutch TP (2010) Contributions of T-type calcium channel isoforms to neuronal firing. *Channels (Austin)* **4**, 475-482.

[563] Carmignoto G, Haydon PG (2012) Astrocyte calcium signaling and epilepsy. *Glia* **60**, 1227-1233.

[564] Sun DA, Sombati S, Blair RE, DeLorenzo RJ (2002) Calcium-dependent epileptogenesis in an in vitro model of stroke-induced "epilepsy". *Epilepsia* **43**, 1296-1305.

[565] Strowbridge BW, Masukawa LM, Spencer DD, Shepherd GM (1992) Hyperexcitability associated with localizable lesions in epileptic patients. *Brain Res* **587**, 158-163.

[566] Schwartzkroin PA (1986) Hippocampal slices in experimental and human epilepsy. *Adv Neurol* **44**, 991-1010.

[567] Babb TL, Brown WJ (1986) Neuronal, dendritic, and vascular profiles of human temporal lobe epilepsy correlated with cellular physiology in vivo. *Adv Neurol* **44**, 949-966.

[568] Barnes CA, Rao G, Orr G (2000) Age-related decrease in the Schaffer collateral-evoked EPSP in awake, freely behaving rats. *Neural Plast* **7**, 167-178.

[569] Barnes CA, McNaughton BL (1985) An age comparison of the rates of acquisition and forgetting of spatial information in relation to long-term enhancement of hippocampal synapses. *Behav Neurosci* **99**, 1040-1048.

[570] Rosenzweig ES, Rao G, McNaughton BL, Barnes CA (1997) Role of temporal summation in age-related long-term potentiation-induction deficits. *Hippocampus* **7**, 549-558.

[571] Foster TC, Kumar A (2007) Susceptibility to induction of long-term depression is associated with impaired memory in aged Fischer 344 rats. *Neurobiol Learn Mem* **87**, 522-535.

[572] Baker J, Libretto T, Henley W, Zeman A (2019) A Longitudinal Study of Epileptic Seizures in Alzheimer's Disease. *Front Neurol* **10**, 1266.

[573] Bell JS, Lonnroos E, Koivisto AM, Lavikainen P, Laitinen ML, Soininen H, Hartikainen S (2011) Use of antiepileptic drugs among community-dwelling persons with Alzheimer's disease in Finland. *J Alzheimers Dis* **26**, 231-237.

[574] Taipale H, Gomm W, Broich K, Maier W, Tolppanen AM, Tanskanen A, Tiihonen J, Hartikainen S, Haenisch B (2018) Use of Antiepileptic Drugs and Dementia Risk-an Analysis of Finnish Health Register and German Health Insurance Data. *J Am Geriatr Soc* **66**, 1123-1129.

[575] Cretin B (2018) Pharmacotherapeutic strategies for treating epilepsy in patients with Alzheimer's disease. *Expert Opin Pharmacother* **19**, 1201-1209.

[576] Zhang MY, Zheng CY, Zou MM, Zhu JW, Zhang Y, Wang J, Liu CF, Li QF, Xiao ZC, Li S, Ma QH, Xu RX (2014) Lamotrigine attenuates deficits in synaptic plasticity and accumulation of amyloid plaques in APP/PS1 transgenic mice. *Neurobiol Aging* **35**, 2713-2725.

[577] Rao SC, Dove G, Cascino GD, Petersen RC (2009) Recurrent seizures in patients with dementia: frequency, seizure types, and treatment outcome. *Epilepsy Behav* **14**, 118-120.

[578] Green KN, LaFerla FM (2008) Linking calcium to Abeta and Alzheimer's disease. *Neuron* **59**, 190-194.

[579] Green KN (2009) Calcium in the initiation, progression and as an effector of Alzheimer's disease pathology. *J Cell Mol Med* **13**, 2787-2799.

[580] Owen EH, Logue SF, Rasmussen DL, Wehner JM (1997) Assessment of learning by the Morris water task and fear conditioning in inbred mouse strains and F1 hybrids:

implications of genetic background for single gene mutations and quantitative trait loci analyses. *Neuroscience* **80**, 1087-1099.

[581]   Severin D, Gallagher M, Kirkwood A (2020) Afterhyperpolarization amplitude in CA1 pyramidal cells of aged Long-Evans rats characterized for individual differences. *Neurobiol Aging* **96**, 43-48.

[582]   Stadtman ER (2001) Protein oxidation in aging and age-related diseases. *Ann N Y Acad Sci* **928**, 22-38.

[583]   Rowley S, Patel M (2013) Mitochondrial involvement and oxidative stress in temporal lobe epilepsy. *Free Radic Biol Med* **62**, 121-131.

[584]   Waldbaum S, Patel M (2010) Mitochondria, oxidative stress, and temporal lobe epilepsy. *Epilepsy Res* **88**, 23-45.

[585]   Geronzi U, Lotti F, Grosso S (2018) Oxidative stress in epilepsy. *Expert Rev Neurother* **18**, 427-434.

[586]   Clemens JA, Meites J (1971) Neuroendocrine status of old constant-estrous rats. *Neuroendocrinology* **7**, 249-256.

[587]   Lu KH, Hopper BR, Vargo TM, Yen SS (1979) Chronological changes in sex steroid, gonadotropin and prolactin secretions in aging female rats displaying different reproductive states. *Biol Reprod* **21**, 193-203.

[588]   Huang HH, Steger RW, Bruni JF, Meites J (1978) Patterns of sex steroid and gonadotropin secretion in aging female rats. *Endocrinology* **103**, 1855-1859.

[589]   Koebele SV, Bimonte-Nelson HA (2016) Modeling menopause: The utility of rodents in translational behavioral endocrinology research. *Maturitas* **87**, 5-17.

[590]   Gibson G, Perrino P, Dienel GA (1986) In vivo brain calcium homeostasis during aging. *Mech Ageing Dev* **37**, 1-12.

[591]   Multhaup G, Ruppert T, Schlicksupp A, Hesse L, Beher D, Masters CL, Beyreuther K (1997) Reactive oxygen species and Alzheimer's disease. *Biochem Pharmacol* **54**, 533-539.

[592]   Butterfield DA, Howard B, Yatin S, Koppal T, Drake J, Hensley K, Aksenov M, Aksenova M, Subramaniam R, Varadarajan S, Harris-White ME, Pedigo NW, Jr., Carney JM (1999) Elevated oxidative stress in models of normal brain aging and Alzheimer's disease. *Life Sci* **65**, 1883-1892.

[593]   Butterfield DA, Yatin SM, Varadarajan S, Koppal T (1999) Amyloid beta-peptide-associated free radical oxidative stress, neurotoxicity, and Alzheimer's disease. *Methods Enzymol* **309**, 746-768.

[594]   Veurink G, Fuller SJ, Atwood CS, Martins RN (2003) Genetics, lifestyle and the roles of amyloid beta and oxidative stress in Alzheimer's disease. *Ann Hum Biol* **30**, 639-667.

[595]   Cecchi C, Fiorillo C, Sorbi S, Latorraca S, Nacmias B, Bagnoli S, Nassi P, Liguri G (2002) Oxidative stress and reduced antioxidant defenses in peripheral cells from familial Alzheimer's patients. *Free Radic Biol Med* **33**, 1372-1379.

VITA

Adam Omar Ghoweri

Education

Moravian College, Bethlehem, PA   **GPA – 3.52**
  Bachelor of Science –May 2015
  Neuroscience; Cellular Neurobiology Track
  Minor: Arabic Studies
  Institutional Honors: Cum Laude

Harrisburg Area Community College, Harrisburg, PA   **GPA – 3.68**
  Associate in Arts – May 2012
  Biology
  Institutional Honors: High Honors

Publications

Peer-Reviewed

"Electrophysiological and Neuronal Calcium Imaging Sex Differences   **2020**
in the 5xFAD Mouse Model"
AO Ghoweri, L Ouillette, HN Frazier, KL Anderson, R-L Lin, JC Gant,
R Parent, GG Murphy, and O Thibault.
Journal of Alzheimer's Disease
doi: 10.3233/JAD-200109

 "Neuronal Calcium Imaging, Excitability and Plasticity Changes   **2020**
in the *Aldh2*$^{-/-}$ Mouse Model of Sporadic Alzheimer's Disease"
AO Ghoweri, P Gagolewicz, HN Frazier, JC Gant, RD Andrew,
BM Bennett, and O Thibault.
Journal of Alzheimer's Disease
doi: 10.3233/JAD-200617

"Molecular Elevation of Insulin Receptor Signaling Improves Memory   **2020**
Recall in Aged Fischer 344 Rats"
Frazier HN, Anderson KL, Ghoweri AO, Lin R-L, Hawkinson TR, Popa GJ,
Sompol P, Mendenhall MD, Norris CM, Thibault O.
Aging Cell
doi: 10.1111/acel.13220

"Elevating Insulin Signaling Using a Constitutively Active Insulin   **2020**
Receptor Increases Glucose Metabolism and Expression of GLUT3

in Hippocampal Neurons.”
Frazier HN, Ghoweri AO, Anderson KL, Lin R-L, Popa GJ, Mendenhall MD,
Reagan LP, Craven RJ, Thibault O.
Frontiers in Neuroscience: Neuroendocrine Science
doi: 10.3389/fnins.2020.00668

“The effects of bacterial endotoxin (LPS) on cardiac and synaptic function   **2020**
in various animal models: Larval *Drosophila*, crayfish, crab, and rodent.”
Ballinger-Boone, C., Anyagaligbo, O., Bernard, J., Bierbower, S.M.,
Dupont-Versteegden, E.E., Ghoweri, A., Greenhalgh, A., Harrison, D.,
Istas, O., McNabb, M., Saelinger, C., Stanback, A., Stanback, M.,
Thibault,O., and Cooper, R.L.
International Journal of Zoological Research
doi: 10.3923/ijzr.2020.XX.XX

“Long-Term Intranasal Insulin Aspart: A Profile of Gene Expression,   **2019**
Memory, and Insulin Receptors in Aged Fischer 344 Rats”
Hilaree N. Frazier, Adam O. Ghoweri, Emily Sudkamp, Eleanor S. Johnson,
Katie L. Anderson, Grant Fox, Keomany Vatthanaphone, Xia Mengfan,
Ruei-Lung Lin, Kendra E. Hargis-Staggs, Nada M. Porter, James R. Pauly,
Eric M. Blalock, and Olivier Thibault
Journals of Gerontology: Medical Sciences
doi: 10.1093/Gerona/glz105

“Broadening the definition of brain insulin resistance in aging and   **2019**
Alzheimer’s disease”
Hilaree N. Frazier, Adam O. Ghoweri, Katie L. Anderson, Ruei-Lung Lin,
Nada M. Porter, and Olivier Thibault
Experimental Neurology
doi: 10.1016/j.expneurol.2018.12.007

“Novel calcium-related targets of insulin in hippocampal neurons”   **2018**
Shaniya Maimaiti, Hilaree N. Frazier, Katie L. Anderson, Adam O. Ghoweri,
Lawrence D. Brewer, Nada M. Porter, Olivier Thibault
Neuroscience
doi: 10.1016/j.neuroscience.2017.09.019

“Expression of a Constitutively Active Human Insulin Receptor in   **2018**
Hippocampal Neurons Does Not Alter VGCC Currents”
Frazier, H N ; Anderson, K L ; Maimaiti, S ; Ghoweri, A O ; Kraner, S D ;
Popa, G J ; Hampton, K K ; Mendenhall, M D ; Norris, C M ; Craven, R J ;
Thibault, O
Neurochemical Research
doi: 10.1007/s11064-018-2510-2

"Nutrition Mythbuster: Protein- How much is enough?"
2020
Adam Ghoweri, Shayan Mohammadmoradi,
Jessie Hoffman, & Sara Police
Health & Wellness
Vol. 17, Issue 7, April 2020
https://issuu.com/rockpointpublishing/docs/hwapril20_digital

"3 Tips to Increase Mental Acuity"
2020
Adam Ghoweri, Courtney Turpin, & Sara Police
Health & Wellness
Vol. 17, Issue 5, February 2020
https://issuu.com/rockpointpublishing/docs/hwfeb20_digital

"5 Healthy Options for Afterschool Snacking"
2019
Adam Ghoweri & Sara Police
Health & Wellness
Vol. 16, Issue 11, August 2019
http://healthandwellnessmagazine.net/5-healthy-options-for-afterschool-snacking.html

"4 Nutrition Tips Every Man Needs" **2018**
Dave Schnell, Adam O. Ghoweri, Kai Zhang, and Nicole Robinson
Health & Wellness Men's Health
Vol. 16, Issue 2, November 2018
https://issuu.com/rockpointpublishing/docs/hwnov18_digital

Scholastic and Professional Accolades

University of Kentucky
    Recipient of DPNS "Student of the Year" Award '19- '20 **2020**

    Recipient of T32 NIH Training Grant **2018**
    Training in Translational Research in Alzheimer's and Related
    Dementia's (TRIAD)
    NIH T32 AG057461

    Passed Qualifying Examination to Become PhD Candidate **2018**

    Recipient of ISN Travel Award **2018**
    Lexington, KY
    For attendance of International Society of Neurogastronomy Conference

Moravian College

Recipient of "The Neuroscience Award"   **2015**
Bethlehem, PA

Recipient of "Honors in Neuroscience"   **2015**
Bethlehem, PA

Selected for Moravian College's Honors Research Program   **2014 – 2015**
Purpose of Project: To determine whether intranasal administration
of DNSP-11, a biologically active synthetic peptide derived from the
human pro-sequence of glial cell line-derived neurotrophic factor
(GDNF), is protective of dopamine neurons of the nigrostriatal pathway
in a striatal 6-hydroxydopamine (6-OHDA) rat model of Parkinson's
disease.

Selected for Moravian College's Student Opportunity for Academic   **2014**
Research (SOAR) Summer Research Grant Program
Project Title: Intranasal Administration of DNSP-11 in a Chronic
6-Hydroxydopamine Model of Parkinson's disease

Affiliations and Professional Academic Roles

National

American Society for Neurochemistry   **2017 - Present**
Member

Society for Neuroscience   **2014 – Present**
Member

University of Kentucky

Book Club Leader   **2019**
Facilitate discussion on Melanie V. Sinche's "Next Gen PhD
A Guide to Career Paths in Science"

Graduate Student Mentor   **2019**
Mentor

Trainees in Research Advisory Committee (TRAC)   **2018 – 2020**
Representative

Nutritional Science and Pharmacology Students Association
Secretary   **2019 – 2020**
Member   **2017 – 2020**

Biomedical Graduate Student Organization
Social Committee Representative   **2018 – 2020**
Member   **2016 – 2020**

Bluegrass Chapter of Society for Neuroscience
Graduate Student Representative   **2018 – 2019**
Member   **2017 – 2020**

Moravian College
Psi Chi International Honor Society in Psychology   **2015 – Present**
Member

Nu Rho Psi National Honor Society in Neuroscience   **2015 – Present**
Member

Gamma Sigma Alpha Greek Academic Honor Society   **2015 – Present**
Member

Beta Beta Beta National Biology Honor Society   **2013 – Present**
Member

Lehigh Valley Chapter of Society for Neuroscience   **2012 – 2015**
Undergraduate Student Member

Moravian College Interfaith Council   **2014 – 2015**
Member

Neuroscience Club
President   **2013 – 2014**
Member   **2012 – 2015**

Middle Eastern Club
President   **2014 – 2014**
Vice President   **2013 – 2014**
Member   **2013 – 2015**

Delta Tau Delta Fraternity
President   **2013 – 2014**
Director of Academic Affairs   **2012 – 2013**
Member   **2012 – 2015**

Harrisburg Area Community College
Phi Theta Kappa Honor Society   **2012 – Present**
Member